Kinetic Investigations of the Oxygen Entry Pathway of the Hypoxia-Inducible Factor (HIF) Prolyl Hydroxylase 2

A thesis submitted to the faculty of Physical Sciences in partial fulfilment of the degree of Master of Science by Research in Chemical Biology

Leah Taylor Kearney
Hertford College
2015

Summary

Human hypoxia inducible factor (HIF) is responsible for mediating the body's response to low O_2 availability. The levels and activity of HIF are regulated by four Fe(II)/2-oxoglutarate (2OG)-dependent oxygenases, prolyl-hydroxylase domains 1-3 (PHD 1-3) and factor-inhibiting HIF (FIH), collectively termed the HIF hydroxylases. [1, 2] The PHDs catalyse hydroxylation of specific prolyl residues in the N - and C - terminal oxygen-dependent degradation domains of HIF-α, targeting it for degradation by the proteasome. FIH catalyses hydroxylation of an asparaginyl residue in the C-terminal transactivation domain,[3] preventing the interaction of HIF-α with the co-transcriptional activator p300. Under hypoxic conditions, the activity of the oxygen-dependent HIF hydroxylases is reduced, causing an increase in cellular HIF-α levels/activity and triggering the transcription of genes that enable the cellular and physiological hypoxic response. [4-7]

PHD2 is reported to be the key O_2 sensor regulating the hypoxic response. [8] It has also been reported to have a high $K_m(O_2)$ value [8-13] and a slow reaction with O_2 in pre-steady state studies, kinetic features that are proposed to be related to its role as an O_2-sensor. [8, 10] We are interested in the molecular features that enable this O_2-sensing role, when other Fe(II)/2OG oxygenases react ~100-fold more rapidly with O_2. To investigate whether restricted O_2 passage to the active site may be responsible for its unusual kinetics, our collaborators (C. Jorgensen and C. Domene, KCL) have conducted molecular dynamic studies to investigate the route of O_2 entry to the PHD2 active site. These studies (unpublished) have indicated that O_2 enters PHD2 via the interface between HIF substrate and a flexible, substrate-binding loop (the β2β3 loop) in PHD2. O_2 is then proposed to reside in a stable 'E-cluster' in PHD2, before moving to the active site. This report describes work conducted to

experimentally verify this predicted O_2 entry pathway into PHD2, and to determine whether aspects of this entry pathway contribute to the slow kinetics of the reaction of PHD2 with O_2.

To validate the role of the β2β3 loop in the reaction of PHD2 with O_2, kinetic studies of PHD2 loop variants were undertaken. These variants were previously developed by Flashman *et al* such that the β2β3 loop of PHD2 was altered to include the loop sequences of PHD1 and PHD3. These loop variants demonstrated reduced O_2 sensitivity, and with the β2β3 loop of PHD3, a more rapid reaction with O_2. These data suggest the β2β3 loop of PHD2 does indeed play an important role in O_2 uptake.

Experimental validation of the stable E-cluster was then undertaken. The site directed mutagenesis of methionine 299 in PHD2 to histidine did not yield different kinetics with respect to O_2, suggesting either replacement of methionine 299 with histidine does not alter the O_2 'stabilising' characteristics of the E-cluster or the E-cluster is not significant in O_2 kinetics. Tryptophans 258 and 389 also form part of the E cluster. Laser-induced excitation of molecular O_2 to O_2* was used to attempt to modify and thus identify amino acid residues in regions where O_2 was stably bound, i.e. the E-cluster. This approach was technically challenging, and results obtained were inconclusive. Further investigations using this method would require substantial optimisation.

Stopped-flow tryptophan fluorescence quenching studies confirmed that these residues encounter a quenching species upon introduction of O_2, supporting the hypothesis that they are present on the O_2 uptake pathway. Interestingly, the rate of tryptophan fluorescence quenching of the $PHD2_{variant}$.CODD.Fe(II).2OG complex by O_2 correlates with the PHD2 WT rate of product turnover [10] suggesting the quenching is correlated with product turnover.

The results reported here imply that the rate limiting step with respect to PHD2 and O_2 is prior to O_2 reaching the E cluster.

Overall the thesis supports the hypothesis that PHD2's β2β3 loop is involved in PHD2's O_2–sensing capability. Experiments were unable to verify the existence of an E-cluster, including the finding that O_2 encounters two tryptophans present along the proposed O_2 uptake pathway in PHD2 at the same rate as PHD2 catalysis. The findings of this study suggest that the β2β3 loop of PHD2 may be a key molecular feature involved in O_2 sensing by PHD2, a factor that could be taken into account when designing PHD2 inhibiting or activating therapies.

1. R. K. Bruick and S. L. McKnight, *Science*, 2001, **294**, 1337-1340.
2. D. Lando, D. J. Peet, D. A. Whelan, J. J. Gorman and M. L. Whitelaw, *Science*, 2002, **295**, 858-861.
3. K. S. Hewitson, L. A. McNeill, M. V. Riordan, Y.-M. Tian, A. N. Bullock, R. W. Welford, J. M. Elkins, N. J. Oldham, S. Bhattacharya, J. M. Gleadle, P. J. Ratcliffe, C. W. Pugh and C. J. Schofield, *J Biol Chem*, 2002, **277**, 26351-26355.
4. J. Myllyharju, *Acta Physiologica*, 2013, **208**, 148-165.
5. W. G. Kaelin and P. J. Ratcliffe, *Mol Cell*, 2008, **30**, 393-402.
6. C. J. Schofield and P. J. Ratcliffe, *Nat Rev Mol Cell Bio*, 2004, **5**, 343-354.
7. G. L. Semenza, *Physiology*, 2004, **19**, 176-182.
8. H. Tarhonskaya, A. P. Hardy, E. A. Howe, N. D. Loik, H. B. Kramer, J. S. O. McCullagh, C. J. Schofield and E. Flashman, *J Biol Chem*, 2015.
9. E. Flashman, L. M. Hoffart, R. B. Hamed, J. M. Bollinger, C. Krebs and C. J. Schofield, *Febs J*, 2010, **277**, 4089-4099.
10. H. Tarhonskaya, R. Chowdhury, I. K. H. Leung, N. D. Loik, J. S. O. McCullagh, T. D. W. Claridge, C. J. Schofield and E. Flashman, *Biochem J*, 2014, **463**, 363-372.
11. M. Hirsilä, P. Koivunen, V. Günzler, K. I. Kivirikko and J. Myllyharju, *J Biol Chem*, 2003, **278**, 30772-30780.
12. J. H. Dao, R. J. M. Kurzeja, J. M. Morachis, H. Veith, J. Lewis, V. Yu, C. M. Tegley and P. Tagari, *Anal Biochem*, 2009, **384**, 213-223.
13. D. Ehrismann, E. Flashman, D. N. Genn, N. Mathioudakis, K. S. Hewitson, P. J. Ratcliffe and C. J. Schofield, *Biochem J*, 2007, **401**, 227-234.

Tiomnaithe do Jasmine

Acknowledgements

First and foremost I would like to thank Dr Emily Flashman for giving me the opportunity to pursue this degree. Her guidance, encouragement and patience not only made this pursuit possible, but enjoyable. I could not have asked for better.

I would also like to thank Professor Christopher Schofield for his boundless scientific enthusiasm and support throughout the year.

I extend my sincerest gratitude to Dr Hanna Tarhonskaya, for paving the way with her extraordinary know-how. Her mentoring and friendship were invaluable.

I would like to thank Mr Gareth Langley, Dr Hanna Tarhonskaya, Ms Rebecca Hancock, Dr Tom McAllister and Dr Emily Flashman for taking the time to proofread my thesis chapters.

I thank Dr Carmen Domene and Mr Christian Jorgensen of King's College London for their incisive modelling studies. I thank Prof Claire Vallance, Dr Simon-John King and Mr Dean James of the Vallance group for their key role in facilitating the laser experiments. It was a pleasure to work with you all. I would like to thank Dr Akane Kawamura and Dr Tom McAllister for allowing me to partake in their project with PHD2 and 3C and for providing the necessary peptides and background information.

I would like to thank Prof Luet Wong for allowing me to occupy his lab space and for answering my incessant questions.

I thank Dr James Wickens for all his help with UPLC, optimizing the method by which we analysed succinate turnover. His help and dedication were incredible. I'm sincerely grateful.

I thank Ms Rebecca Hancock for primers, fluorescence tips and her FOXY-guru skills.

I also thank Ms Joanna Bonnici for providing cells, primers and peptides – not to mention great fun (and food and my Slinky).

I would like to thank Mr Herminio Mansojubier for providing media, Dr Zhihong Zhang and Dr Rasheduzzaman Chowdhury for their help and support, Mr Colin Sparrow for his help with MALDI-TOF MS, Dr Adam Hardy and Ms Wendy Sobey for their constant supply of laboratory help and know-how and Mr Thomas Leissing for his helpful Pymol tutorials and study breaks. To all I am truly grateful.

To the rest of the CJS, Flashman, Kawamura and Loenarz group members, I could not have asked for better compatriots! You made coming to work very easy.

To my friends both here, home, and in far flung places, I cannot thank you enough for your company and endless support. On this occasion I extend a special thank you to Mr Eoin Lyons, Ms Arika Downey, Ms Leoma Williams, Ms Rosie Worster and Ms Anne Makena who in tough times ensured I saw this through.

To my grandparents, Mr and Mrs Dan and Joan Taylor, I owe you a lifetime of gratitude. Thank you for everything you have done and will undoubtedly do.

To my mother, Helen, thank you for making sure I ate my vegetables and turned up to school.

To my entire family, of which there are too many members to mention, I owe every last one of my successes to you.

Table of Contents

Abbreviations

2OG – 2-Oxoglutarate

2TY - 2 Tryptone Yeast

APS - Ammonium Persulfate

Asp(D) - Aspartic acid (Aspartate)

CAD - HIF *C*-terminal transcriptional activation domain

CHCA - α-Cyano-4-hydroxycinnamic acid

CODD – C-Terminal Oxygen Dependent Degradation Domain

DNA - Deoxyribonucleic acid

DSBH - Double stranded beta helix

E. coli - *Escherichia coli*

EDTA - Ethylenediaminetetracetic acid

ESI-MS - Electron-spray Ionisation Mass Spectrometry

FIH - Factor Inhibiting HIF

FPLC - Fast Protein Liquid Chromatography

HEPES - 4-(2-hydroxyethyl)-1-piperazineethanesulfonic acid

HIF-1α – Hypoxia-Inducible Factor -1α

IFA - Intrinsic Fluorescence Assay

IPTG - Isopropyl β-D-1-Thiogalactopyranoside

LCMS – Liquid Chromatography Mass Spectrometry

MALDI-TOF-MS – Matrix-Assisted-Laser-Desorption/Ionisation Time-of-Flight MS

MES - 2-(N-morpholino)ethanesulfonic acid hydrate

MLCT - Metal-to-ligand charge transfer

mPAHX – Mature phytanoyl-CoA hydroxylase

MS - Mass Spectrometry

MS-MS – Tandem Mass Spectrometry

MW - Molecular Weight

NMR – Nuclear Magnetic Resonance Spectroscopy

NODD - N-Terminal Oxygen Dependent Degradation Domain

NOG - N-oxaylglycine

PDB - Protein Data Bank

PHD 2 - Prolyl-Hydroxylase-Domain 2 wild type

PHD 2.1 – PHD 2 with loop region of Prolyl-Hydroxylase-Domain 1

PHD 2.3 - PHD 2 with loop region of Prolyl-Hydroxylase-Domain 3

PHD.D315E - PHD 2, Aspartic Acid 315 – Glutamic Acid

PHD.M299H - PHD 2, Methionine 299 – Histidine

PHD.W334F/W367F - PHD 2, Tryptophan 334/367 – Phenylalanine

$PPHD_{putida}$ - Prokaryotic Prolyl Hydroxylase

pVHL - Von Hippel-Lindau tumour suppressor protein

RPM - Revolutions per Minute

SDS-PAGE - Sodium Dodecyl Sulphate-Polyacrylamide Gel Electrophoresis

SOC – Super Optimal Broth

TauD - Taurine Dioxygenase

TEMED - N,N,N',N'-tetramethyl-ethane-1,2-diamine

Tris -HCl Tris(hydroxymethyl)aminomethane

vCPH - Viral collagen prolyl-4-hydroxylase

WT - Wild-Type

Standard abbreviations for amino acids, SI-units/prefixes and chemical elements are used throughout

Chapter 1: Introduction

The hypoxia-inducible factor system

All aerobic organisms require O_2 to survive, with chronic reduction in O_2 supply to tissues resulting in a state of hypoxia. This hypoxic state is known to induce numerous profound physiological responses including increased red blood cell production and changes to the expression of cytokines and growth factors that influence vascular re-modelling and inflammation. [3, 4] The body's response to hypoxia is regulated by the hypoxia-inducible transcription factor (HIF) in cells, inducing the transcription of a number of genes responsible for adapting to the hypoxic conditions. These genes include erythropoietin (EPO), vascular endothelial growth factor (VEGF) and glucose transporter 1 (GLUT1) and glycolytic enzymes allowing for increased anaerobic ATP synthesis. [5-7]

Hypoxia-inducible factor (HIF) is an α,β-heterodimeric transcription factor that mediates cellular responses to low oxygen concentrations via the transcriptional activation of specific genes involved in both tumorigenesis and angiogenesis. [8] Specifically, the promotion of angiogenesis associated with upregulated HIF can facilitate the vascularisation of tumours,[8, 9] and has therefore been proposed to be linked to tumorigenesis. [10] Conversely, HIFα upregulation has resulted in tumour suppression in certain cases, with HIF-1α and HIF-2α causing opposite effects in the same cell type. [11-14] Therefore understanding how HIF levels are regulated is important in rationalising certain pathological processes.

HIF consists of two subunits: HIF-α and HIF-β. Although HIF-α has three isoforms, only cellular levels of HIF-α and not those of HIF-β vary with respect to O_2 availability. [15] In hypoxia, levels of HIF-α increase, and it forms a heterodimer with HIF-β in the nucleus,

promoting HIF target gene expression. By contrast, under normal O_2 conditions, or normoxia, HIF-α levels are reduced, resulting in a deficiency of the active HIF-α,β heterodimer and suppression of the hypoxic response.

Both the cellular levels of HIF-α and its transcriptional activity are regulated by post-translational modifications in direct response to changes in cellular O_2 concentrations. Under normoxic conditions, HIF-1/2α are hydroxylated by four 2 oxoglutarate (2OG)/Fe(II) dependent oxygenases; three prolyl hydroxylase domain enzymes (PHD1-3) and an asparaginyl hydroxylase (factor inhibiting HIF-1, FIH), collectively termed the HIF hydroxylases. [16, 17] The hydroxylation of two prolyl residues targets HIF for proteosomal degradation by the von Hippel-Lindau tumour suppressor protein (pVHL) E3 ubiquitin ligase complex. [18-20]

The two aforementioned hydroxylation sites in HIF-1α have been identified: the *N*- and *C*-terminal oxygen dependent degradation domains (NODD and CODD, respectively). [21] Two prolyl-residues, in NODD (Pro402 in human HIF-1α) and CODD (Pro564 in human HIF-1α), undergo *trans*-4-hydroxylation catalysed by PHD1-3, [16, 22-24] resulting in a hydroxyproline residue. [24] While both PHD1 and 2 can hydroxylate NODD and CODD, PHD3 exhibits a striking preference for CODD, [25-28] only hydroxylating NODD after prolonged incubation. [29] Crystal structures of pVHL with HIF-1α CODD peptide reveal a mechanism by which HIF is targeted. In pVHL there exists a hydrophobic pocket with which the hydroxyproline of HIF interacts. The hydroxyl group of the hydroxyproline displaces a H_2O molecule from pVHL and subsequently forms a hydrogen bond to nearby residues. The resulting increase in the strength of interaction between pVHL and the hydroxylated species of HIF-α relative to that

of the unhydroxylated is, at least in part, responsible for the recognition of HIF by pVHL and degradation. [30]

HIF-mediated transcription of genes is facilitated by the interaction of the HIF *C*-terminal transcriptional activation domain (CAD) with the CBP/p300 transcriptional coactivators. FIH, the fourth HIF hydroxylase, is responsible for regulating this HIF1/2α transcriptional activity via the hydroxylation of asparaginyl residues 803 and 851 in HIF 1α and HIF 2α respectively. These hydroxylated asparaginyl residues block the interaction of the CAD with the CBP/p300 transcriptional coactivators, downregulating the hypoxic response. Structurally, this hydrophobic CAD-CBP/p300 interaction is disrupted via a steric clash induced *via* the hydroxylation of the β-carbon of the asparaginyl 803 residue. [31, 32]

2OG/Fe(II) dependent oxygenases

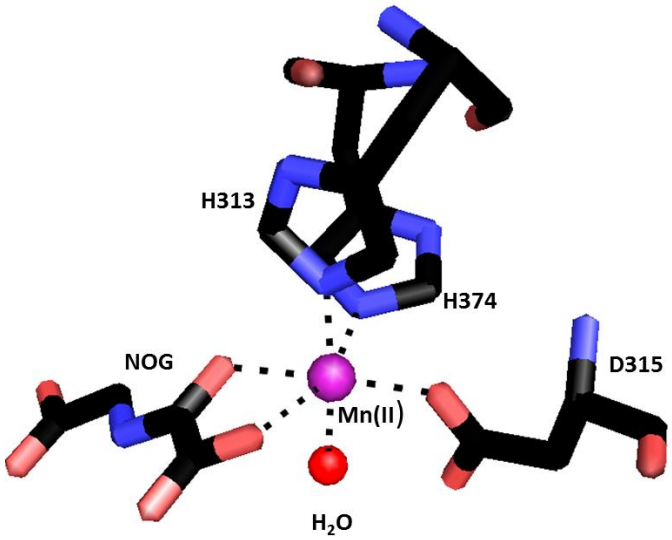

Figure 1: *The octahedral coordination of the Mn(II) metal centre in the PHD2.Mn(II).N-oxalylglycine(NOG).CODD structure. Mn(II) is coordinated by histdines 313 and 374, aspartate 315, H_20 and NOG – an unreactive 2OG analogue. This conserved HXD/E…H motif is found in all Fe(II)/2OG dependent oxygenases. PDB ID: 3HQR* [1]

The HIF hydroxylases are part of a large superfamily of Fe(II)/2OG dependent enzymes, responsible for catalysing hydroxylation and demethylation in animals, and a far wider range of oxidative reactions in plants and microorganisms (the HIF hydroxylases are to be

discussed in more detail later). [33-36] 2OG oxygenases utilize Fe(II) and 2OG to facilitate the 2-electron oxidation of 2OG, resulting in the decarboxylation of 2OG to succinate and the oxidation of an alkyl substrate (see below). [2,33,37,38] Structural analyses of the 2OG oxygenases reveal not only homology in co-factor and co-substrate selection, but also conserved structural features, with a common active site motif and a double-stranded β-helix (DSBH) fold. [39] The active site consists of an Fe(II) centre coordinated by a HXD/E…H facial triad motif, [40] with the 2OG binding to the Fe(II) centre in a bi-dentate manner and a H_2O molecule completing the octahedral Fe(II) complexation. While the 'prime' substrate binds in close proximity to the facial triad, it is not directly coordinated to Fe(II) (Fig 1).

Mechanism of Fe(II)/2OG related enzymes

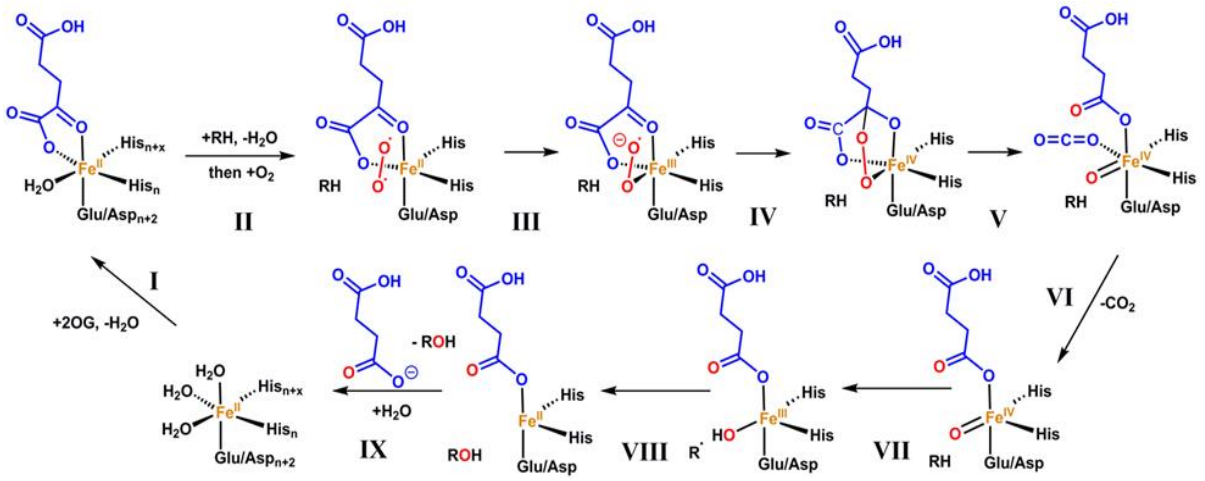

Figure 2: *Outline of the proposed consensus mechanism of Fe(II)/2OG dependent oxygenases. Following formation of an enzyme.Fe(II).2OG.substrate complex (I) O_2 binds to the active site Fe^{II} (II) forming an Fe(III)-superoxo species which decarboxylates 2OG to succinate (IV, V). Following this, the Fe(IV)-oxo species forms (VI) and the substrate becomes hydroxlated via a radical mechanism (VII-VIII), hydroxylated substrate and succinate leave, followed by Fe(II) coordination of three H_2O with 2OG coordination displacing two H_2O molecules (IX-I).*

Spectroscopic, structural and kinetic studies of a number of 2OG oxygenases such as deacetoxycephalosporin C synthase (DAOCS), viral collagen prolyl-4-hydroxylse (vCPH) and taurine deoxygenase (TauD) led to the proposal of a consensus mechanism (Figure 2). [37, 41-43]

A series of spectroscopic transient kinetic studies supported this mechanism, with the exception of the Fe(III)-superoxo species which has thus far not been directly observed for 2OG dependent oxygenases. [37, 38, 44-47] The Fe(IV)-oxo and Fe(III)-OH reaction intermediates (Fig 2, VII and VIII respectively) were observed by combining stopped-flow and rapid quench experiments with spectroscopic characteristics. [37, 38, 48] Upon mixing of the TauD.Fe(II).2OG.taurine complex with O_2 saturated buffer, a strong absorbance feature at a maximum of 318 nm was formed. This species gave way to the formation of the 520 nm absorbance feature decay, corresponding to the loss of the metal-to-ligand charge transfer (MLCT) band of the reactant TauD.Fe(II).2OG.taurine complex. [48] Rapid freeze-quench Mössbauer spectroscopy and cryoreductant electron paramagnetic resonance (EPR) concluded that the 318 nm intermediate was a high-spin Fe(IV) species proposed to participate in 2OG oxygenase catalysis. [38] The second intermediate formed upon the degradation of the 520 nm species, with spectral characteristics assigning an Fe oxidation state of (II). [37, 48] The hydroxylation step of the alkyl substrate is thought to proceed *via* a radical rebound mechanism, whereby a radical substrate species reacts with an Fe(III)-OH complex. [33]

Further kinetic and spectroscopic evidence from vCPH work supported the mechanism proposed for TauD [42] with the halogenases CytC3 and SyrB2 employing the same consensus mechanism. [49, 50] Importantly, these studies illustrated a fast O_2 activation, with the Fe(IV)-oxo intermediate formation times around 10 – 100 ms. This is important in the context of PHD2 (one of three PHD isoforms involved in HIF modulation) as the formation of its Fe(IV)-oxo intermediate was not observed in stopped-flow experiments and the O_2 activated reaction was ~100 fold slower than TauD. [48] When similar kinetic and spectroscopic studies

were conducted on PHD2, it was found that although the Fe(IV)-oxo didn't accumulate, its reaction following addition of O_2 was significantly slower than that of the previously studied enzymes, e.g. rate of product formation (0.0095±0.0012 s^{-1} , [51]). This was found to be the case for all substrates of PHD2 (HIF 1/2alpha, NODD/CODD, including with long substrates). It was proposed that this slow reaction with oxygen is connected to its role as an oxygen sensor.

The HIF-hydroxylases

Sequence alignment of the *C*-terminally located catalytic domains of the three PHD isoforms show that the enzymes exhibit sequence homology, and possess typical structures shared by other 2OG oxygenases (DBSH fold and HXD/E…H facial triad, [52, 53]). The *N*-termini of the PHDs, however, differ significantly. The PHD1 *N*-terminus is predicted to be disordered; PHD3 does not have an extended *N*-terminus, whilst the *N*-terminus of PHD2 contains a MYND-type zinc finger domain. This domain is thought to be conserved in at least one of the PHDs in all animals. [54] Further to this, PHD2 is expressed ubiquitously throughout the body, the suppression of which results in embryonic fatalities in mice. [55, 56] PHD1 and PHD3, however, are found predominately in the testes and heart respectively, [57, 58] with mice in knockout studies of both PHD1 and PHD3 reaching adulthood. [59] Together with mRNA expression patterns and structural and kinetic analyses of PHD2, these data indicate that PHD2 is the most important of the three PHD isoforms in normoxia. [56]

As the HIF-hydroxylase enzymes are Fe(II)/2OG dependent oxygenases, it is suggested that they employ the same consensus hydroxylation mechanism (Figure 2). [53, 60] However, unlike other 2OG oxygenases, the PHDs are also known to act as O_2 sensors, based on their low-affinity for O_2. [61] PHDs 1 and 3 are reported to have high K_m values for O_2 of ~250 μM, [62, 63]

while a K_m values for O_2 have been reported to be between 250 µM and 1.7 mM for PHD2. [52, 62-66] By comparison, FIH has a significantly lower K_m for O_2 of ~100 µM, [62, 66], taurine dioxygenase (TauD) has a $K_m(O_2)$ value of ~76 µM and mature phytanoyl-CoA hydroxylase (mPAHX) has a $K_m(O_2) \approx 93$ µM. [62]

Figure 3: *Overlay of the crystal structures of PHD 2 with (PDB ID: 3HQR) [1] and without (PDB ID 2G19) [2] substrate in grey and blue respectively. The pink region denotes the β2β3 loop region of interest folded over locking the substrate in place. The C-terminal oxygen dependent domain of HIF (CODD) substrate is depicted here in* ***black****.*

A series of crystal structures of PHD2, both in the presence [1] and absence [53] of bound HIF-1α CODD 19mer substrate, illustrate a mobile loop region connecting β loops 2 and 3. Binding of substrate to PHD2 is accompanied by a change in β2β3 loop conformation, enclosing the substrate (Fig 3). [1] This β2β3 loop region has been connected with substrate recognition, [52] and has the potential to alter PHD2 kinetics with respect to O_2 (as reported here). PHD2 exhibits unusually slow activation with respect to O_2 compared to other 2OG oxygenases – a feature that, together with its unusually high K_m value for O_2, has been linked to its O_2 sensing function in cells. [67]

Identifying the features responsible for PHD2's slow reaction with O_2 has recently been the subject of increased scientific attention. Tarhonskaya *et al* reported on the kinetics of a

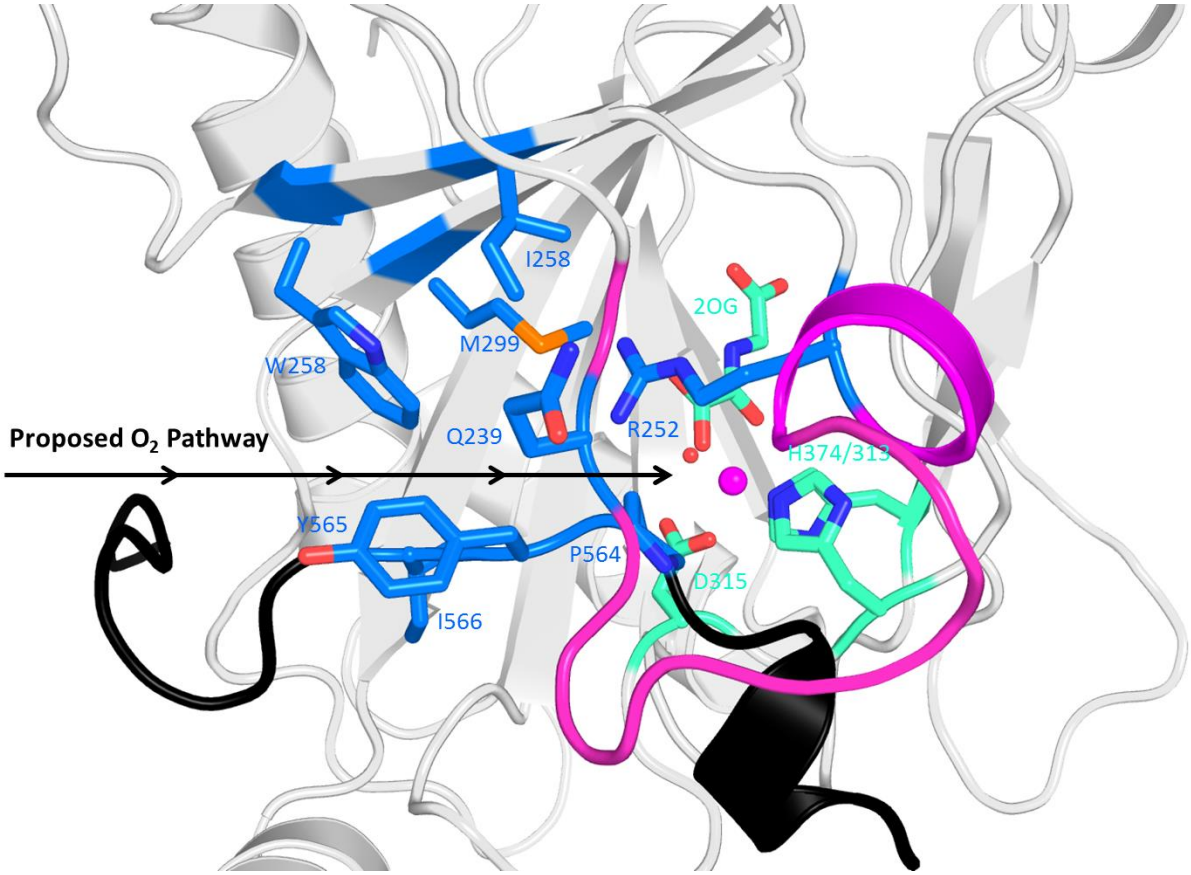

Figure 4: *The proposed O_2 pathway in PHD2, with the interacting residues in the proposed E-cluster shown in **blue**, the β2β3 loop in **pink**, CODD substrate in **black** and the PHD2 in **grey**. The Mn(II) at the active site is depicted here in **purple**, coordinated by the HXD…H triad in **green**. PDB ID: 3HQR* [1]

variant of PHD2, in which the aspartate of the HXD/E…H catalytic triad was substituted with a glutamate residue. [51] Although the rate of reaction with O_2 was increased relative to wild type (WT) enzyme, this was attributed to a weakened interaction with Fe(II) and/or the final Fe(II)-coordinating H_2O molecule. The change observed in the O_2 kinetics were insignificant with respect to other, more efficient 2OG oxygenases, [51] illustrating that the underlying mechanisms by which PHD2 acts as an O_2 sensor remain undefined.

Thesis objectives

While research to date sufficiently confirms the 2OG oxygenase consensus mechanism, it is still unclear as to how PHD2, in particular, behaves in the presence of O_2. Certain structural features such the catalytic triad and the β2β3 loop have been connected to PHD2 activity

and substrate selection, but the exact mechanism by which PHD2 reacts slowly with O_2 remains undetermined. Molecular dynamic simulations were recently conducted by our collaborators, Jorgensen *et al* (unpublished) to probe for O_2 entry pathways into PHD2 in order to determine whether the rate limiting step with respect to the reaction with O_2 is in O_2 delivery to the active site, or O_2 activation at the active site. Interestingly, these studies revealed a single potential O_2 pathway to PHD2's active site which includes a "pocket" in which O_2 is proposed to interact non-covalently prior to active site entry – termed the "E-cluster" (Fig 4). This is interesting in light of the results revealing TauD, a member of the same 2OG/Fe(II) dependent family, to have multiple potential O_2 uptake pathways (Jorgensen *et al*, unpublished). There is a barrier to activation moving from this stabilizing pocket to the active site – providing a hypothesis by which the slow kinetics of PHD2 could be rationalised. As both the proposed E-cluster and O_2 pathway form at the interface between HIF substrate (19-mer-CODD) and the flexible, substrate-binding loop in PHD2 (β2β3), this further supports the hypothesis that the β2β3 loop is connected to PHD kinetic activity. Specifying the underlying features that enable PHD2's unusual kinetic behaviour could elucidate the structural and mechanistic basis of O_2 sensing and provide a platform upon which new therapeutics could be designed.

The aims of this thesis are:

1) To kinetically characterise PHD2 β2β3 loop variants to elucidate whether or not the loop can affect PHD2's behaviour with respect to O_2;
2) To validate PHD2's proposed O_2 uptake pathway *via* intrinsic tryptophan fluorescence of a PHD2 tryptophan variant;

3) To build on modelling studies conducted by Jorgensen *et al* (unpublished), experimentally verifying the proposed E-cluster. This is to be carried-out using singlet state O_2;

4) To kinetically characterise PHD2 in the presence of a proposed activating peptide, 3C, to understand if hydroxylation of the CODD substrate is increased in the presence of 3C.

References

1. R. Chowdhury, M. A. McDonough, J. Mecinovic, C. Loenarz, E. Flashman, K. S. Hewitson, C. Domene and C. J. Schofield, *Structure*, 2009, **17**, 981-989.
2. I. J. Clifton, M. A. McDonough, D. Ehrismann, N. J. Kershaw, N. Granatino and C. J. Schofield, *J Inorg Biochem*, 2006, **100**, 644-669.
3. F. J. Giordano, *Arteriosclerosis, Thrombosis, and Vascular Biology*, 2010, **30**, 641-642.
4. B. P., *C R Acad Sci Paris* 1882, **94**, 805–807.
5. L. E. Huang and H. F. Bunn, *J Biol Chem*, 2003, **278**, 19575-19578.
6. P. J. Ratcliffe, *Blood purification*, 2002, **20**, 445-450.
7. N. V. Iyer, L. E. Kotch, F. Agani, S. W. Leung, E. Laughner, R. H. Wenger, M. Gassmann, J. D. Gearhart, A. M. Lawler, A. Y. Yu and G. L. Semenza, *Genes & Development*, 1998, **12**, 149-162.
8. K. S. Hewitson and C. J. Schofield, *Drug Discov Today*, 2004, **9**, 704-711.
9. P. Carmeliet, Y. Dor, J. M. Herbert, D. Fukumura, K. Brusselmans, M. Dewerchin, M. Neeman, F. Bono, R. Abramovitch, P. Maxwell, C. J. Koch, P. Ratcliffe, L. Moons, R. K. Jain, D. Collen and E. Keshert, *Nature*, 1998, **394**, 485-490.
10. B. Keith, R. S. Johnson and M. C. Simon, *Nature reviews. Cancer*, 2012, **12**, 9-22.
11. K. Kondo, W. Y. Kim, M. Lechpammer and W. G. Kaelin, Jr., *PLoS biology*, 2003, **1**, E83.
12. J. K. Maranchie, J. R. Vasselli, J. Riss, J. S. Bonifacino, W. M. Linehan and R. D. Klausner, *Cancer cell*, 2002, **1**, 247-255.
13. J. Mazumdar, M. M. Hickey, D. K. Pant, A. C. Durham, A. Sweet-Cordero, A. Vachani, T. Jacks, L. A. Chodosh, J. L. Kissil, M. C. Simon and B. Keith, *Proc Natl Acad Sci U S A*, 2010, **107**, 14182-14187.
14. T. Acker, A. Diez-Juan, J. Aragones, M. Tjwa, K. Brusselmans, L. Moons, D. Fukumura, M. P. Moreno-Murciano, J. M. Herbert, A. Burger, J. Riedel, G. Elvert, I. Flamme, P. H. Maxwell, D. Collen, M. Dewerchin, R. K. Jain, K. H. Plate and P. Carmeliet, *Cancer cell*, 2005, **8**, 131-141.
15. G. L. Wang, B. H. Jiang, E. A. Rue and G. L. Semenza, *Proc Natl Acad Sci U S A*, 1995, **92**, 5510-5514.
16. R. K. Bruick and S. L. McKnight, *Science*, 2001, **294**, 1337-1340.
17. D. Lando, D. J. Peet, D. A. Whelan, J. J. Gorman and M. L. Whitelaw, *Science*, 2002, **295**, 858-861.

18. S. Salceda and J. Caro, *Journal of Biological Chemistry*, 1997, **272**, 22642-22647.
19. L. E. Huang, J. Gu, M. Schau and H. F. Bunn, *Proc. Natl. Acad. Sci. U. S. A.*, 1998, **95**, 7987-7992.
20. M. S. Wiesener, H. Turley, W. E. Allen, C. Willam, K. U. Eckardt, K. L. Talks, S. M. Wood, K. C. Gatter, A. L. Harris, C. W. Pugh, P. J. Ratcliffe and P. H. Maxwell, *Blood*, 1998, **92**, 2260-2268.
21. N. Masson, C. Willam, P. H. Maxwell, C. W. Pugh and P. J. Ratcliffe, *Embo Journal*, 2001, **20**, 5197-5206.
22. M. Ivan, K. Kondo, H. Yang, W. Kim, J. Valiando, M. Ohh, A. Salic, J. M. Asara, W. S. Lane and W. G. Kaelin, Jr., *Science (Washington, DC, U. S.)*, 2001, **292**, 464-468.
23. P. Jaakkola, D. R. Mole, Y. M. Tian, M. I. Wilson, J. Gielbert, S. J. Gaskell, A. von Kriegsheim, H. F. Hebestreit, M. Mukherji, C. J. Schofield, P. H. Maxwell, C. W. Pugh and P. J. Ratcliffe, *Science*, 2001, **292**, 468-472.
24. A. C. R. Epstein, J. M. Gleadle, L. A. McNeill, K. S. Hewitson, J. O'Rourke, D. R. Mole, M. Mukherji, E. Metzen, M. I. Wilson, A. Dhanda, Y. M. Tian, N. Masson, D. L. Hamilton, P. Jaakkola, R. Barstead, J. Hodgkin, P. H. Maxwell, C. W. Pugh, C. J. Schofield and P. J. Ratcliffe, *Cell*, 2001, **107**, 43-54.
25. D. A. Chan, P. D. Sutphin, S. E. Yen and A. J. Giaccia, *Mol Cell Biol*, 2005, **25**, 6415-6426.
26. D. Ehrismann, E. Flashman, D. N. Genn, N. Mathioudakis, K. S. Hewitson, P. J. Ratcliffe and C. J. Schofield, *The Biochemical journal*, 2007, **401**, 227-234.
27. E. Flashman, E. A. L. Bagg, R. Chowdhury, J. Mecinovic, C. Loenarz, M. A. McDonough, K. S. Hewitson and C. J. Schofield, *The Journal of biological chemistry*, 2008, **283**, 3808-3815.
28. M. Hirsila, P. Koivunen, V. Gunzler, K. I. Kivirikko and J. Myllyharju, *The Journal of biological chemistry*, 2003, **278**, 30772-30780.
29. P. Koivunen, M. Hirsila, K. I. Kivirikko and J. Myllyharju, *The Journal of biological chemistry*, 2006, **281**, 28712-28720.
30. W. C. Hon, M. I. Wilson, K. Harlos, T. D. Claridge, C. J. Schofield, C. W. Pugh, P. H. Maxwell, P. J. Ratcliffe, D. I. Stuart and E. Y. Jones, *Nature*, 2002, **417**, 975-978.
31. S. J. Freedman, Z. Y. Sun, F. Poy, A. L. Kung, D. M. Livingston, G. Wagner and M. J. Eck, *Proc Natl Acad Sci U S A*, 2002, **99**, 5367-5372.
32. S. A. Dames, M. Martinez-Yamout, R. N. De Guzman, H. J. Dyson and P. E. Wright, *Proc Natl Acad Sci U S A*, 2002, **99**, 5271-5276.
33. R. P. Hausinger, *Crit Rev Biochem Mol*, 2004, **39**, 21-68.
34. C. Loenarz and C. J. Schofield, *Trends in biochemical sciences*, 2011, **36**, 7-18.
35. J. J. Hutton, Jr., A. Kaplan and S. Udenfriend, *Archives of biochemistry and biophysics*, 1967, **121**, 384-391.
36. L. J. Walport, R. J. Hopkinson and C. J. Schofield, *Current opinion in chemical biology*, 2012, **16**, 525-534.
37. J. C. Price, E. W. Barr, L. M. Hoffart, C. Krebs and J. M. Bollinger, *Biochemistry-Us*, 2005, **44**, 8138-8147.
38. J. M. Bollinger, J. C. Price, L. M. Hoffart, E. W. Barr and C. Krebs, *European Journal of Inorganic Chemistry*, 2005, **2005**, 4245-4254.
39. W. Aik, M. A. McDonough, A. Thalhammer, R. Chowdhury and C. J. Schofield, *Current opinion in structural biology*, 2012, **22**, 691-700.

40. K. D. Koehntop, J. P. Emerson and L. Que, Jr., *Journal of biological inorganic chemistry : JBIC : a publication of the Society of Biological Inorganic Chemistry*, 2005, **10**, 87-93.
41. J. E. Baldwin, R. M. Adlington, R. T. Aplin, N. P. Crouch, G. Knight and C. J. Schofield, *J Chem Soc Chem Comm*, 1987, 1651-1654.
42. L. M. Hoffart, E. W. Barr, R. B. Guyer, J. M. Bollinger and C. Krebs, *P Natl Acad Sci USA*, 2006, **103**, 14738-14743.
43. C. J. Schofield and Z. Zhang, *Current opinion in structural biology*, 1999, **9**, 722-731.
44. D. M. Arciero, A. M. Orville and J. D. Lipscomb, *J Biol Chem*, 1985, **260**, 4035-4044.
45. V. J. Chen, A. M. Orville, M. R. Harpel, C. A. Frolik, K. K. Surerus, E. Munck and J. D. Lipscomb, *J Biol Chem*, 1989, **264**, 21677-21681.
46. K. Pohl, K. Wieghardt, B. Nuber and J. Weiss, *J Chem Soc Dalton*, 1987, 187-192.
47. G. Schenk, M. Y. M. Pau and E. I. Solomon, *Journal of the American Chemical Society*, 2004, **126**, 505-515.
48. J. C. Price, E. W. Barr, B. Tirupati, J. M. Bollinger and C. Krebs, *Biochemistry-Us*, 2003, **42**, 7497-7508.
49. M. L. Matthews, C. M. Krest, E. W. Barr, F. H. Vaillancourt, C. T. Walsh, M. T. Green, C. Krebs and J. M. Bollinger, *Biochemistry-Us*, 2009, **48**, 4331-4343.
50. D. P. Galonic, E. W. Barr, C. T. Walsh, J. M. Bollinger and C. Krebs, *Nat Chem Biol*, 2007, **3**, 113-116.
51. H. Tarhonskaya, R. Chowdhury, I. K. H. Leung, N. D. Loik, J. S. O. McCullagh, T. D. W. Claridge, C. J. Schofield and E. Flashman, *Biochem J*, 2014, **463**, 363-372.
52. E. Flashman, E. A. L. Bagg, R. Chowdhury, J. Mecinovic, C. Loenarz, M. A. McDonough, K. S. Hewitson and C. J. Schofield, *J Biol Chem*, 2008, **283**, 3808-3815.
53. M. A. McDonough, V. Li, E. Flashman, R. Chowdhury, C. Mohr, B. M. R. Lienard, J. Zondlo, N. J. Oldham, I. J. Clifton, J. Lewis, L. A. McNeill, R. J. M. Kurzeja, K. S. Hewitson, E. Yang, S. Jordan, R. S. Syed and C. J. Schofield, *P Natl Acad Sci USA*, 2006, **103**, 9814-9819.
54. C. Loenarz, M. L. Coleman, A. Boleininger, B. Schierwater, P. W. Holland, P. J. Ratcliffe and C. J. Schofield, *EMBO Rep*, 2011, **12**, 63-70.
55. K. Takeda, V. C. Ho, H. Takeda, L. J. Duan, A. Nagy and G. H. Fong, *Mol Cell Biol*, 2006, **26**, 8336-8346.
56. E. Berra, E. Benizri, A. Ginouves, V. Volmat, D. Roux and J. Pouyssegur, *Embo J*, 2003, **22**, 4082-4090.
57. C. L. Cioffi, X. Q. Liu, P. A. Kosinski, M. Garay and B. R. Bowen, *Biochem Bioph Res Co*, 2003, **303**, 947-953.
58. M. E. Lieb, K. Menzies, M. C. Moschella, R. J. Ni and M. B. Taubman, *Biochem Cell Biol*, 2002, **80**, 421-426.
59. J. Myllyharju, *Acta Physiologica*, 2013, **208**, 148-165.
60. K. S. Hewitson, L. A. McNeill, M. V. Riordan, Y.-M. Tian, A. N. Bullock, R. W. Welford, J. M. Elkins, N. J. Oldham, S. Bhattacharya, J. M. Gleadle, P. J. Ratcliffe, C. W. Pugh and C. J. Schofield, *J Biol Chem*, 2002, **277**, 26351-26355.
61. J. Aragones, P. Fraisl, M. Baes and P. Carmeliet, *Cell Metab*, 2009, **9**, 11-22.
62. D. Ehrismann, E. Flashman, D. N. Genn, N. Mathioudakis, K. S. Hewitson, P. J. Ratcliffe and C. J. Schofield, *Biochem J*, 2007, **401**, 227-234.
63. M. Hirsilä, P. Koivunen, V. Günzler, K. I. Kivirikko and J. Myllyharju, *J Biol Chem*, 2003, **278**, 30772-30780.

64. J. H. Dao, R. J. M. Kurzeja, J. M. Morachis, H. Veith, J. Lewis, V. Yu, C. M. Tegley and P. Tagari, *Anal Biochem*, 2009, **384**, 213-223.
65. J. R. Tuckerman, Y. G. Zhao, K. S. Hewitson, Y. M. Tian, C. W. Pugh, P. J. Ratcliffe and D. R. Mole, *Febs Lett*, 2004, **576**, 145-150.
66. P. Koivunen, M. Hirsila, V. Gunzler, K. I. Kivirikko and J. Myllyharju, *J Biol Chem*, 2004, **279**, 9899-9904.
67. E. Flashman, L. M. Hoffart, R. B. Hamed, J. M. Bollinger, C. Krebs and C. J. Schofield, *Febs J*, 2010, **277**, 4089-4099.

Chapter 2: Protein expression, purification and characterisation

2.1 Introduction

This Chapter describes the detailed processes by which PHD2 WT and four PHD2 variants, namely; PHD2.1, PHD2.3, PHD2 W334F/W367F and PHD2 M299H were expressed, purified and subsequently characterised for further use in the experiments conducted in this thesis. Preliminary investigations of their activity are shown, alongside purification and characterisation data.

2.2 Results and Discussion

2.2.1 Expression, purification and characterisation of PHD2 WT

The DNA sequence encoding $PHD2_{181\text{-}426}$ had previously been ligated into the pET-24a vector (Novagen). [1] PHD2 WT was expressed in *Escherichia coli (E.coli)* BL21(DE3) cells at 18 °C, overnight after IPTG induction (IPTG added after an optical density, OD_{600}, of 1.2 was reached). The clarified PHD2 lysate was purified via S Sepharose 50 mL (SSEPH50), cation exchange chromatography (Fig 1, A, see Materials and Methods). SSEPH50 purified fractions 12-17 were seen to contain protein of the correct mass (~27 kDa) according to the MW marker (Fig 1, A and C), corresponding to eluted fractions with the highest absorbance at 280 nm. PHD2 is known to co-purify with Fe(II) at the active site [2] which must be removed to generate homogenous apo-PHD2 such that stoichiometric levels of Fe(II) could be subsequently added. As such, the eluted fractions were concentrated to >50 mg/mL before being diluted to 1 mg/mL in a 2:3 ratio of 0.5 mM EDTA and 20 mM ammonium acetate to facilitate bound Fe(II) removal.

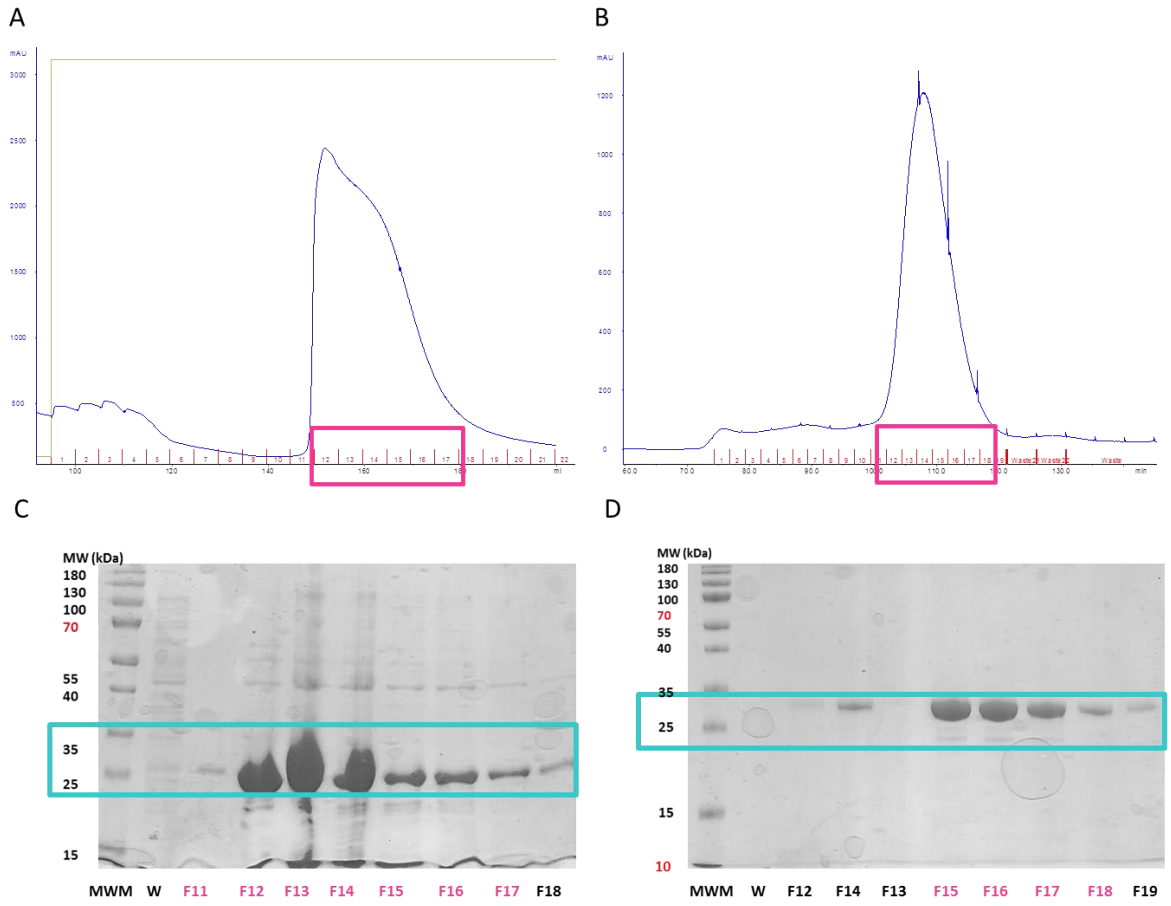

Figure 1: *Purification of PHD2 WT showing; A) the SSEPH50 elution profile B) the S75300 size exclusion elution profile, with the UV trace in* ***blue*** *and fractions of interest highlighted in* ***red*** *for both; C) an SDS-PAGE gel showing the contents of the fractions eluted from the SSEPH50 column and D) from the S75300 with the protein at 27 kDa highlighted. The protein-containing fractions are highlighted in* ***pink*** *on both the chromatogram trace (A and B) and the SDS-PAGE gels (C and D).*

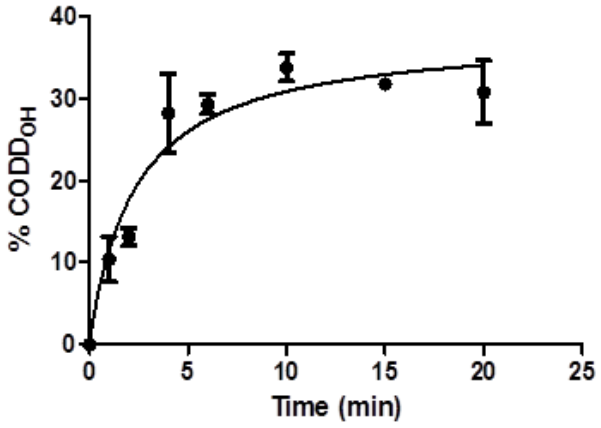

Figure 2: *Time course assay for PHD2 WT under the conditions; 100 µM CODD, 50 µM Fe(II), 4 mM L-ascorbate, 300 µM 2OG and 4 µM enzyme at 37 °C, n = 3. Error bars represent standard deviation.*

After incubation overnight with EDTA, the protein was concentrated to ~2 mL to enable loading onto an S75 300 mL size exclusion column (Fig 1, B). The resulting fractions believed to contain protein from the S75300 purification chromatogram were analysed by 12% acrylamide sodium dodecylsulfate-polyacrylamide gel

electrophoresis (SDS-PAGE) to ensure the fractions of interest contained protein and to confirm the protein's mass of 27 kDa. (Fig 1, C and D) The SDS-PAGE gels confirm the presence of protein of the correct mass (Fig 1, D) in fractions 15-18. These fractions were buffer exchanged into 50 mM Tris/HCl, pH 7.5 then concentrated to ~1 mM. Aliquots were stored at -80 °C. Liquid chromatography mass spectrometry (LC-MS) of purified PHD2 confirmed the expected 27643.3 kDa mass for PHD2 to within 4 Da (Fig 3). The expression yielded 11 mg/L of purified apoenzyme.

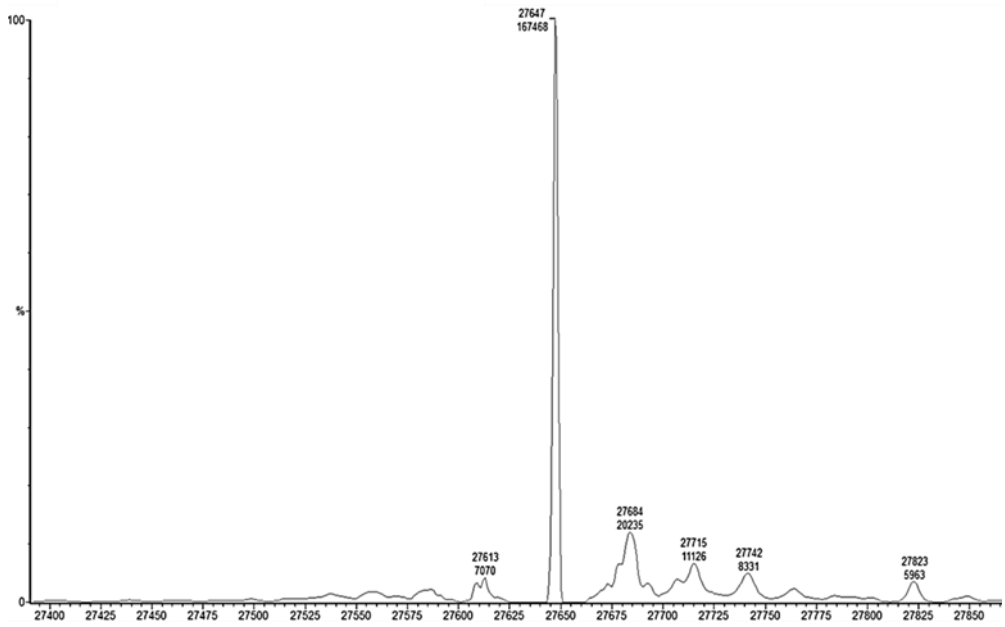

Figure 3: *LCMS spectrum for PHD2 WT, depicting a MW of 27647 Da (expected 27643 Da)*

To test purified enzyme activity, time-course assays using the HIF-1$\alpha_{556\text{-}574}$ CODD 19-mer substrate, sequence DLDLEMLAPYIPMDDDFQL were performed. The assay conditions included: 50 µM Fe(II), 300 µM 2OG, 100 µM CODD and 4 mM sodium ascorbate, incubated with 4 µM of PHD2 at 37 °C. Aliquots of the assay were quenched in 1% formic acid, followed by vortexing and snap-freezing in liquid nitrogen. These conditions are analogous to those performed previously by Flashman [3, 4] and Tarhonskaya *et al*. [5, 6] Matrix Assisted

Laser Desorption Ionisation Time-of-Flight Mass Spectrometry (MALDI-TOF-MS) was used to determine the extent of CODD hydroxylation at each time point. PHD2 WT activity was confirmed (Fig 2).

2.2.2 Expression, purification and characterisation of PHD2.1

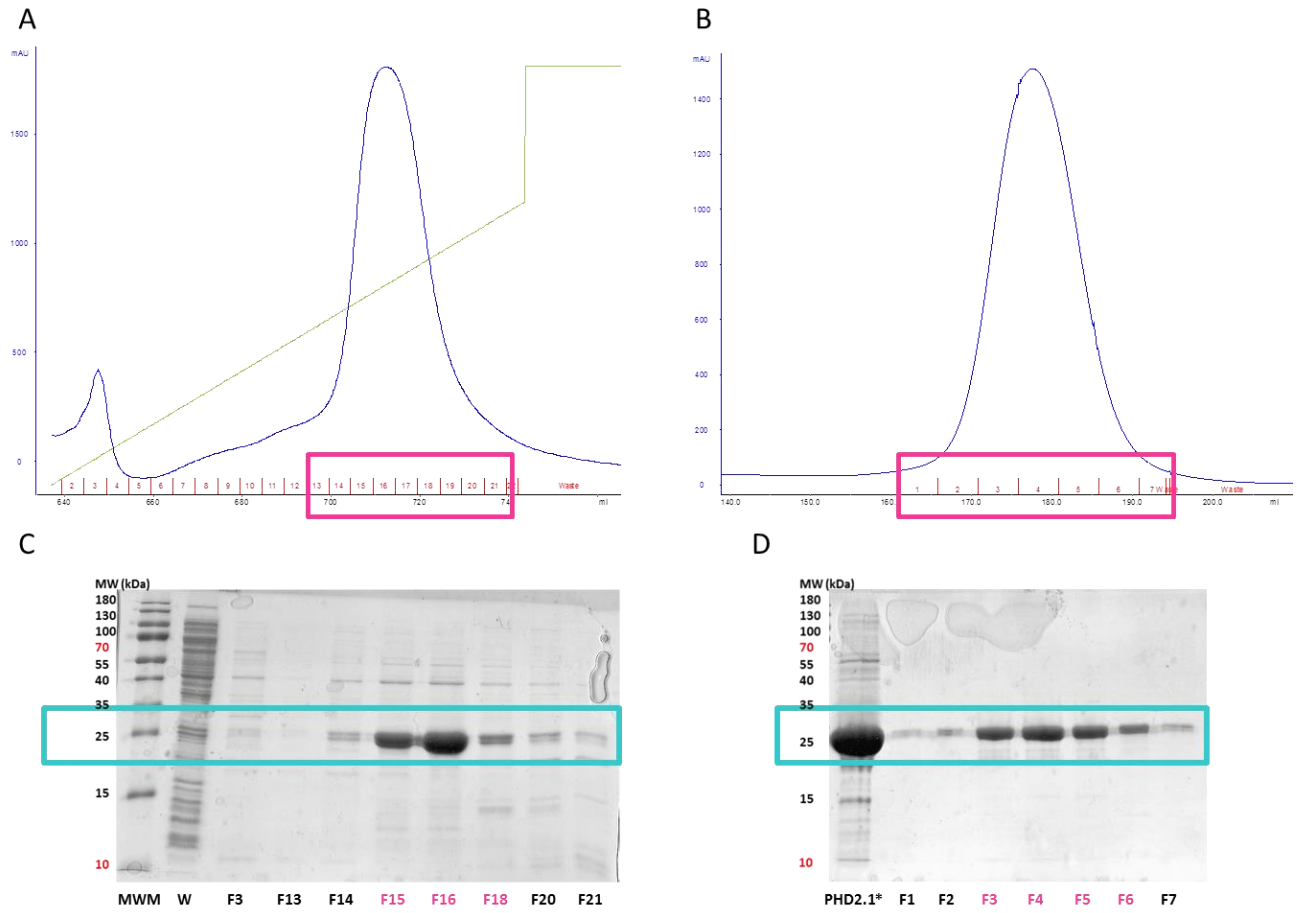

Figure 4: *Purification of PHD2.1 showing; A) the SSEPH50 elution profile B) the S75300 size exclusion elution profile, with the UV trace in* ***blue*** *and fractions of interest highlighted in* ***red*** *for both; C) an SDS-PAGE gel showing the contents of the fractions eluted from the SSEPH50 column and D) from the S75300 with the protein at 27 kDa highlighted. The protein-containing fractions are highlighted in* ***pink*** *on both the chromatogram trace (A and B) and the SDS-PAGE gels (C and D).*

PHD2.1 and PHD2.3 chimeras were generated previously by Dr Emily Flashman [3] whereby the β2β3 loop (residues 238 – 250) of the $PHD2_{181-426}$ catalytic domain was replaced with that of either PHD1 or PHD3 (termed PHD2.1 and PHD2.3 respectively). [3] PHD2.1 was expressed and purified using the same conditions as for PHD2, save for expression, which

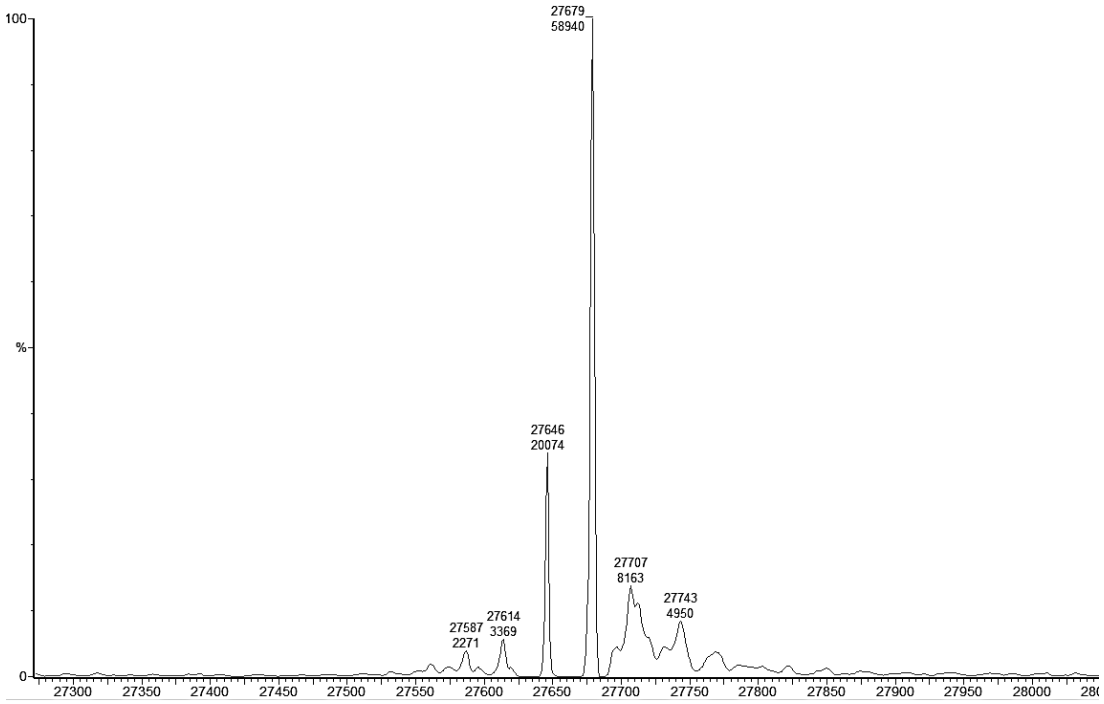

Figure 5: *LCMS spectrum for PHD2.1, depicting a MW of 27679 Da and an unknown impurity at 27646 Da. Expected MW of PHD2.1 (27673 Da)*

was conducted at 37 °C for four hours after induction with IPTG (see detailed procedures outlined in Materials and Methods.). SSEPH50 purified fractions 15-18 were seen to contain protein of the correct MW (Fig 4, A and C). These eluted fractions were concentrated to >50 mg/mL before being diluted to 1mg/mL in a 2:3 ratio of 0.5 mM EDTA and 20 mM ammonium acetate to remove any Fe(II) bound to the enzyme. After incubation overnight with EDTA, the protein was concentrated to ~2 mL to enable loading onto an S75 300 mL size exclusion column (Fig 4, B). Eluted fractions that indicated they contained protein (fractions with the highest absorbance at 280 nm) were collected and run on a 12% SDS-PAGE (Fig 4, D). Fractions 3- 6 were identified on the gel as containing protein of the correct mass. These fractions were buffer exchanged into 50 mM Tris/HCl, pH 7.5 then concentrated to ~1 mM. Aliquots were stored at -80 °C. Liquid chromatography mass spectrometry (LC-MS) of purified PHD2.1 confirmed the expected 27673.5 Da MW of the chimera to within 6 Da (Fig 5). This expression of PHD2.1 yielded 7 mg/L of active enzyme.

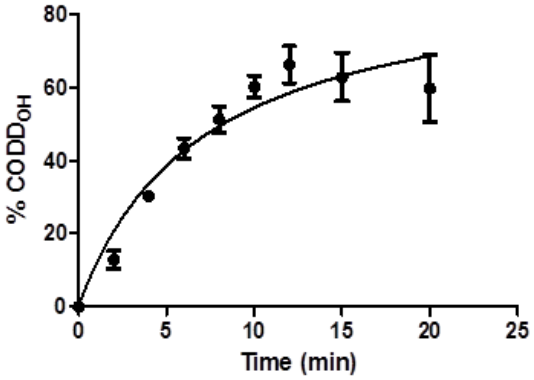

Figure 6: *Time course assay for the PHD2.1 variant under the conditions; 125 µM CODD, 50 µM Fe(II), 4 mM L-ascorbate, 300 µM 2OG and 4 µM enzyme at 37 °C, n = 3. Error bars represent standard deviation.*

To test purified enzyme activity, an assay under the following conditions was conducted; 50 µM Fe(II), 300 µM 2OG, 125 µM CODD and 4 mM sodium ascorbate, incubated with 4 µM of PHD 2.1 at 37 °C, n = 3 with aliquots quenched in 1% formic acid, followed by vortexing and snap-freezing in liquid nitrogen. The results (Fig 6) confirmed PHD2.1's activity, with a similar activity to that which is reported for PHD2 WT (70 – 80% hydroxylation, after 20 minutes, R. Hancock, Part II thesis, Fig 2).

2.2.3 Expression, purification and characterisation of PHD2.3

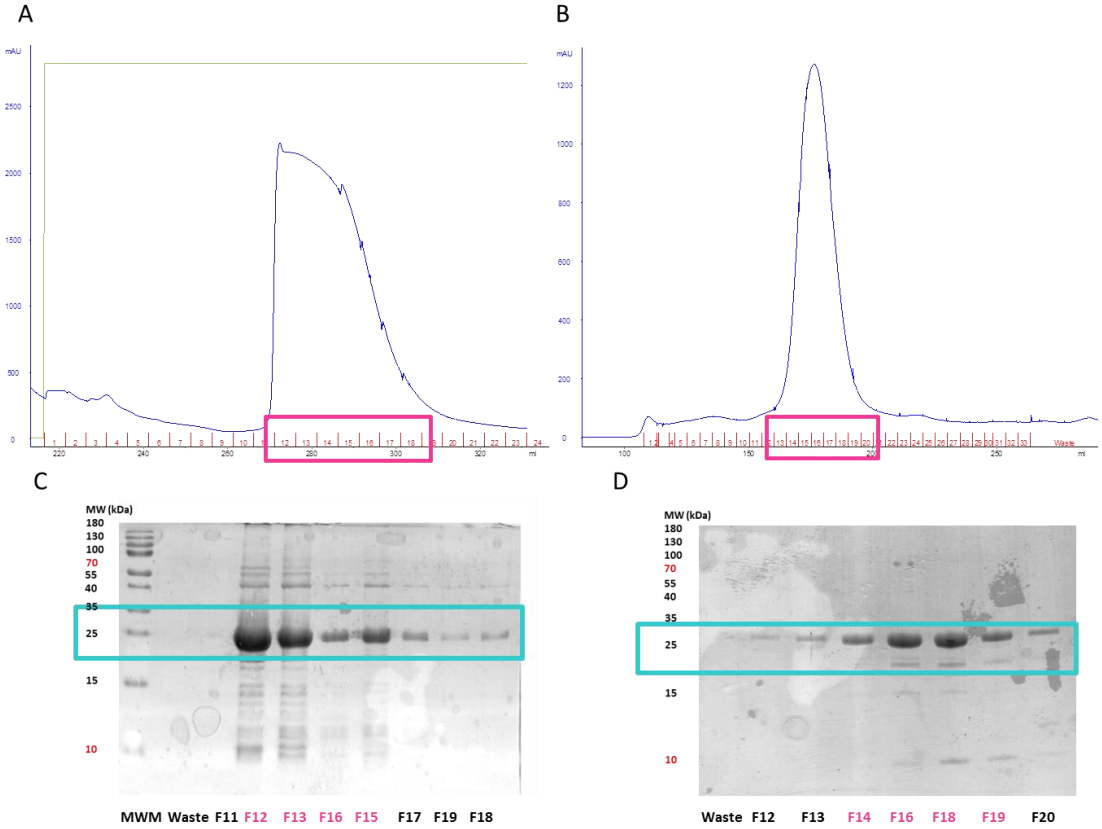

Figure 7: *Purification of PHD2.3 showing; A) the SSEPH50 chromatogram B) the S75300 size exclusion chromatogram, with the UV trace in **blue** and fractions of interest highlighted in **red** for both; C) an SDS-PAGE gel showing the contents of the fractions eluted from the SSEPH50 column and D) from the S75300 with the protein at 27 kDa highlighted. The protein-containing fractions are highlighted in **pink** on both the chromatogram trace (A and B) and the SDS-PAGE gels (C and D).*

PHD2.3 was expressed and purified in the same manner as PHD2.1 (as outlined in Materials and Methods). The SSEPH50 and S75300 chromatograms and SDS-PAGE gels of purified PHD2.3 confirmed the presence of enzyme of the correct MW of 27 kDa (Fig 7). The expression yielded 4 mg/L of purified, active and PHD2.3. LC-MS confirmed the correct expected MW of 27698.6 Da to within 5 Da (Fig 8).

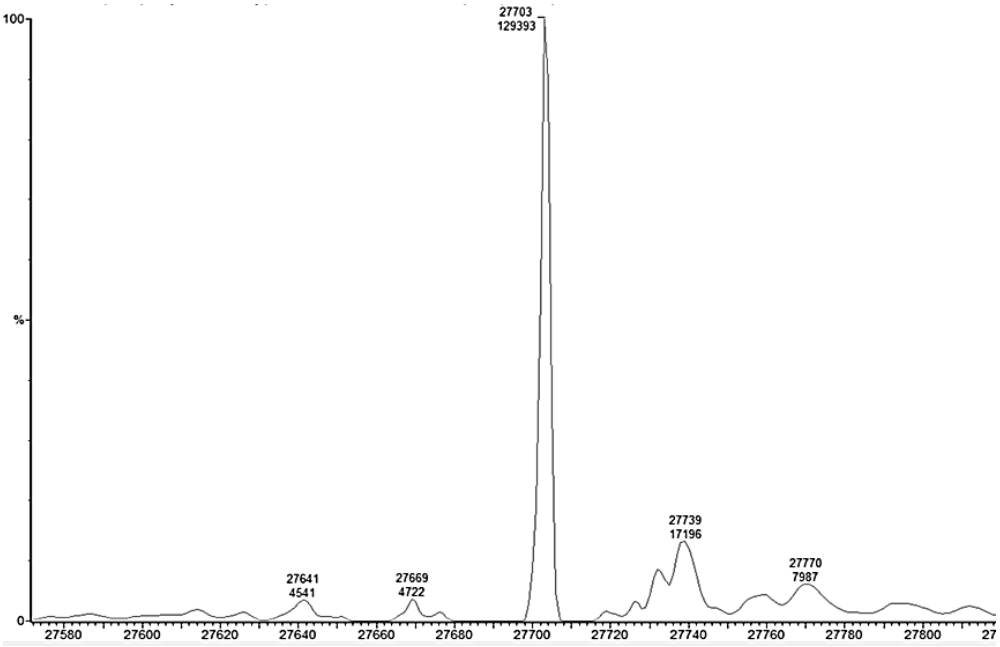

Figure 8: *LCMS spectrum for PHD2.3, depicting a MW of 27703Da (Expected 27698 Da)*

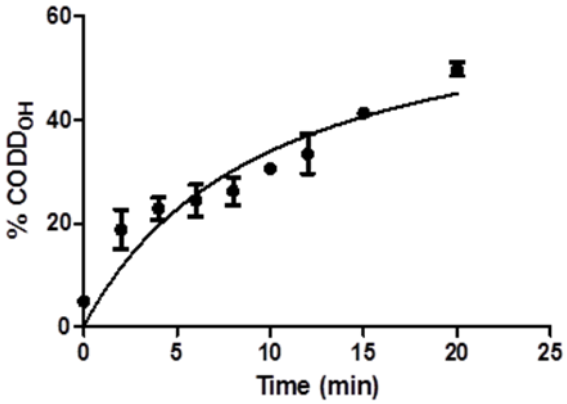

Figure 9: *Time course assay for the PHD2.3 variant under the conditions; 100 µM CODD, 50 µM Fe(II), 4 mM L-ascorbate, 300 µM 2OG and 4 µM enzyme at 37 °C, n = 3. Error bars represent standard deviation.*

An assay under the conditions: 100 µM CODD, 50 µM Fe(II), 4 mM L-ascorbate, 300 µM 2OG and 4 µM PHD2.3 at 37 °C, at n = 3 confirmed PHD2.3 activity, albeit to a slightly lower percentage hydroxylation (50%) than that reported here for PHD2.1.

This could be due to reduced PHD2.3 stability by comparison to PHD2 2.1 and

therefore increased levels of inactive PHD2.3. For example, during pre-steady state studies (and therefore under anaerobic conditions) PHD2.3 appeared less-stable, with considerably more enzyme precipitation observed upon the introduction of Fe(II) than observed for PHD2.1.

2.2.4 Expression, purification and characterisation of PHD2 M299H

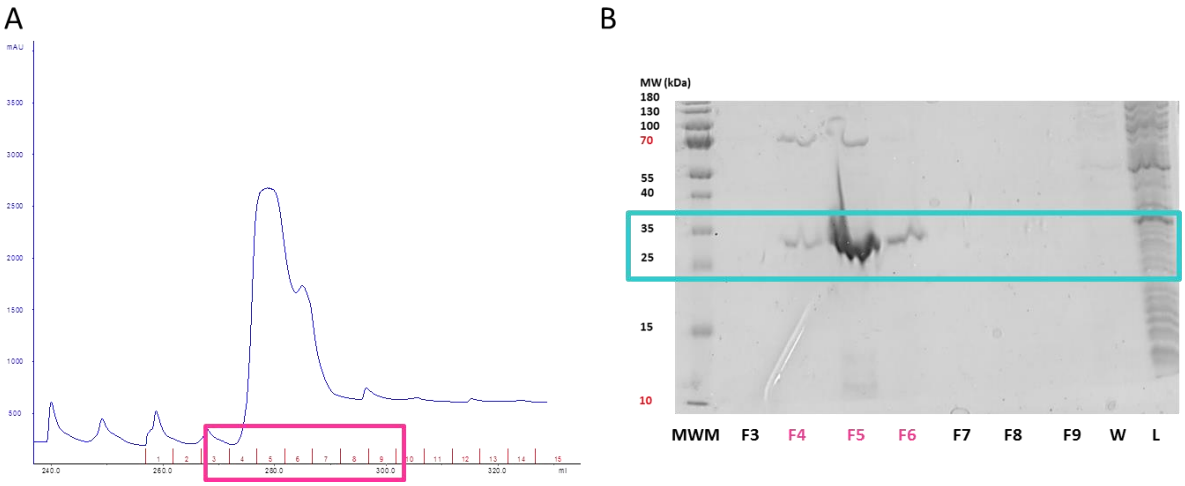

Figure 11: *Purification of the PHD2 M299H variant showing; A) the SSEPH50 chromatogram with the UV trace in **blue** and fraction numbers in **red** and B) an SDS-PAGE gel showing the contents of the fractions eluted from the SSEPH50 column with the 27 kDa MW marker highlighted. The concentrated protein-containing fractions are highlighted in **pink** on both the chromatogram trace (A and B)*

A construct encoding PHD2 M299H had been previously designed by R. Chowdhury using a pET-28a vector, and the plasmid extracted and the sequence verified by E. Bagg (Part II thesis). Note: the pET28a vector has a different N terminus to that of pET24a. The purified and thrombin-cleaved N-terminus of PPHD2 M299H has the added residues, GSHM, due to the additional

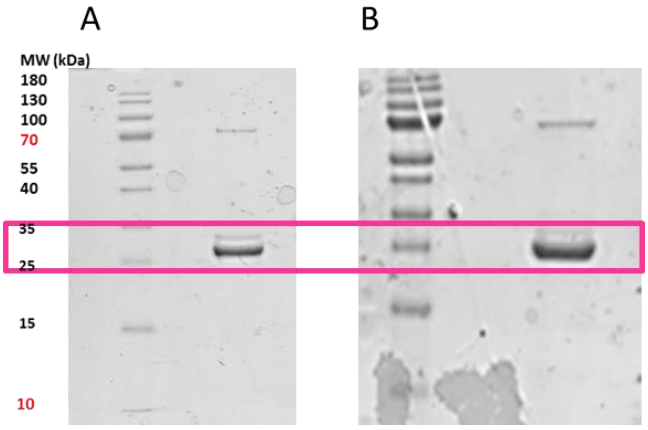

Figure 10: *The SDS-PAGE results for PHD2 M299H A) 12 hrs and B) 18 hrs after incubation with thrombin. The pink band highlights the separate bands with cleaved (28.1 kDa) and un-cleaved (29.9 kDa) His-Tag protein.*

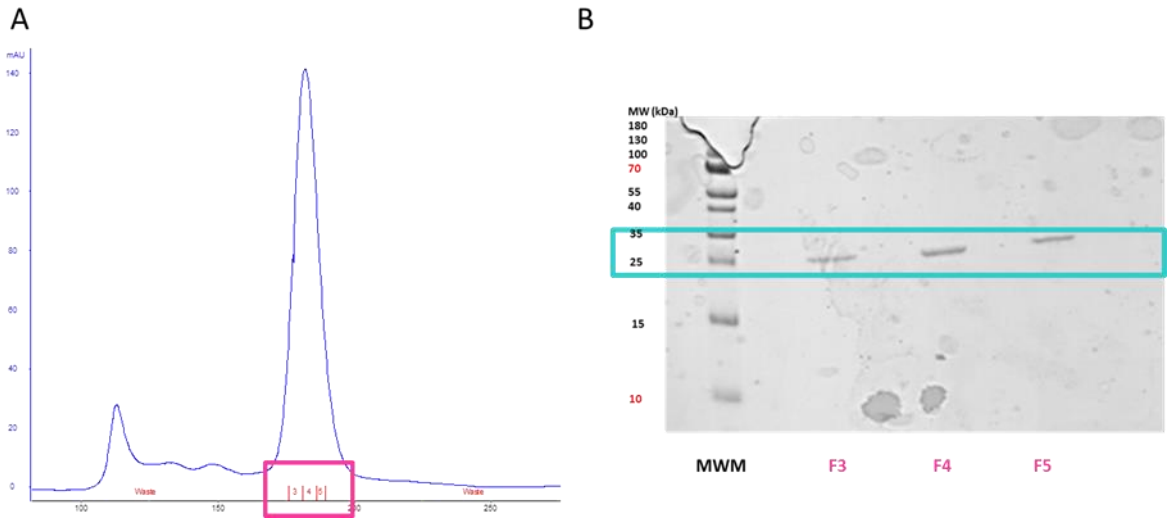

Figure 12: *Purification of the PHD2 M299H variant showing; A) the S75300 chromatogram with the UV trace in **blue** and fraction numbers in **red** and B) an SDS-PAGE gel showing the contents of the fractions eluted from the S75300 column with the 27 kDa MW marker highlighted. The concentrated protein-containing fractions are highlighted in **pink** on both the chromatogram trace (A and B)*

thrombin cleavage site and His-tag synonymous with the pET28a vector.

As the PHD2 M299H primers had been previously designed using a pET-28a vector with a polyhistidine tag, the PHD2M299H clarified lysate was not purified using the S Sepharose 50 mL column, but rather with a HisTrap™ Ni Sepharose™ 5 mL column, which utilizes immobilized Ni(II) affinity chromatography. The purification was carried-out as described in Materials and Methods.

The HisTrap™ purification (Fig 10) was followed by thrombin cleavage to remove the polyhistidine tag (his-tag). This was so as to ensure the protein structure and activity was as comparable to PHD2 WT and its variants as possible for subsequent kinetic analysis. Thrombin cleavage was carried-out as described Materials and Methods. The fractions of interest from the HisTrap™ column (fractions 4-6, Fig 10, B) were incubated in 1 unit of thrombin per mg of PHD2 M299H for a total of 18 hours. Two SDS-PAGE gels were run at 12 and 18 hours to determine the extent of his tag cleavage. The double band of the cleaved (28.1 kDa) and un-cleaved (29.9 kDa) PHD2 M299H is visible (Fig 11). After 18 hours of

incubation it was thought the process had reached equilibrium. The cleaved protein was subsequently diluted in a 2:3 ratio of 0.5 mM EDTA and 20 mM ammonium acetate to facilitate bound Fe(II) removal. The protein was left to incubate for 12 hours in EDTA prior to size exclusion chromatography (Fig 12). The size exclusion purification process only yielded 0.5 mg/L of purified protein due to an unsuspected hardware malfunction on the ÄKTA purification system. LC-MS confirmed the expected MW of 28062 Da for the PHD2 M299H variant to within 3 Da (Fig 13).

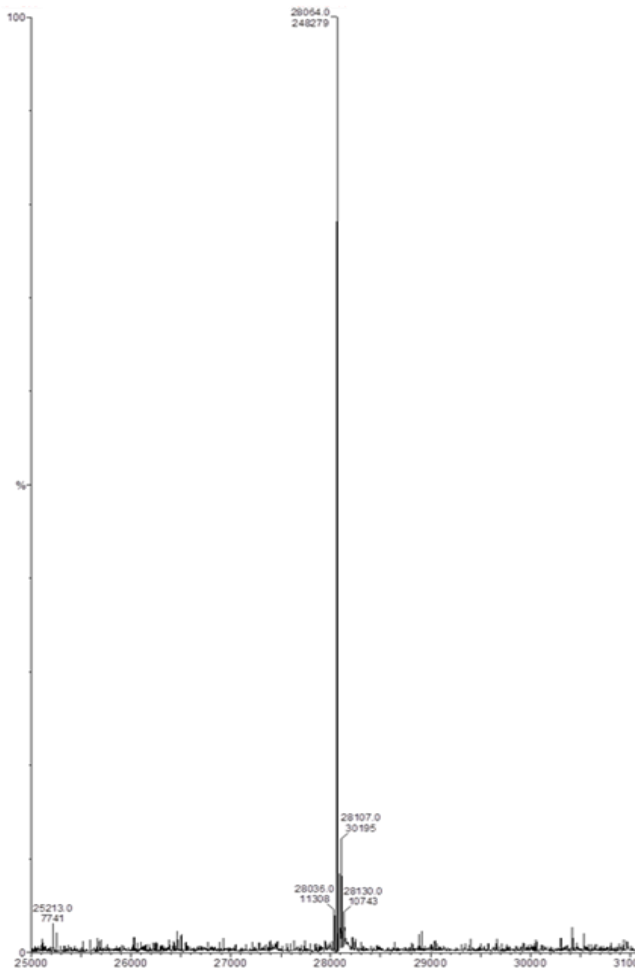

Figure 13: *LCMS spectrum for PHD2 M299H, depicting a MW of 28064 Da (expected 28062 Da)*

An activity assay under the conditions: 50 µM CODD, 50 µM Fe(II), 4 mM L-ascorbate, 300 µM 2OG and 4 µM PHD2 M299H at 37 °C, at n = 3 confirmed enzyme activity (Fig 14).

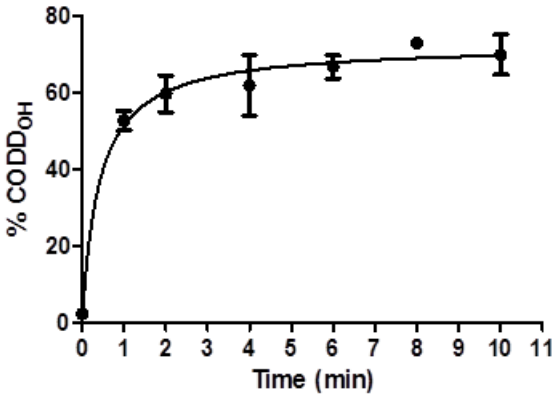

Figure 14: *Time course activity assay for the PHD2 M299H variant under the conditions: 50 µM CODD, 50 µM Fe(II), 4 mM L-ascorbate, 300 µM 2OG and 4 µM enzyme at 37 °C, n = 3*

2.2.5 *Expression, purification and characterisation of PHD2 W334F/W367F*

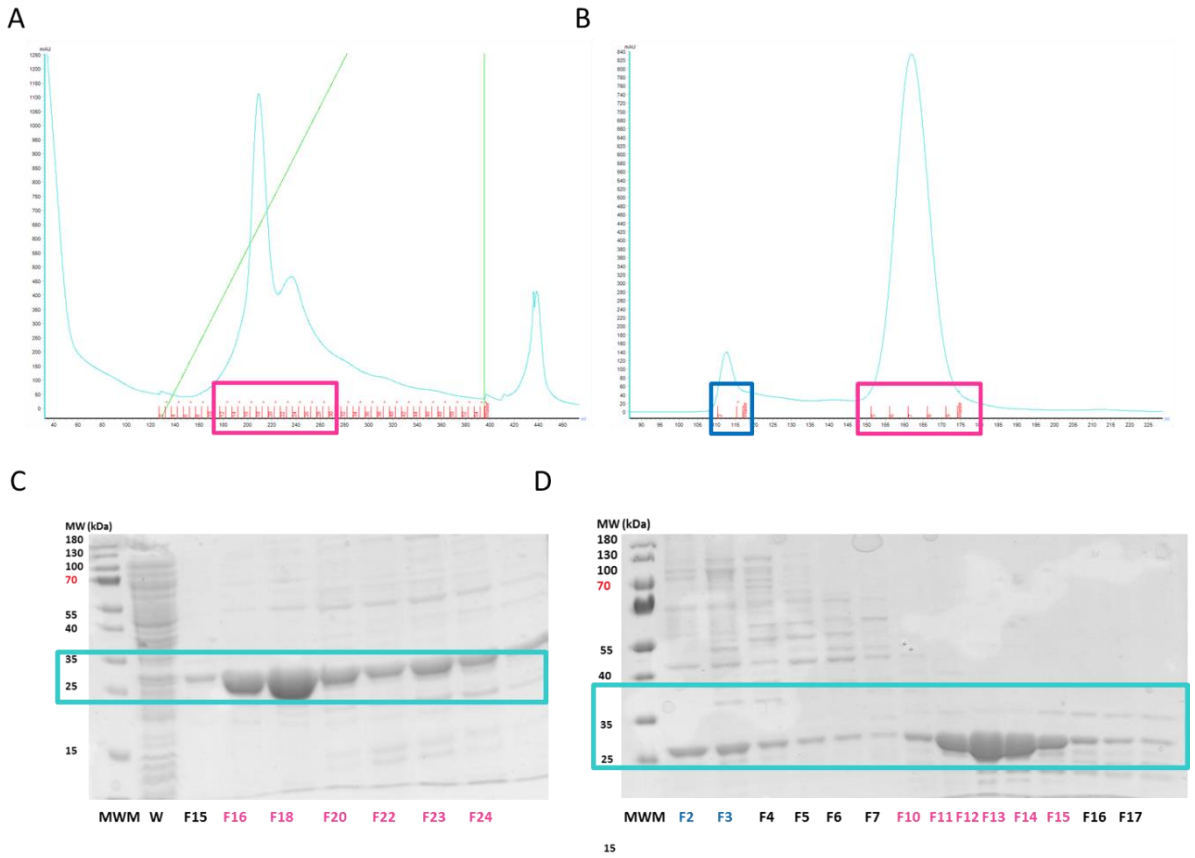

Figure 15: *Purification of PHD2 W334F/W367F showing; A) the SSEPH50 chromatogram B) the S75300 size exclusion chromatogram, with the UV trace in* ***blue,*** *the percentage buffer B gradient in* ***green*** *and fractions of interest highlighted in* ***red*** *for both; C) an SDS-PAGE gel showing the contents of the fractions eluted from the SSEPH50 column and D) from the S75300 with the protein at 27 kDa highlighted. The protein-containing fractions are highlighted in* ***pink*** *on both the chromatogram trace (A and B) and the SDS-PAGE gels (C and D).The fractions highlighted in* ***blue*** *are those of "Peak I" of the S75300 elution profile.*

The pET-24a-PHD2 W334F/W367F plasmid had previously been generated by site directed mutagenesis by R. Hancock (Part II thesis). The PHD2 W334F/W367F variant was expressed and purified using the same methods outlined for PHD2 WT (See Materials and Methods) using both SSEPH 50 cation exchange and S75300 size exclusion chromatography. For both the SSEPH50 and S75300 elution profiles for the PHD2 W334F/W367F two peaks were observed in the elution profiles, resulting in "Peak I" and "Peak II" (Fig 15, A and B). The resulting elution fractions from both peaks were run on SDS-PAGE gels and were found to contain protein of the correct MW (Fig 15, C and D). The fractions from both peaks were

concentrated separately for kinetic analysis. The expression yielded 3 mg/L of purified, active enzyme.

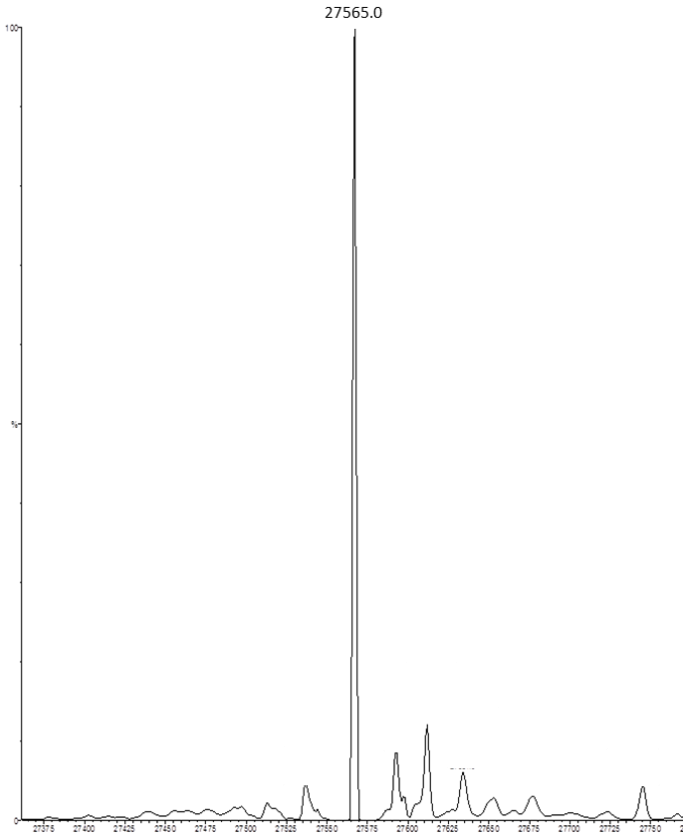

Figure 16: *LCMS spectrum for PHD2 W334F/W367F depicting a MW of 27567Da (Expected 27565Da)*

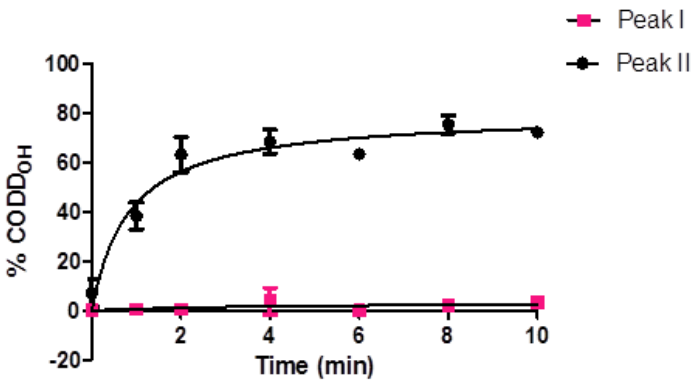

Figure 17: *Time course assay for PHD2 W334F/W367F testing "Peak I" (**black**) and "Peak II" (**pink**) respectively from the S75300 elution profile under the conditions; 100 µM CODD, 50 µM Fe(II), 4 mM L-ascorbate, 300 µM 2OG and 4 µM enzyme at 37 °C, n = 3. Error bars represent standard deviation.*

To test the activity of the purified enzyme, assays were run for both sets of concentrated fractions, from both peaks I and II of the S75300 elution profile. The assay conditions included; 100 µM CODD, 50 µM Fe(II), 4 mM L-ascorbate, 300 µM 2OG and 4 µM enzyme at 37 °C, n = 3. Interestingly, the protein collected from peak I was inactive (Fig 17, **pink** data points) while the protein collected in peak II was active (Fig 17, **black** data points), suggesting the possibility of protein aggregation in peak I. LC-MS confirmed the expected MW of 27565 Da (Fig 16).

2.2.6 Comparative assay of PHD 2 variants, PHD2.1, PHD2.3, PHD2 W367F/W334F and PHD2 M299H

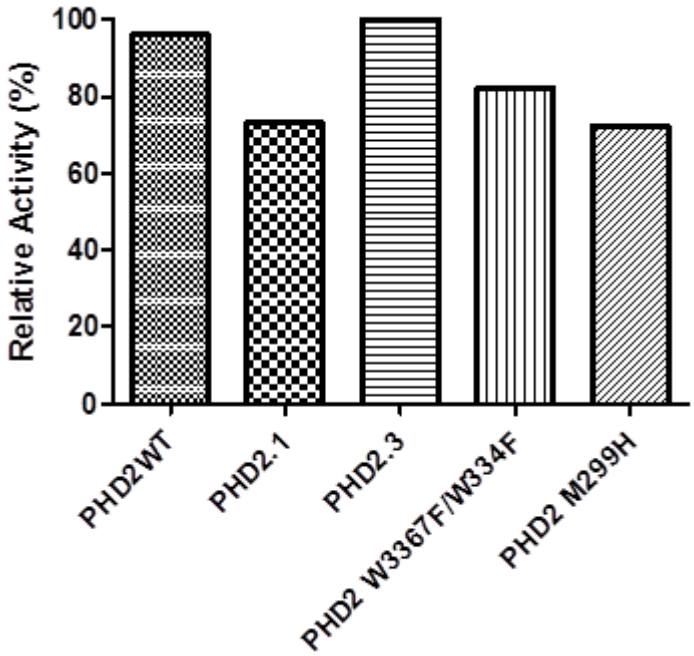

Figure 18: *Relative activity of PHD2.1, PHD2.3, PHD2 W367F/W334F, PHD2 M299H and PHD2 WT at 15 minutes. The conditions included; 100 µM CODD, 50 µM Fe(II), 4 mM L-ascorbate, 300 µM 2OG and 2 µM enzyme at 37 °C, n = 3. The activity is relative to the maximum activity achieved by PHD.2.3.*

To ensure the enzymes produced exhibited similar activity, a comparative activity was run. This run compared the activity of the four variants, PHD2.1, PHD2.3, PHD2 W367F/W334F, PHD2 M299H and wild type PHD2 (Fig 18). The assays were conducted on the same day, under the same conditions (kinetic experimental outline in Chapter 3). The conditions included; 100 µM CODD, 50 µM Fe(II), 4 mM L-ascorbate, 300 µM 2OG and 2 µM enzyme at 37 °C, n = 3. The highest percentage CODD hydroxylation at the 15 minute time point was achieved by PHD2.3. The activities outlined in Fig 18 are relative to this maximum. PHD2 WT and PHD2.3 exhibit similar activity, with PHD2 WT at 96% maximum activity. PHD2.1, PHD2 W367F/W334F and PHD2 M299H have slightly lower activities at 73%, 82% and 72% maximum activity respectively. The enzymes express sufficient activity for further kinetic analysis. The differences seen here are not thought to be significant and could represent different stabilities and/or variability in kinetics across the chimerae (see Chapter 3).

2.3 Conclusion

PHD2 WT and its variants were all found to express and purify according to those procedures outlined by Flashman *et al* [3] and R. Hancock (Part II thesis). The enzymes were active and stable after storage at -80 °C, therefore suitable for the further kinetic assays described in this Thesis.

2.4 Materials and Methods

2.4.1 Transformation

~50ng of plasmid were added to 30 µl aliquots of *E.coli* BL21 (DE3) competent cells. The cells and plasmids were incubated on ice for 20 min, followed by heat shock at 42 °C for 45 s. 200 µl of super optimal broth (SOC) was added to aid cell recovery before incubation on ice for a further 2 min. The cells were incubated at 37 °C for 45 min in the water bath. The transformed cells were spread on a Luria-Bertani agar plate and incubated O/N at 37 °C

*Note: All handing of agar plates, both inoculated and unused was conducted in a laminar-flow hood

2.4.2 Pre-culture preparation

A single colony was selected from the agar plate and used to inoculate 100 ml 2YT media. The inoculated media was incubated overnight at 37 °C.

2.4.3 Protein expression

600 µl of 30 mg/ml Kanamycin was added to each 600 ml of LB growth media, to a final concentration of 30 µg/ml. The flasks and antibiotic were then pre-heated to 37 °C to avoid pre-culture shock and subsequent cell death. The two, 100 mL pre-cultures was added and incubated at 37 °C until OD_{600} reached approximately 1.2 (1.5 max). Once OD_{600} ~ 1.2 was reached, isopropyl 1–β-D thiogalactopyranoside (IPTG) was added to a final concentration of

0.5 mM to induce protein expression. PHD 2.1, PHD 2.3 and PHD2 M299H-containing cells were harvested 4 hours after IPTG induction at 37 °C. PHD 2 W.T. and PHD2 W334F/W367F growths were left O/N at 18 °C after IPTG induction.

2.4.4 Harvesting cells

Cells were harvested via centrifugation at 36375 RCF, 4 °C for 10 min. The pellet was frozen at -80 °C.

2.4.5 Cell lysate preparation

Cell pellet was re-suspended at 4 °C in ~100 ml of 0.1 M MES, pH 5.8 (S SEPH 50 – Buffer A) and a small amount of DNAse I (tip of a spatula). The cell suspension was sonicated at 60% amplitude for 45 s on, 45 s off, four times using a Soniprep 150 sonicator (MSE). The sonicated lysate was centrifuged at 23666 RCF for 20 min, at 4 °C. The resulting supernatant was centrifuged a second time, at 43,589 RCF, for 10 min, 4 °C. This solution was then filtered using a 0.45 µm filter to give a clarified lysate.

2.4.6 Purification using S SEPH 50 – cation exchange

Buffer A; 0.1 M MES, pH 5.8

Buffer B; 0.1 MES, 1M NaCl, pH 5.8

Column was equilibrated with 2 column volumes (CV) of H_2O, 2 CV of 1 M NaCl, 2 CV of buffer A. Once equilibrated, the filtered lysate was loaded at a flow rate of 2.5 ml/min (or less). Once loaded, the column was washed with Buffer A. The protein was eluted with Buffer B. Fractions of interest (according to SDS-PAGE results) were concentrated in a 10,000 MWCO ultracentrifugation device, at 37690 RCF at 4 °C until the sample volume was ~1-2 ml.

The sample was suspended in 0.5 M EDTA pH 8.0 and incubated on ice for 10 min. The sample was centrifuged at 37690 RCF at 4 °C to remove any precipitate. The remaining supernatant was "topped-up" using 20 mM ammonium acetate. The EDTA/ammonium acetate ratio was 2:3, bringing the final protein concentration to 1 mg/ml. The solution was incubated O/N at 4 °C

2.4.7 Purification using a 5 mL HisTrap™ - Ni(II) affinity chromatography

Binding buffer; 20 mM NaH_2PO_4, 0.5 M NaCl, 40 mM imidazole, pH 7.4

Elution buffer; 20 mM NaH_2PO_4, 0.5 M NaCl, 400 mM imidazole, pH 7.4

Stripping buffer; 20 mM NaH_2PO_4, 0.5 M NaCl, 50 mM EDTA, pH 7.4

Charging buffer; 0.1 M $NiSO_4$

The column was first manually stripped and charged prior to use on the ÄKTA system. The column was stripped with 5-10 CV (25-50 mL) of stripping buffer to remove bound Ni(II) (the column turned white indicating loss of Ni(II)). Note: If the column has recently been re-charged this step is unnecessary, can proceed directly to washing with Milli-Q® water. After stripping, the column was recharged with 2.5 mL of charging buffer then washed after charging with 5-10 CV of binding buffer and 5-10 CV of Milli-Q® water. The column was washed with 3-5 CV of Milli-Q® water. The column was equilibrated using 5 CV of binding buffer at a flow rate of 1mL/min. The lysate was applied and then washed with 10-15 CV or until the absorbance reached a steady baseline. The protein was eluted using elution buffer until the absorbance reached a steady baseline. Once fractions were collected the column was stripped and re-charged, as described previously, and stored in 20% ethanol. The concentrated fractions were diluted in 0.5 M EDTA pH 8.0 and incubated on ice for 10 min. The sample was centrifuged at 37690 RCF at 4 °C to remove precipitate. The remaining

supernatant was “topped-up” using 20 mM ammonium acetate. The EDTA/ammonium acetate ratio was 2:3, bringing the final protein concentration to 1 mg/ml. The solution was incubated O/N at 4 °C.

2.4.8 Thrombin cleavage of a polyhistidine tag

Restriction grade thrombin protease was purchased from Novagen®. The protein-containing fractions were incubated in x10 thrombin buffer: 200 mM tris/HCl, 1.5 mM NaCl, 25 mM $CaCl_2$, pH 8.4 with 1 unit of thrombin per mg of protein for 18 hours. The success of the thrombin cleavage was determined by SDS-PAGE analysis, using a 12% acrylamide gel.

2.4.9 Purification using S75 300 – size exclusion

Buffer: 0.1 m Tris/HCl pH 7.5, 0.1 M NaCl

The S75 300 size exclusion column was pre-equilibrated with 1 CV H_2O and 1 CV 0.1 M Tris/HCl pH 7.5, 0.1 M NaCl. The 1 mg/ml PHD protein/EDTA solution was concentrated to ~2 ml then loaded onto the column at 2.5 mL/min. Fractions of interest were collected and then buffer exchanged into 50 mM Tris/HCl pH 7.5 using a 10,000 MWCO ultracentrifugation device. The final protein concentration was determined using a Nanodrop®.

2.5 References

1. D. Ehrismann, E. Flashman, D. N. Genn, N. Mathioudakis, K. S. Hewitson, P. J. Ratcliffe and C. J. Schofield, *Biochem J*, 2007, **401**, 227-234.
2. L. A. McNeill, E. Flashman, M. R. G. Buck, K. S. Hewitson, I. J. Clifton, G. Jeschke, T. D. W. Claridge, D. Ehrismann, N. J. Oldham and C. J. Schofield, *Mol Biosyst*, 2005, **1**, 321-324.
3. E. Flashman, E. A. L. Bagg, R. Chowdhury, J. Mecinovic, C. Loenarz, M. A. McDonough, K. S. Hewitson and C. J. Schofield, *J Biol Chem*, 2008, **283**, 3808-3815.
4. E. Flashman, L. M. Hoffart, R. B. Hamed, J. M. Bollinger, C. Krebs and C. J. Schofield, *Febs J*, 2010, **277**, 4089-4099.
5. H. Tarhonskaya, R. Chowdhury, I. K. H. Leung, N. D. Loik, J. S. O. McCullagh, T. D. W. Claridge, C. J. Schofield and E. Flashman, *Biochem J*, 2014, **463**, 363-372.
6. H. Tarhonskaya, A. P. Hardy, E. A. Howe, N. D. Loik, H. B. Kramer, J. S. O. McCullagh, C. J. Schofield and E. Flashman, *J Biol Chem*, 2015, **290**, 19726-19742.

Chapter 3: Investigating the role of the β2β3 loop in PHD2's reaction with oxygen

3.1 Introduction

Figure 1: *Overlay of the crystal structures of PHD 2 with (PDB ID: 3HQR)* [1] *and without (PDB ID 2G19)* [2] *substrate in **grey** and **blue** respectively. The **pink** region denotes the β2β3 loop region of interest folded over locking the substrate in place. The C-terminal oxygen dependent domain of HIF (CODD) substrate is depicted here in **black**.*

Of the three PHDs, PHD2 (henceforth referred to as PHD2 or WT) is reported to be the key O_2 sensor regulating the hypoxic response. [3] It has also been reported to have a high $K_m(O_2)$ value [3-8] and a slow reaction with O_2 in pre-steady state studies; kinetic features that are proposed to be related to its role as an O_2-sensor. [3, 5] The molecular features that enable this O_2-sensing role are poorly resolved especially given that other Fe(II)/2OG oxygenases with conserved structures and mechanisms react more readily with O_2. Understanding the molecular basis of PHD2's slow kinetics with respect to O_2 could reveal important information about cellular O_2 sensing at the enzymatic level.

Aspects of PHD2's active site have been investigated to probe their contribution to its slowed O_2 kinetics. Although a PHD2D315E variant described by Tarhonskaya *et al* had an increase in the rate of product turnover [5] compared to WT [3], the rate of product turnover of

PHD 1 GQLVSQRAIPPR-SIR

PHD 2 GQLVSQKSDSSK-DIR

PHD 3 GQLAGPRAGVSKRHLR

Figure 2: *Sequence alignment of the β2β3 loop regions of PHD1-3. Hydrophobic residues are in* ***black****, polar non-charged residues are in* ***pink****, positively charged residues are in* ***blue*** *and negatively charged residues are in* ***green****.*

this variant with respect to O_2 only increased slightly with a k = 0.0484 ± 0.006 s^{-1} [5] compared to WT (0.0095±0.0012 s^{-1} [5]). It was rationalised that the increased activity for the PHD2 D315E variant was due to weakened interaction with the active site Fe(II) and/or the iron-bound water, thus potentially increasing the rate at which O_2 binds to the Fe(II) centre. [5] The unusually slow kinetics of PHD2 with respect to O_2 is, however, likely attributed to a series of highly controlled structural features which have yet to be fully elucidated.

In the crystal structure of PHD2 (Figure 1), the mobile loop region linking β strands 2 and 3 (β2β3) loop is seen to be mobile but upon binding of the C-terminal O_2 degradation domain (CODD) substrate stabilizes, "fixing" CODD in place. Molecular dynamic (MD) studies of the PHD2.Mn.NOG.CODD complex by Jorgensen *et al* (unpublished) propose that the β2β3 loop and CODD substrate form part of PHD2's single O_2 uptake pathway, with the removal of the loop resulting in a range of O_2 uptake pathways and decreased O_2 selection (these MD studies are elaborated upon in Chapter 4). The studies also revealed a stabilizing pocket or "E-cluster" in which O_2 is proposed to interact non-covalently prior to active site entry. Should this observation be experimentally verifiable, it could provide a rationale for slowed PHD2 kinetics with respect to O_2.

As the β2β3 loop is suggested to form part of the O_2 entry pathway and also to be part of the E-cluster, changes in the loop sequence may therefore induce altered kinetic behaviour in terms of O_2. Flashman *et al* report upon the substrate selectivity of two PHD2 variants,

Enzyme	*K_m(CODD)*	*k_{cat}*
PHD2 WT	36.7 ± 9.0 μM	0.0033±0.003 s^{-1}
PHD2.1	63 ± 15.7 μM	0.031 ±0.004 s^{-1}
PHD2.3	6.4 ± 0.2 μM	0.016 ± 0.003 s^{-1}

Table 1: K_m(CODD) and k_{cat} values for PHD 2 WT and the PHD 2.1 and PHD 2.3 chimerae. All values depicted in this table were collected by Dr Emily Flashman. [9]

PHD2.1 and PHD2.3, whereby the β2β3 loop in PHD2, were replaced by the β2β3 loop sequences from PHD1 and PHD3 respectively. The chimerae were reported to hydroxylate both the N-terminal Oxygen Degradation Domain (NODD, Fig 3) and CODD 19-mer peptides as efficiently as $PHD2_{181–426}$ and to decarboxylate 2OG similarly in the presence of both NODD and CODD under standard assay conditions. [9] PHD2.3 was found to exhibit a striking preference for CODD, with a k_{cat} value approximately half that of either $PHD2_{181–426}$ or PHD2.1 (0.016 ± 0.003 s^{-1}). PHD2.3 also experienced a ~10 fold drop in K_m (6.4 ± 0.2 μM) in terms of CODD compared with PHD2.1 (63 ± 17.2 μM) and ~5 fold drop compared with PHD2 (36.7 ± 9.0 μM), see Table 1. [9] No significant change was observed for NODD hydroxylation for either chimera compared to WT. [9] This result is particularly important as it highlighted the β2β3 loop as a possible reason for PHD3's near absolute preference for CODD over NODD. [6, 10, 11] Both PHD2.1 and PHD2.3 illustrated much higher association rate constants for CODD. [9] The k_{cat} values, however, did not reflect this marked increase in

binding strength, suggesting the loop is predominately involved in substrate binding rather than hydroxylation.[9]

NODD ALTLLAPAAGDTIISLD

CODD DLEMLAPYIPMDDDFQL

Figure 3: *Alignment of the sequences of the N-terminal oxygen degradation domain (NODD) and C-terminal oxygen degradation domain (CODD) 19-mer peptides respectively. The proline targeted for hydroxylation, proline 405 and 564 of NODD and CODD respectively, are highlighted here in* ***green****.*

The reaction of the PHD2.1 and PHD2.3 variants with respect to oxygen, however, remains unexplored. Due to the β2β3 loop proximity to the proposed O_2-entry pathway for PHD2 (Jorgensen *et al,* unpublished), these chimerae would provide good models by which to begin to prove the importance of this O_2-entry pathway in the O_2-sensing characteristics of the PHDs. Variation in O_2 kinetics across the PHD2.1 and PHD2.3 variants would suggest changes in sensitivity to O_2 with respect to the β2β3 loop –unravelling which factors contribute to PHD2's slowed O_2 kinetics compared to other Fe(II)/2OG oxygenases.

Further to understanding the detailed kinetic mechanism of PHD2 with oxygen, uncovering characteristic O_2 kinetic traits across the three PHDs could prove insightful in terms of the human hypoxic response. The three PHD isoforms are found to manifest distinct patterns of cellular expression. [6, 12-15] Therefore in different cell types, isoform-specific patterns of PHD expression alter both the relative abundance of the PHDs and their relative contribution to the regulation of HIF – depending on their individual reactivity with O_2. This has the potential to give some insight into how certain cell types are prioritized under low O_2 conditions *in vivo*. Furthermore, with different substrate selectivity for each PHD for each HIF-α terminal, differential PHD inhibition has the potential to selectively alter the characteristics of HIF activation.[16]

In this Chapter, using the chimerae to test the modelling data, the kinetic analysis of PHD2.1 and PHD2.3 in terms of both CODD and O_2 are described. It describes the steady state (CODD and O_2) and pre-steady state analysis of each chimera, with a view to elucidating the structural basis for altered kinetics with respect to O_2.

3.2 Results and Discussion

3.2.1 Steady state kinetic studies of PHD 2.1 and 2.3 variants

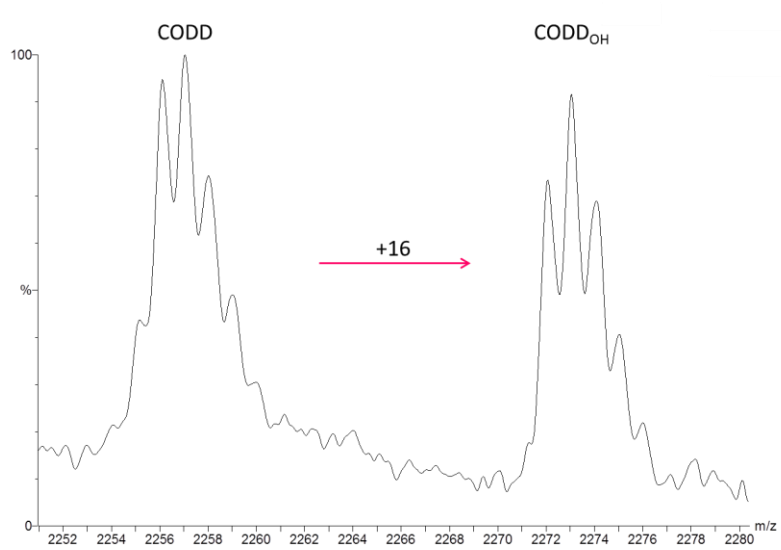

Figure 4: *Example of a typical MALDI-TOF spectrum, highlighting the +16 shift consistent with CODD hydroxylation in the presence of enzyme, 2OG, Fe(II), CODD and ascorbate.*

To investigate the O_2 kinetics of the loop mutants, it was first necessary to generate a K_m(CODD) value for both chimerae, to ensure the concentration of CODD used in studies on O_2 dependence was not limiting. For the purposes of this study, a HIF-1α-19-mer CODD peptide was used, a HIF peptide length known to be optimal. [17] All assays were conducted at 37 °C, 4 µM PHD2.1 or 2 µM PHD2.3 (chosen protein concentrations are rationalised later), 50 µM Fe(II), 4 mM L-ascorbate, 300 µM 2OG with CODD peptide concentrations varied from 10 – 125 µM, quenching aliquots in 1% formic acid at defined time points. CODD hydroxylation at various time points was quantified using MALDI-TOF MS. In Fig 4, the +16 Da shift observed upon CODD hydroxylation is illustrated. This change over time was monitored, generating a time course like those seen in Fig 5.

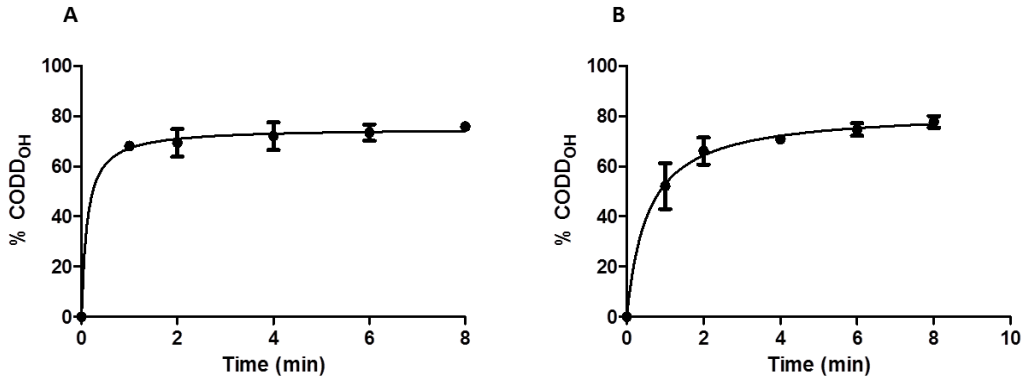

Figure 5: *Time course for PHD2.3 in the presence of 100 µM CODD, 50 µM Fe(II), 4 mM L-ascorbate, 300 µM 2OG and A) 4 µM and B) 2 µM of PHD2.3 at 37 °C. In A) the initial rate zone is undefined as the reaction plateaued within an immeasurable time range. In B) the initial rate zone is more defined, and a steady state rate for CODD$_{OHn}$ is calculable.*

Enzyme concentrations were varied from 2-4 µM to account for the different kinetics of the chimerae and allow for the accurate determination of initial rates at low peptide concentrations. As K_m ≈ [Substrate], where $V_{max} = k_{cat}[ES] = k_{cat}[E]_T$ under the steady state approximation different enzyme concentrations will not affect the K_m obtained. Optimising the enzyme concentration will increase the accuracy with which the initial rates are generated (Fig 5). For example in Fig 5 are two time courses for PHD2.3 in the presence of 13.5 µM CODD and A) 4 µM and B) 2 µM of PHD2.3. In Fig 5 A) the initial rate zone, where the steady state approximation applies, is undefined as the reaction plateaued within an immeasurable time range. However, in Fig 5 B) the initial rate zone is more defined, and a steady state rate for CODD hydroxylation ($CODD_{OHn}$) is calculable. It was on this basis a concentration of 2 µM PHD2.3 was chosen for K_m(CODD) studies. A concentration of 4 µM for PHD2.1 was initially chosen based on studies conducted with PHD2 WT; this generated well-defined curves negating the need for optimization.

As CODD (Fig 3) contains two methionine residues it raises the possibility of methionine oxidation, a factor previously observed for PHD2. Therefore it was imperative background methionine oxidation be subtracted to ensure only enzyme-mediated-prolyl hydroxylation

was being factored into K_m measurements. A no-enzyme control (100 µM CODD, 50 µM Fe(II), 4 mM L-ascorbate and 300 µM 2OG) determined the average background methionine oxidation over the time course to be stable and 7% using MALDI-TOF MS in negative ion mode. This value was subtracted as a baseline from all K_m(CODD) and $K_m(O_2)$ time courses generated.

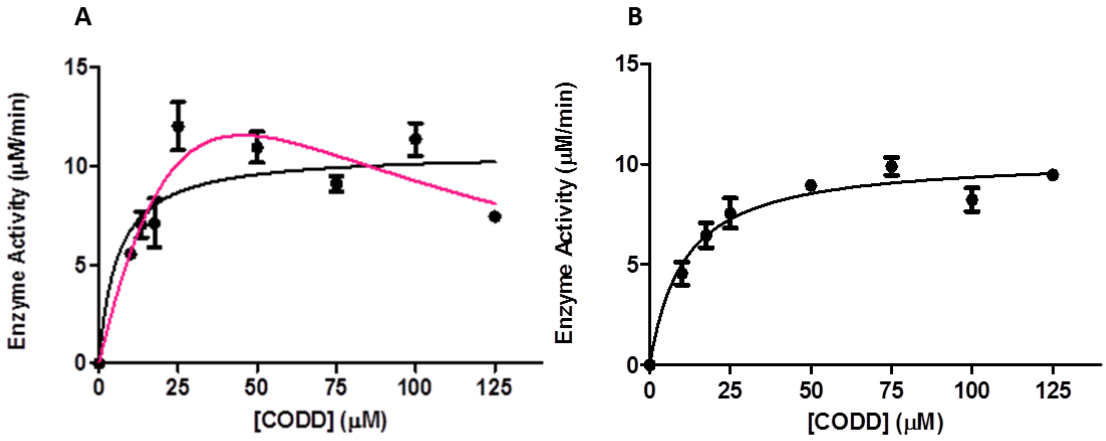

***Figure 6**: Michaelis-Menten graphs for A) PHD2.3 and B) PHD2.1 in terms of CODD. All time courses performed at atmospheric O_2 with 50 µM Fe(II), 4 mM L-ascorbate, 300 µM 2OG and A) 4 µM and B) 2 µM of PHD2.3 at 37 °C. HIF-1α CODD 19-mer peptide concentrations varied from 10 to 125 µM. The Michaelis-Menten fit for PHD2.3 (A) is shown by the **black** line, with the Michaelis-Menten peptide inhibition fit shown in **pink**.*

The initial rate data for PHD2.1 and PHD2.3 was plotted and fitted using the Michaelis-Menten (MM) fit on Graphpad Prism® version 5.04. Steady-state plots revealed the K_m values for the variants as shown in Table 1. Interestingly, the K_m(CODD) for PHD2.1 is comparable to WT (11 ± 3 µM and 9 ±3 µM [5] respectively), whereas the K_m(CODD) generated for PHD2.3 was approximately half that of either PHD2 or PHD2.1 with K_m(CODD) = 6 ± 4 µM (Table 1, Fig 6) indicating higher substrate affinity. Flashman *et al* [9] revealed that both the PHD2.1 and PHD2.3 chimerae had much higher association rate constants for CODD (29.5 (±11.7)×10^5 M^{-1} s^{-1} and 61.3(±28.0)×10^5 M^{-1} s^{-1} respectively, compared with just 1.34 (±0.63)×10^5 M^{-1} s^{-1} for PHD2). [9] Both the K_m(CODD) and association rate constant

generated for PHD2.3 not only highlight the β2β3 loop as an important factor in substrate recognition, but illustrates that the β2β3 loop can also promote different kinetics. Peptide inhibition effects were noted while acquiring K_m(CODD) for PHD 2.3. A peptide inhibition

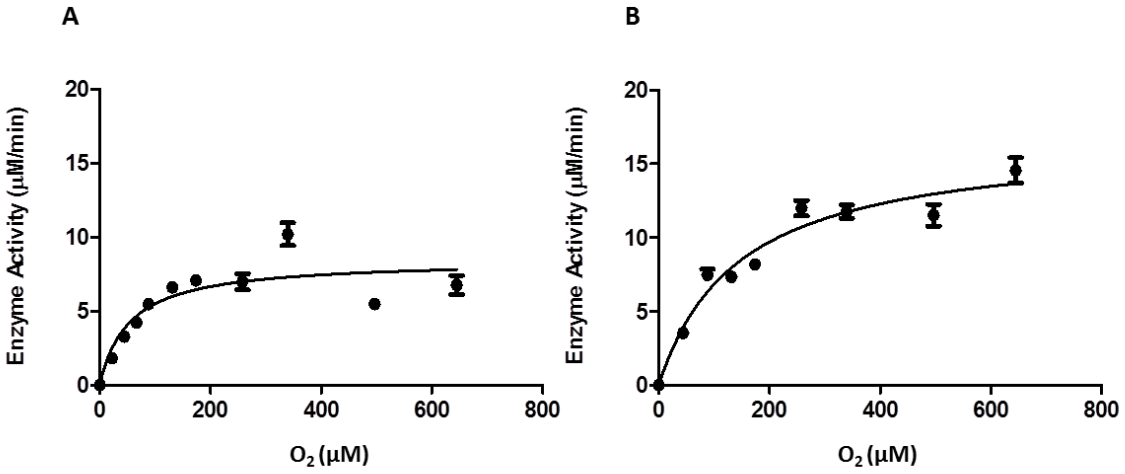

Figure 7: *$K_m(O_2)$ graphs for A) PHD2.3 and B) PHD2.1. All time courses were performed under the conditions; 4 μM PHD2, 50 μM Fe(II), 4 mM L-ascorbate, 300 μM 2OG, HIF-1α CODD 19-mer peptide, at 37 °C in Tris·HCl 50 mM, pH 7.5.O2 concentrations were varied from 5 to 80%.*

model (pink line in Fig 6, A) was used to validate this.

Moving from K_m(CODD) to $K_m(O_2)$ studies, it was imperative the experimental design ensure neither peptide concentrations nor inhibition effects be limiting. To avoid possible peptide inhibition effects noted while acquiring the K_m(CODD) for PHD 2.3 in $K_m(O_2)$ studies, a CODD concentration of 25 μM was chosen for PHD2.3 $K_m(O_2)$ studies (a concentration ~4 fold higher than K_m^{app}(CODD)), as it was the concentration at which PHD2.3 achieved the highest rate activity. A concentration of 100 μM CODD used for both PHD2.1 and PHD2 WT $K_m(O_2)$ studies. A time-point of 2, 2 and 1 min were chosen for PHD 2, 2.1 and 2.3 respectively, as both these time intervals are known to be within the initial rate zones of their respective CODD concentrations. Samples were quenched at the defined time points at various O_2

concentrations at n = 3. These points were plotted to form the Michaelis-Menten curve, generating $K_m(O_2)$.

In $K_m(O_2)$ studies, PHD2.3 had a value over 6 fold lower than that of WT with a $K_m(O_2)$ = 54 ± 9 μM and 355 ± 80 μM respectively and almost 3 fold lower than PHD2.1 $K_m(O_2)$ = 145 ± 37 μM (Table 1 and Fig 7). Different $K_m(O_2)$ values amongst the chimerae are particularly interesting as it implies the β2β3 loop contributes to the affinity of PHD2 for O_2. The variation in sensitivity for O_2 seen here for these chimerae compared to WT could be due to an increase in the rate of O_2 uptake as a result of a disruption of stabilization features in PHD2.

To ensure the validity of the decreased $K_m(O_2)$ values for both PHD2.1 and 2.3, the PHD2 WT $K_m(O_2)$ was repeated and found to be in agreement with previous findings by Tarhonskaya *et al*; $K_m(O_2)$ = 355 ± 80 μM and >450 μM [5] respectively (Table 2). The difference in the value was thought to be acceptable, as enzyme activity can vary due to slight differences in purification procedures. Hence the results for PHD2.1 and PHD2.3 are thought to be validated and contrasting with that of PHD2 WT.

Enzyme	*Steady State*		*Pre-Steady State*
	$K_m(O_2)$	*K_m(CODD)*	*Rate CODD hydroxylation*
PHD2 WT	355 ± 80 μM	9 ± 3 μM [5]	0.0095±0.0012 s^{-1} [5]
PHD2.1	145 ± 37 μM	11 ± 3 μM	0.0112±0.0019 s^{-1}
PHD2.3	54 ± 9 μM	6 ± 4 μM	0.0762±0.0089 s^{-1}

Table 2: *Steady and pre-steady state values for PHD 2 WT and the β2β3 loop chimerae PHD2.1 and 2.3. PHD2 WT values for Km(CODD) and rate of CODD hydroxylation were generated by Tarhonskaya et al* [5]

3.2.2 Pre-steady state kinetic studies of PHD 2.1 and 2.3 variants

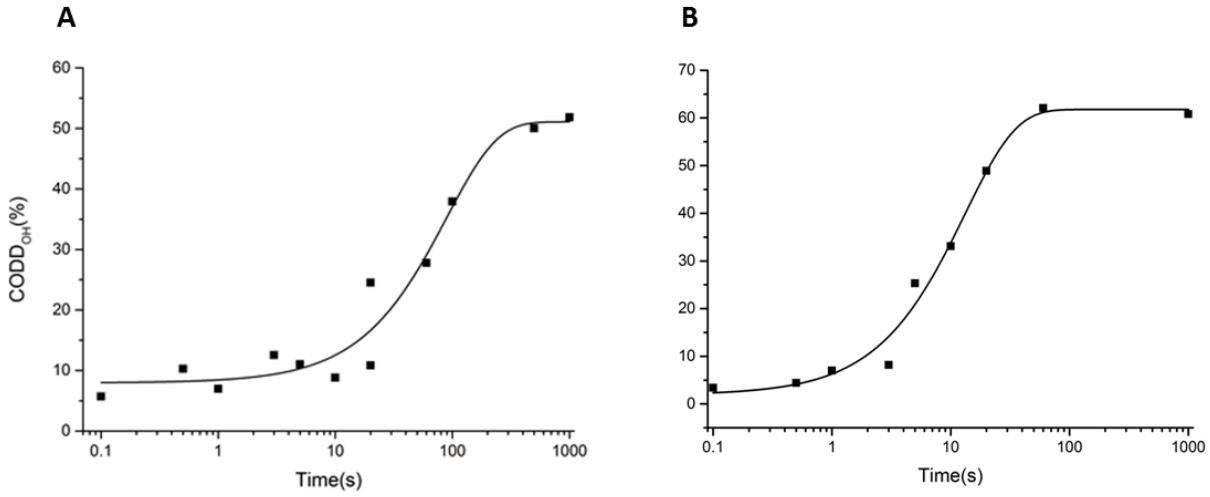

Figure 8: *Pre-steady state study of reaction of O_2 with A) PHD2.1 and B) PHD2.3. Conditions: anaerobic 0.8 mM enzyme, 1 mM CODD, 0.5 mM $Fe(NH_4)_2(SO_4)_2$ and 5 mM 2OG were mixed with saturated O_2 solution IN 1:1 ratio, 5°C, on a rapid quench flow equipment (RQF-63, TG-K Scientific, UK) n=1. Reactions were performed in an anaerobic glove box (Belle Technologies, Weymouth, UK) at < 6ppm O_2. Rates of product turnover were calculated via Origin 8.51 software, with data fitted with a single exponential function* $\boldsymbol{y = A1 * exp\left(-\frac{x}{t1}\right) + y0}$.

Given the differences observed in $K_m(O_2)$ for the chimerae and the suggested link between pre-steady state and K_m values, pre-steady-state (PSS) studies were performed on PHD2.1 and PHD2.3, to see if these chimeras exhibit faster PSS kinetics than WT (Fig 8, Table 1). The experiments were conducted under anaerobic conditions, using a rapid quench flow apparatus. Reactions were initiated by mixing an anaerobically prepared PHD2.1/2.3.Fe^{II}.2OG.CODD complex with O_2-saturated buffer and quenched at defined time points using 1% trifluoroacetic acid (TFA). PSS samples were analysed by MALDI-TOF MS to analyse the rate of CODD hydroxylation. PHD2 is known to react slowly with O_2 in pre-steady state kinetic experiments [18], which is proposed to be linked to its O_2 sensing role. [4] Under PSS conditions, the rate of CODD hydroxylation of PHD2.1 with O_2 was very similar to that of WT (0.0095 ± 0.0012 s^{-1} [5]), generating a value of k = 0.0112 ± 0.0019 s^{-1} (Table 1 and Fig 8, A). In contrast the rate of CODD hydroxylation was faster for the PHD2.3 variant than WT, with a rate of 0.0762 ± 0.0089 s^{-1} (Table 1 and Fig 8, B).

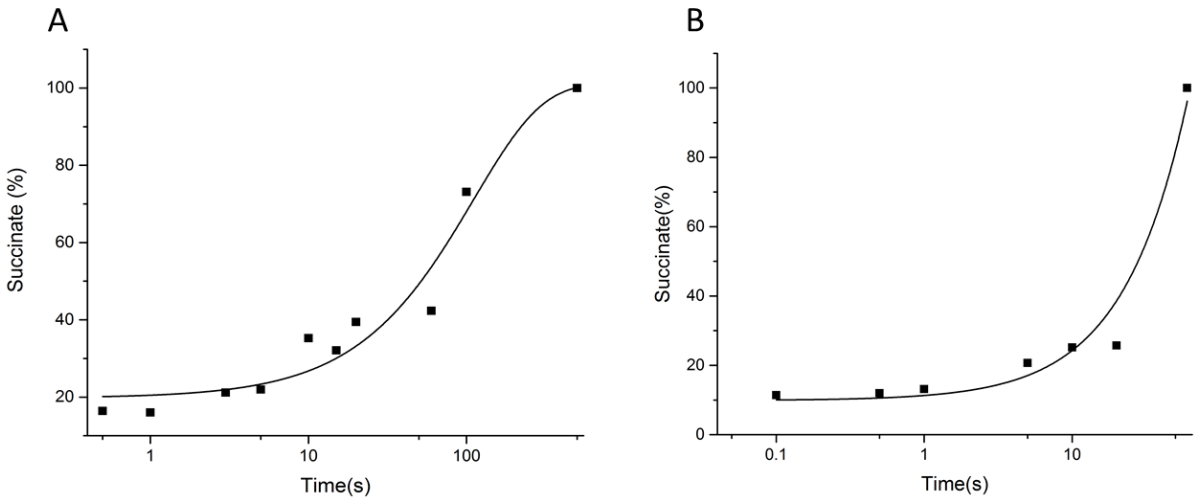

Figure 9: *Succinate turnover analysis for A) PHD2.1 and B) PHD2.3 respectively. Chromatographic separations were performed at 50 °C using a Waters ACQUITY ™ BEH Amide 1.7 µm, 2.1 mm×100 mm column using a Thermo U3000 chromatography system coupled to a Thermo Q-Exactive S mass spectrometer. Instrument control and data processing were performed using Thermo Xcalibur Software. The following eluents were used: mobile phase A: 10% water, 90% (v/v) acetonitrile and 10mM ammonium formate; mobile phase B: 50%water, 50% (v/v) acetonitrile and 10mM ammonium formate. The mass spectrometer was operated using a heated electrospray (HESI-II) probe, all analysis was performed in positive ion mode. Rates of succinate turnover were calculated via Origin 8.51 software, with data fitted with a single exponential function* $\boldsymbol{y = A1 * exp\left(-\frac{x}{t1}\right) + y_0}$.

MD studies based on the crystal structure analysis of the PHD2.Mn.NOG.CODD complex, suggest the interface between the β2β3 loop and CODD peptide are integral in forming a single O_2 uptake pathway in PHD2 – with the removal of the loop resulting in reduced selectivity in O_2 uptake. The formation of the proposed O_2 delivery pathway upon substrate binding (and the different kinetics of the chimeras with respect to WT) indicates the loop may be able to control accessibility of O_2 to the PHD2 active site. Should the composition of the loop change, as is the case for the PHD2.1 and PHD2.3 chimerae, it is reasonable to believe PHD2's accessibility to O_2 could also change – thus promoting different O_2 kinetics.

The $K_m(O_2)$ values for PHD2.1 and PHD2.3 are 145 ± 37 µM and 54 ± 9 µM respectively, ~3 and ~6 fold lower than WT (355 ± 80 µM). While the PHD2.3 $K_m(O_2)$ and PSS value correlate, in that the lower $K_m(O_2)$ correlates with a more rapid rate of reaction in PSS, the PHD2.1 PSS

value does not reflect the decreased $K_m(O_2)$ observed for this chimera. This could be indicative that the oxygen sensory role of PHD2 is not entirely disrupted by changing the loop to that of PHD1. K_m takes into account the affinity of binding as well as k_{cat}, whereas in in PSS studies saturating binding conditions are used, so the differences in PHD2.1 and PHD2.3 K_m values may reflect different affinities for O_2, in line with the first interaction with O_2 likely being via β2β3 loop. Furthermore, for $K_m(O_2)$ studies the enzyme does not have to undergo the stressful de-oxygenating process required for PSS analysis. If the PHD2.1 variant were sensitive to environmental changes, the PSS kinetics could be hampered by comparison to $K_m(O_2)$. The observed rate changes in these chimerae, however, imply a significant structural role for the β2β3 loop in terms of oxygen uptake.

To complement the pre-steady state results generated for the PHD2.1 and 2.3 chimeras, succinate turnover analysis was conducted. This is the process by which the turnover of 2OG to succinate by the loss of CO_2 is quantified, with a view to calculating a rate of 2OG turnover. As 2OG conversion to succinate is coupled to CODD hydroxylation in a 1:1 ratio in productive catalysis, the turnover rate should be comparable that of CODD hydroxylation under PSS conditions. The rate of succinate turnover for PHD2.1 was k = 0.0090 ± 0.0017 s^{-1} (Fig 9, A), a comparable rate to that of CODD hydroxylation under PSS conditions for PHD2.1 (k = 0.0112 ± 0.0019 s^{-1}). The rate of succinate turnover for PHD2.3 was not calculated due to a lack of analysable points and therefore inability to fit the curve using the single exponential function $\mathrm{y} = \mathrm{A1} * \exp\left(-\frac{\mathrm{x}}{\mathrm{t1}}\right) + \mathrm{y}_0$ (Fig 9, B). The levels of succinate in some of the PHD2.3 PSS samples were below the levels of detectability. A series of optimization techniques and mass spectrometers were used, but to no avail.

3.3 Conclusions

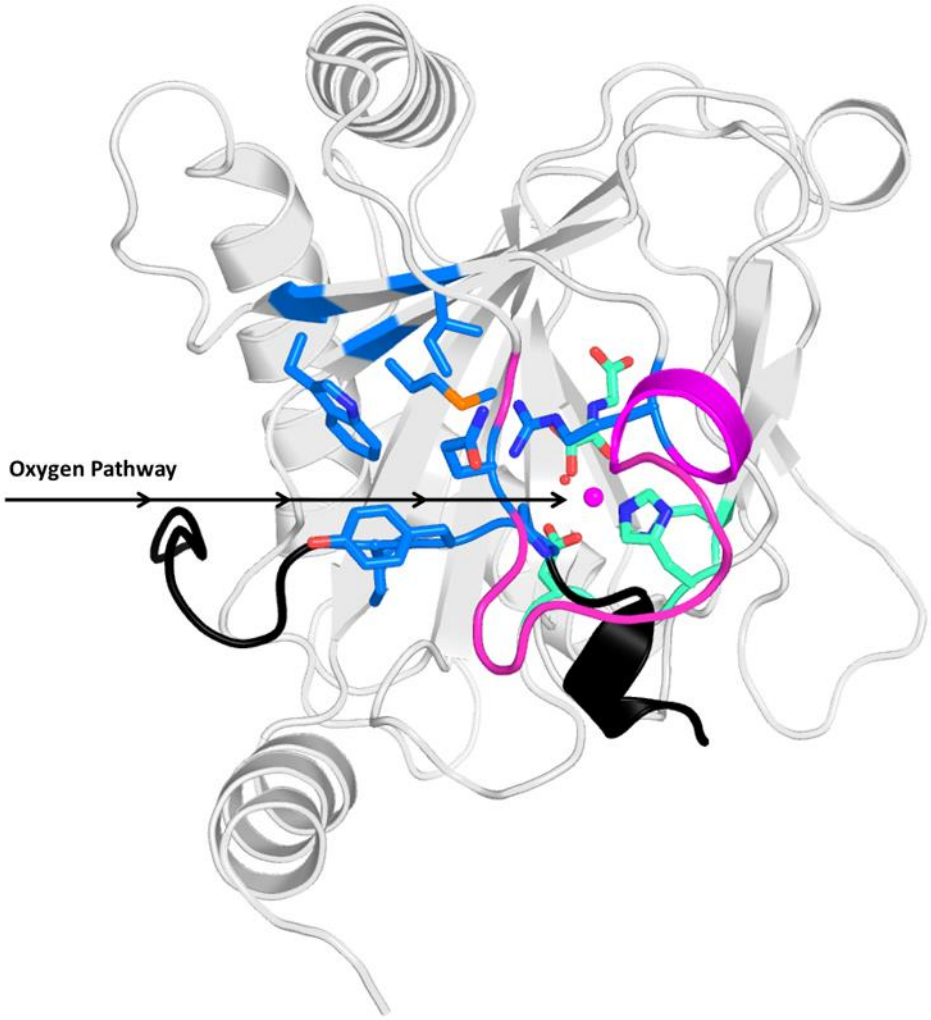

Figure 10: *The proposed O_2 pathway in PHD2, with the interacting residues proposed to be in the E-cluster shown in **blue**, the β2β3 loop in **pink**, CODD substrate in **black** and the PHD2 in **grey**. The Mn metal centre is depicted here in **purple**, coordinated by the HXD…H triad in **green**. This clearly illustrates the direct oxygen uptake pathway from bulk solvent, to the e-cluster and finally to the active site. PDB ID: 3HQR* [1]

The purpose of the work described in this Chapter was to investigate the kinetics of the PHD2.1 and PHD2.3 chimerae with respect to O_2 to try and validate the proposal that O_2 entry to the PHD2 active site occurs via the β2β3 loop:CODD interface. The results show that both PHD2.1 and PHD2.3 generated very different $K_m(O_2)$ values compared to that of PHD2 WT; 145 ± 37 μM, 54 ± 9 μM and >450 μM respectively with PSS rates of CODD hydroxylation determined as k = 0.0112 ± 0.0019 s^{-1}, k = 0.0762 ± 0.0089 s^{-1} and 0.0095±0.0012 s^{-1} [5] respectively (Table 1). These results indicate that the loop is likely to contribute to O_2 uptake by PHD2. The different kinetics observed for the chimeras imply

different O_2 interaction affinities or mechanisms. This work supports the findings of our collaborators Jorgensen *et al* (unpublished) which proposed this route of O_2 entry to the PHD2 active site.

Previous work carried-out by Flashman *et al*, [9] concluded that CODD binds to both PHD2.1 and PHD2.3 more strongly by comparison to WT, due to their significantly higher association constants. As the loop is the region of greatest variability across the three PHDs, the position and stability of the loop may vary from PHD1-3, affecting the overall pathway structure and/or E-cluster stability and therefore accessibility to O_2. The different O_2 kinetics of these chimeras validates this hypothesis, presenting O_2 kinetics as a function of changes made to the β2β3 loop. There may be characteristics of the O_2 entry pathway that are both rate limiting and affected directly by the β2β3 loop-CODD interaction. It would be interesting to probe the O_2 kinetics of PHD2 using an altered substrate to further establish the importance of the β2β3 loop-CODD interface. It is worth noting here, that kinetic studies conducted by Tarhonskaya *et al*, [3] revealed similar O_2 kinetics of PHD2 in the presence of NODD compared to CODD (< 450 μM). Should the β2β3 loop-CODD interaction play such an important role in O_2 uptake, it would be unexpected that the O_2 kinetics of PHD2 in the presence of NODD should be similar to that of CODD. This study relates O_2 kinetic behaviour directly to the structure of PHD2.

The enzymes, both WT and various chimerae, studied in this project are truncated to omit PHD 2's N-terminus (PHD $2_{181-426}$). PHD 2 has an MYND-type zinc finger at its N-terminus, a feature not shared with the PHD 1 and 3 isomers. It is acknowledged that the omission of this domain could indeed affect PHD 2 kinetics with respect to both substrate and O_2. The MYND-type zinc finger may adopt a binding conformation that could alter the β2β3 loop and/or O_2 access to the active site. The aim of this chapter, however, was to study the β2β3

loop contribution to O_2 uptake across the three PHD isoforms, by looking for O_2 affinity variations with respect to the different β2β3 loops inserted into the PHD 2 sequence. The larger, biological consequence of such changes cannot, therefore, be accurately inferred from this data. It simply serves as a structural analysis of PHD2 via kinetic studies.

3.4 Materials and Methods

3.4.1 Steady-state analysis of PHD2.1 and PHD2.3 with respect to CODD peptide

A 100 µl reaction mixture was made up to a final concentration of: 300 µM 2OG, 50 µM $Fe(NH_4)_2(SO_4)_2$, 4 mM sodium ascorbate (analogous to previous experiments performed by Flashman *et al* [4]), 4 µM of enzyme (PHD2.3 at 2 µM, see Fig 5)). The assays were run at CODD peptide concentrations of 10 µM, 13.5 µM, 17.5 µM, 25 µM, 50 µM, 75 µM, 100 µM and 125 µM, at 37 °C. 10 µl samples were quenched in 10 µl of 1% formic acid, immediately vortexed and snap frozen in liquid nitrogen.

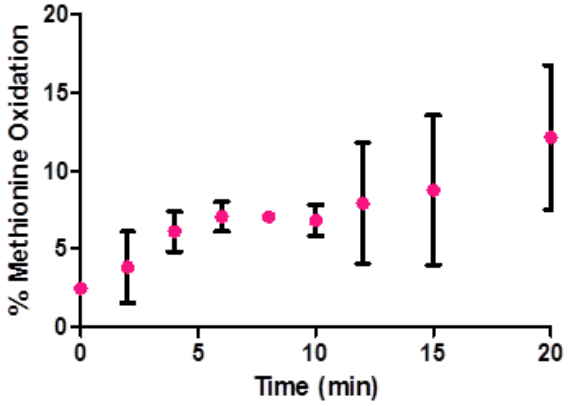

Figure 11: *No enzyme control performed at atmospheric O_2 with 50 µM Fe(II), 4 mM L-ascorbate, 300 µM 2OG, 100 µM CODD at 37 °C. Samples analysed via MALDI-TOF MS.*

For MALDI-MS analysis, samples were thawed over ice, with 2 µl of the sample added to 1 µl of α-cyano-4-hydroxycinnamic acid (CHCA) matrix in 50% MeCN, 50% H_2O (0.1% CF_3COOH). The samples were analysed using MALDI-TOF MS in negative ion mode. Initial rates were calculated via initial rate analysis and plotted against [S]. The data was fit with the Michaelis-Menten model on GraphPad Prism® 5.04 software, where $v = \frac{[S]V_{max}}{K_m + [S]}$. A no-enzyme control was used to subtract background CODD methionine oxidation (Fig 9). The average background methionine oxidation across a 20 minute time course was found to be 7%.

3.4.2 Steady-state analysis of PHD2.1 and PHD2.3 in terms of O_2

Assays were conducted whereby reagents were added to the following final concentrations; 300 µM 2OG, 50 µM $Fe(NH_4)_2(SO_4)_2$, 4 mM sodium ascorbate, 4 µM PHD2 WT and PHD2.1 or 2 µM PHD2.3 and 100/25 µM CODD. Mass-flow controllers (Brooks Instrument) were used to fix O_2 concentrations. O_2 concentrations included: 5%, 10%, 15%, 20%, 30%, 40%, 60% and 80% (80% is the maximum permitted oxygen concentration for safety reasons). 50 mM Tris/HCl, pH 7.5 and CODD were equilibrated at the desired [O_2] for 10 min in 1.1 mL sealed glass vials (with septum for reagent addition) at 37 °C prior to further reagent addition. Once equilibrated, the remaining cofactors were added via Hamilton® gastight syringes to a final volume of 100 µl, with the enzyme addition marking the time-point beginning. The reaction was incubated at 37 °C for the required time and quenched with 100 µl of 1% formic acid. Samples were frozen on dry ice and then stored at -20 °C prior to further analysis

3.4.3 Pre-Steady State analysis of PHD2.1 and PHD2.3

Experiments were performed using rapid quench flow equipment (RQF-63, TG-K Scientific, UK) in an anaerobic glove box (Belle Technologies, Weymouth, UK) where [O_2] < 6 ppm. Reactions were conducted in 50 mM HEPES, pH 7.5 (analogous to previous experiments performed by Tarhonskaya *et al*). [5] 50 mM HEPES, pH 7.5, 50 mM HEPES, 15% glycerol pH 7.5, Milli-Q H_2O, 1% (v/v) CF_3COOH and protein mixtures were de-oxygenated via vacuum and stored under argon. Oxygenated 50 mM HEPES, pH 7.5 was stored on ice during oxygenation and the experiment to facilitate greater O_2 solvation. 2OG, Fe(II) and CODD solids were pre-weighed and placed in the glove box to enable solutions to be made with anaerobic buffer. Reagents were mixed in the glove box to a final concentration of 0.8 mM enzyme, 1 mM CODD, 0.5 mM $Fe(NH_4)_2(SO_4)_2$ and 5 mM 2OG. 2OG and CODD were mixed

first, followed by enzyme and Fe(II). Samples were collected via 'interrupt mode', using loop "4" (for 0.1 s time points and above). Samples were quenched with 1% (v/v) CF_3COOH. Prior to MALDI-TOF MS analysis, the samples were treated with 1:1 acetone and centrifuged at 14k for 10 min to precipitate the protein (high protein concentrations can obscure CODD MALDI-TOF MS signal, however with this separation technique clear CODD analysis is facilitated). Rates of product turnover were calculated via Origin 8.51 software, with data fitted with a single exponential function; $y = A1 * \exp\left(-\frac{x}{t1}\right) + y_0$.

Quenched pre-steady state samples were further analysed for coupled succinate turnover by LC-MS. The samples were concentrated in a 4k molecular weight cut-off (MWCO) tube at 14k for 1 hour, separating the enzyme from succinate. Chromatographic separations were then performed at 50 °C using a Waters ACQUITY ™ BEH Amide 1.7 µm, 2.1 mm×100 mm column using a Thermo U3000 chromatography system coupled to a Thermo Q-Exactive S mass spectrometer. Instrument control and data processing were performed using Thermo Xcalibur Software. The following eluents were used: mobile phase A: 10% water, 90% (v/v) acetonitrile and 10mM ammonium formate; mobile phase B: 50%water, 50% (v/v) acetonitrile and 10mM ammonium formate. The system was calibrated on the day of the analysis and its mass accuracy with external calibration (as used for these experiments) is 5ppm for 24 hours following calibration. The mass spectrometer was operated using a heated electrospray (HESI-II) probe, all analysis was performed in positive ion mode. Electrospray source conditions were adjusted to maximise sensitivity. Rates of succinate turnover were calculated via Origin 8.51 software, with data fitted with a single exponential function $y = A1 * \exp\left(-\frac{x}{t1}\right) + y_0$.

3.5 References

1. R. Chowdhury, M. A. McDonough, J. Mecinovic, C. Loenarz, E. Flashman, K. S. Hewitson, C. Domene and C. J. Schofield, *Structure*, 2009, **17**, 981-989.
2. I. J. Clifton, M. A. McDonough, D. Ehrismann, N. J. Kershaw, N. Granatino and C. J. Schofield, *J Inorg Biochem*, 2006, **100**, 644-669.
3. H. Tarhonskaya, A. P. Hardy, E. A. Howe, N. D. Loik, H. B. Kramer, J. S. O. McCullagh, C. J. Schofield and E. Flashman, *J Biol Chem*, 2015, **290**, 19726-19742.
4. E. Flashman, L. M. Hoffart, R. B. Hamed, J. M. Bollinger, C. Krebs and C. J. Schofield, *Febs J*, 2010, **277**, 4089-4099.
5. H. Tarhonskaya, R. Chowdhury, I. K. H. Leung, N. D. Loik, J. S. O. McCullagh, T. D. W. Claridge, C. J. Schofield and E. Flashman, *Biochem J*, 2014, **463**, 363-372.
6. M. Hirsilä, P. Koivunen, V. Günzler, K. I. Kivirikko and J. Myllyharju, *J Biol Chem*, 2003, **278**, 30772-30780.
7. J. H. Dao, R. J. M. Kurzeja, J. M. Morachis, H. Veith, J. Lewis, V. Yu, C. M. Tegley and P. Tagari, *Anal Biochem*, 2009, **384**, 213-223.
8. D. Ehrismann, E. Flashman, D. N. Genn, N. Mathioudakis, K. S. Hewitson, P. J. Ratcliffe and C. J. Schofield, *Biochem J*, 2007, **401**, 227-234.
9. E. Flashman, E. A. L. Bagg, R. Chowdhury, J. Mecinovic, C. Loenarz, M. A. McDonough, K. S. Hewitson and C. J. Schofield, *J Biol Chem*, 2008, **283**, 3808-3815.
10. M. O. Landazuri, A. Vara-Vega, M. Viton, Y. Cuevas and L. del Peso, *Biochem Bioph Res Co*, 2006, **351**, 313-320.
11. A. C. Epstein, J. M. Gleadle, L. A. McNeill, K. S. Hewitson, J. O'Rourke, D. R. Mole, M. Mukherji, E. Metzen, M. I. Wilson, A. Dhanda, Y. M. Tian, N. Masson, D. L. Hamilton, P. Jaakkola, R. Barstead, J. Hodgkin, P. H. Maxwell, C. W. Pugh, C. J. Schofield and P. J. Ratcliffe, *Cell*, 2001, **107**, 43-54.
12. D. Dupuy, I. Aubert, V. G. Dupérat, J. Petit, L. Taine, M. Stef, B. Bloch and B. T. Arveiler, *Genomics*, 2000, **69**, 348-354.
13. N. Erez, M. Milyavsky, N. Goldfinger, E. Peles, A. V. Gudkov and V. Rotter, *Oncogene*, 2002, **21**, 6713-6721.
14. C. L. Cioffi, X. Qin Liu, P. A. Kosinski, M. Garay and B. R. Bowen, *Biochem Bioph Res Co*, 2003, **303**, 947-953.
15. F. Oehme, P. Ellinghaus, P. Kolkhof, T. J. Smith, S. Ramakrishnan, J. Hutter, M. Schramm and I. Flamme, *Biochem Biophys Res Commun*, 2002, **296**, 343-349.
16. R. J. Appelhoff, Y. M. Tian, R. R. Raval, H. Turley, A. L. Harris, C. W. Pugh, P. J. Ratcliffe and J. M. Gleadle, *J Biol Chem*, 2004, **279**, 38458-38465.
17. P. Koivunen, M. Hirsila, K. I. Kivirikko and J. Myllyharju, *J Biol Chem*, 2006, **281**, 28712-28720.
18. R. P. Hausinger, *Crit Rev Biochem Mol*, 2004, **39**, 21-68.

Chapter 4: Experimental verification of a proposed stable O_2 binding site adjacent to the active site: the "E-cluster"

4.1 Introduction

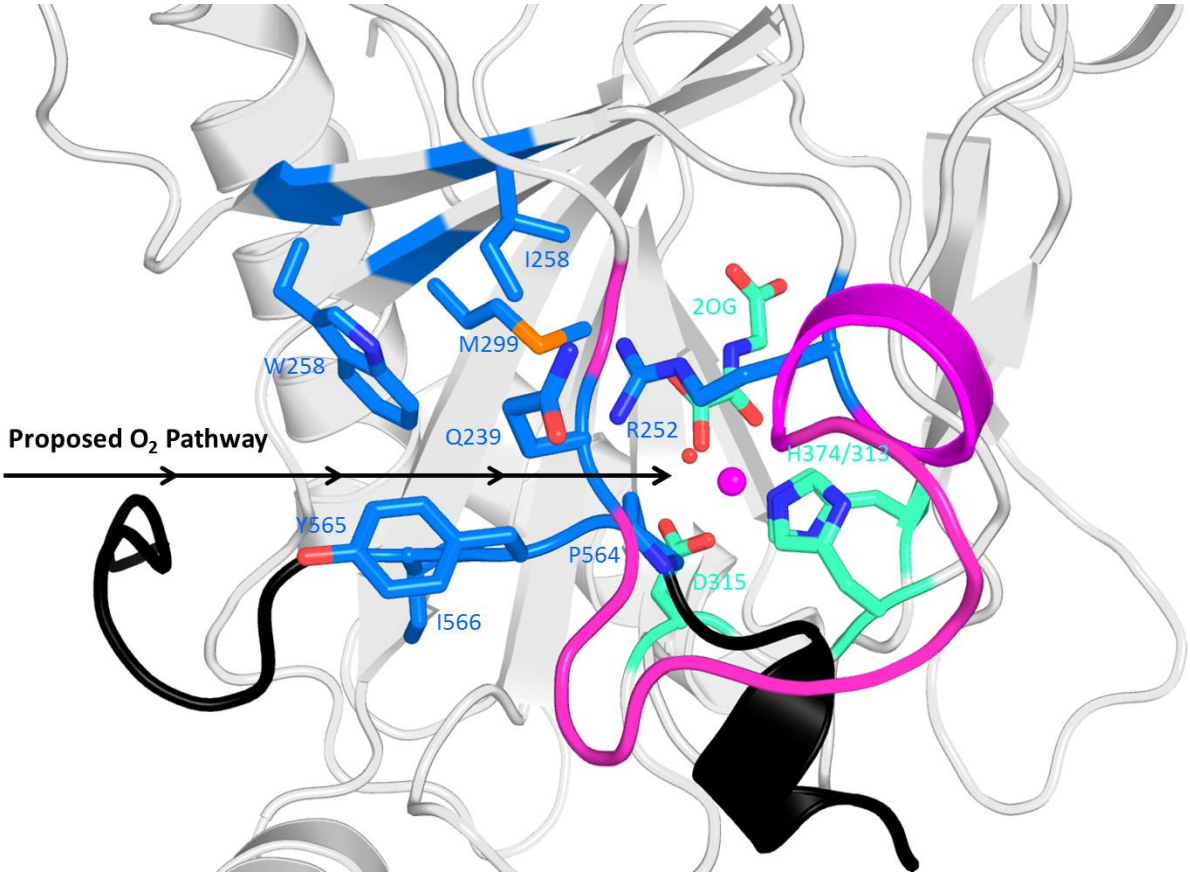

Figure 1: *The proposed O_2 pathway in PHD2, with the interacting residues in the proposed E-cluster shown in **blue**, the β2β3 loop in **pink**, CODD substrate in black and the PHD2 in **grey**. The Mn(II) at the active site is depicted here in **purple**, coordinated by the HXD…H triad in **green**. PDB ID: 3HQR* [1]

The work conducted by our collaborators, revealing a potential O_2 pathway to the PHD2 active site, suggested not only the importance of the interaction between the β2β3 loop and HIF-α in determining the diffusive entry trajectory of O_2 in the PHD2.CODD complex (supported by kinetic studies of PHD2 loop variants with respect to O_2, Ch. 3), but also identified a 'pocket' in which molecular O_2 appears to interact non-covalently 8 - 8.5 Å from the active site prior to active site entry (Fig 1 and Fig 2) – this was termed the 'E-cluster'. In

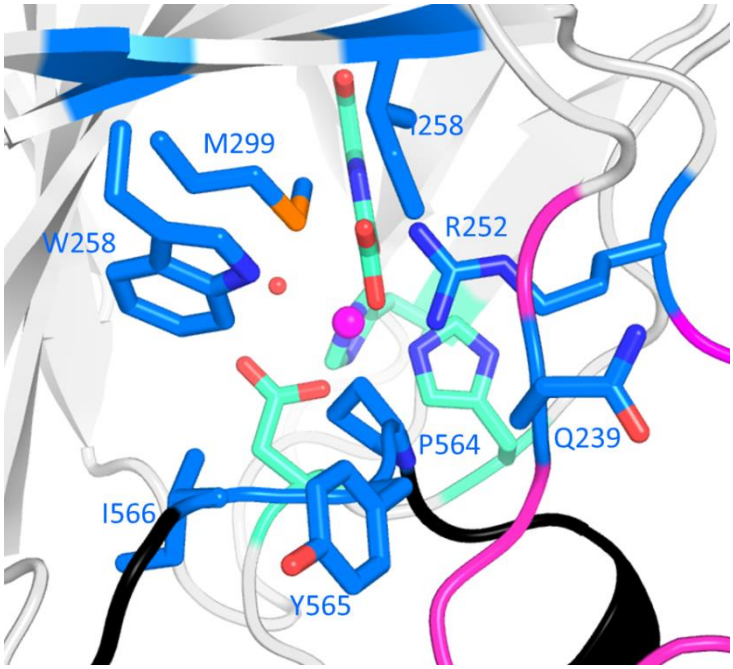

Figure 2: *A view of the proposed e-cluster shown in **blue**, the β2β3 loop in **pink**, CODD substrate in black and the PHD2 in **grey**. The Mn(II) metal centre is depicted here in **purple**, coordinated by the HXD…H triad in **green**. PDB ID: 3HQR* [1]

this "E-cluster" Adaptive Biasing Force (ABF) and non-equilibrium Steered Molecular Dynamics (SMD) MD simulations suggest O_2 is stabilized by 2.0-2.3 kcal mol^{-1} over the active site (or "G-cluster"), with the E-cluster representing the global minimum. Classical MD simulations calculated a residence time of 10^1 – 10^2 nanoseconds for O_2 in the E-cluster under the modelled conditions. This preluding E-cluster is only fully formed upon binding of the CODD substrate (Fig 1 and Fig 2) – employing the use of CODD residues tyrosine 565, isoleucine 566 and proline 564. The remaining residues contributing to the E-cluster are derived from PHD2 – methionine 299, arginine 252, tryptophan 258, isoleucine 256 and glutamine 239 with glutamine 239 and arginine 252 found on the β2β3 loop (Fig 2). The theoretical identification of this E-cluster with its proposed stability in terms of non-covalent O_2 binding may further rationalize the slow kinetics of PHD2.

The aim of the work outlined in this Chapter was to experimentally verify the proposed stabilisation of O_2 binding at the E-cluster. Techniques used to verify the proposed O_2 entry pathway and E-cluster include: site-directed mutagenesis of a key residue in the E-cluster with the investigation of the subsequent O_2 kinetics, tryptophan fluorescence quenching to

monitor interaction of O_2 with two tryptophan residues in and around the proposed E-cluster and attempting to "trap" O_2 in the E-cluster *via* laser-induced activation of O_2 to reactive O_2*, to induce O_2 reaction with local residues.

4.2 Results and Discussion

4.2.1 Site-directed mutagenesis of key amino acids – methionine 299

Site-directed mutagenesis was thought of as an effective method of de-stabilizing the proposed cluster and promoting different O_2 kinetics with respect to PHD2. The first approach was to determine whether any PHD2 variants studied previously by the C. J. Schofield or E. Flashman groups were directed at residues in the E-cluster. PHD2 M299H was identified as a known active variant (produced by E. Bagg, Part II thesis), investigated previously because Scotti *et al* reported a large difference in activity towards O_2 for a pseudomonas PHD or PPHD (48 ± 9 µM), [8] where methionine 299 is replaced by a histidine in the PPHD sequence. Methionine 299 is a key residue in the proposed E-cluster (Fig 1 and Fig 2), therefore it was rationalized that its replacement might alter PHD2 kinetics with respect to O_2. Investigations were therefore carried-out to probe the O_2 kinetics of this variant in case disruption of the E-cluster would be observed. The expression, purification and characterisation data for

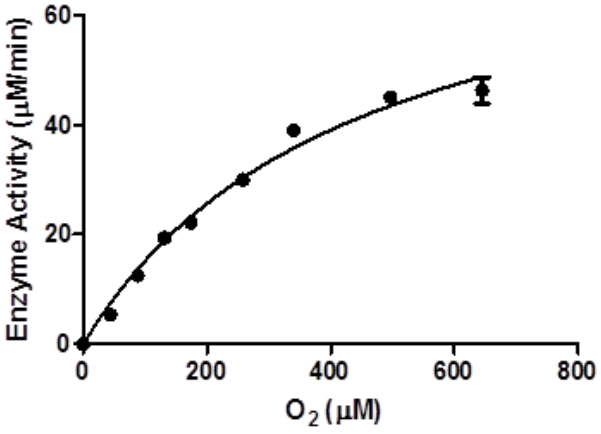

Figure 3: *$K_m^{app}(O_2)$ for the PHD2 M299H variant. $K_m^{app}(O_2)$ = 439 ± 78 µM. Conditions: 4 µM PHD2, 50 µM Fe(II), 4 mM L-ascorbate, 300 µM 2OG, 100 µM HIF-1α CODD 19-mer peptide and O_2 (5 to 80%) in Tris·HCl 50 mM, pH 7.5 at 37 °C*

the PHD2 M299H variant can be found in Chapter 2. An activity assay revealed the expressed PHD2 M299H variant to be active (Chapter 2).

The K_m^{app} (O_2) was determined according to the procedure outlined in Materials and Methods, Chapter 3. The conditions included: 4 μM PHD2, 50 μM Fe(II), 4 mM L-ascorbate, 300 μM 2OG, 100 μM HIF-1α CODD 19-mer peptide and varied O_2 concentrations (5 to 80%) in Tris·HCl 50 mM, pH 7.5 at 37 °C. The K_m^{app} (O_2) for PHD2 M299H was determined to be 439 ± 78 μM, by comparison to >450 μM for that of PHD2 WT. [3] The difference in K_m^{app} is not thought to be significant, suggesting either replacement of methionine 299 with histidine does not alter the O_2 'stabilizing' characteristics of the E-cluster or the E-cluster is not significant in O_2 kinetics.

4.2.2 Intrinsic tryptophan fluorescence of PHD2 W334F/W367F

Many spectroscopic and kinetic techniques have been used to better understand what governs PHD2's slow reaction with oxygen. [3, 9-11] While some Fe(II)/2OG oxygenases have been studied *via* intrinsic tryptophan fluorescence, [12, 13] such studies have yet to be reported for PHD2. Of the 20 naturally occurring amino acids, tryptophan, tyrosine and phenylalanine are fluorescent due to their conjugated side-chains. Tryptophan possesses an indole ring, the fluorescence of which possesses the highest quantum yield of the aromatic amino acids side chains. [14] Tryptophan residues are highly sensitive to changes in their local environment (solvent interactions, conformational changes and interactions with other residues) and as such increases in their fluorescence intensity and fluorescence quenching have been widely used to study protein conformational changes and interactions. [15-20] Tryptophan residues in proteins absorb light at 280 nm and their fluorescence emission

occurs at a maximum of 350 nm. [21] Tryptophan fluorescence in the context of a protein, however, is far more complicated as tryptophan fluorescence is highly anisotropic.[22]

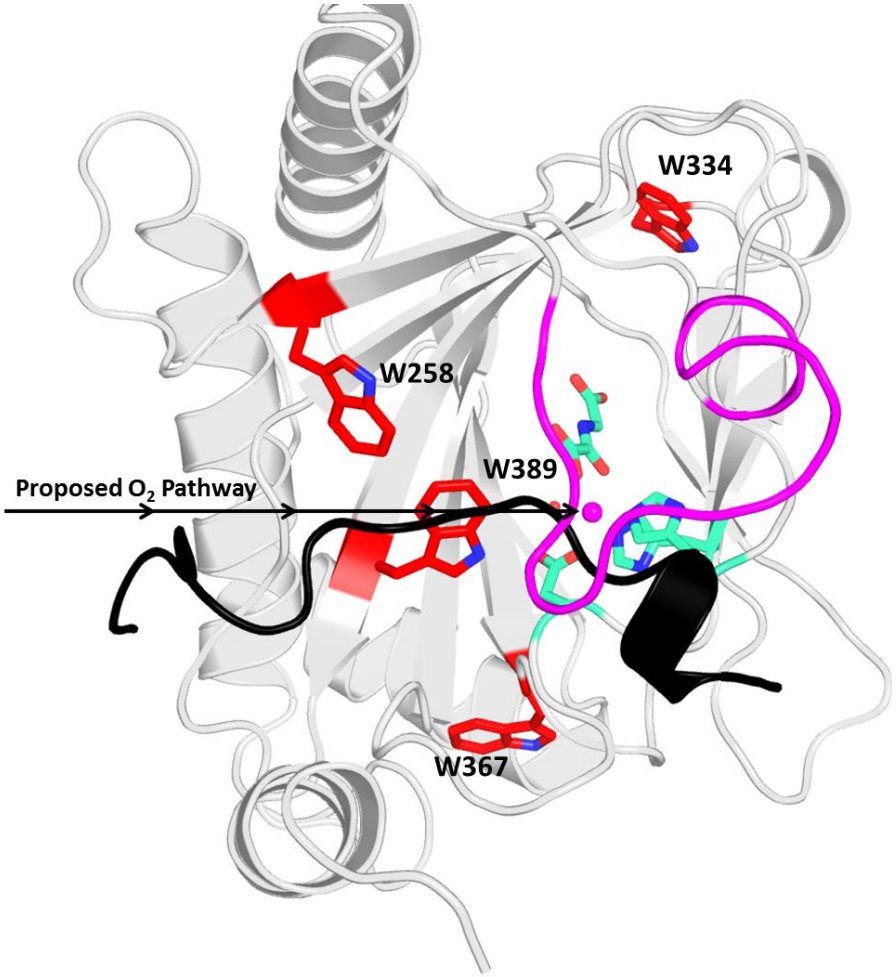

Figure 4: *View of a crystal structure of PHD2 illustrating the position of tryptophan residues relative to each other and the proposed O_2 pathway. Tryptophan residues 258, 389, 334 and 367 shown in **red**, the β2β3 loop in **pink**, CODD substrate in **black** and the PHD2 in **grey**. The Mn(II) metal centre is depicted here in **purple**, coordinated by the HXD…H triad in **green**. PDB ID: 3HQR* [1]

Fluorescence quenching occurs as a result of an excited state fluorophore interacting with a quencher. Quenchers may include substrate or O_2, or be other nearby intrinsically fluorescent residues. The quenching of intrinsic protein fluorescence can therefore be revealing, both structurally and mechanistically. [23] Large quenchers such as acrylamide [24] cannot easily penetrate a protein's structure so will selectively quench external residues, whereas smaller quenchers, like O_2, can diffuse through the protein and interact with internal residues.

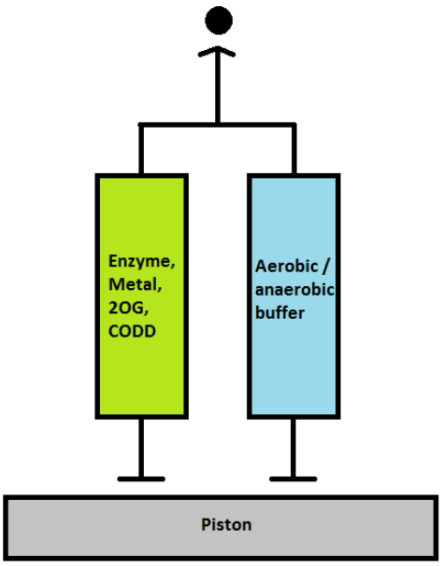

Figure 5: *A schematic of the Applied Photophysics SX20 Stopped Flow system with the separate chambers for buffer and complex storage prior to analysis. The piston moves upwards to initiate the reaction*

To elucidate certain mechanistic features of an enzyme's kinetic behaviour, stopped-flow transient kinetic analysis coupled with fluorescence allows the time-scale of such mechanistic changes to be monitored. This allows for the analysis of rate-limiting processes during the catalytic cycle. As O_2 is a known quencher, [25] observing intrinsic tryptophan fluorescence quenching upon the introduction of O_2 to a $PHD2_{variant}$.CODD.Fe(II).2OG complex could experimentally support the presence of tryptophans along the proposed O_2 entry pathway.

$PHD2_{181–426}$ has four tryptophans; W334, W367, W258 and W389, with W258 and W389 located in the proposed E-cluster (Fig 4). The other two external tryptophans have previously been mutated to phenylalanine by site directed mutagenesis to produce a PHD2 W334F/W367F variant which hydroxylates CODD at the same rate and hydroxylates NODD at a higher rate compared to WT (R. Hancock, Part II thesis). Expression, purification and characterisation data for the PHD2 W334F/W367F variant are described in Chapter 2. The pre-steady state kinetics of tryptophan fluorescence quenching were investigated, initiating by rapidly mixing anaerobic (<60 ppm O_2) PHD2.Fe(II).2OG.CODD complex with O_2 saturated buffer using an Applied Photophysics SX20 Stopped Flow system. Fluorescence quenching

was monitored using a photodiode array detector (320 nm wavelength cut-off filter for the photomulitplier tube with a monochromator excitation and emission slit width of 4 mm).

The fluorescence quenching data was analysed using Origin 8.51 software with a single exponential function $\mathbf{y = A1 * exp\left(-\frac{x}{t1}\right) + y_0}$. All tryptophan fluorescence assays were conducted at 5 °C (as per previous pre-steady state experiments conducted with PHD2), typically under the conditions 80 µM PHD2 W334F/W367F, 50 µM Fe(II) 500 µM 2OG and 100 µM CODD. Control reactions were performed in buffer that had undergone treatment with vaccum and argon to remove O_2 (deoxygenated buffer). Spectra gathered in deoxygenated buffer were subtracted from reactions with O_2-saturated buffer - to eliminate possible non-specific background interference. The fluorescence quenching rates determined here for each complex are as a result of n=3 averaged spectra, with the active PHD2 W334F/W367F.2OG.Fe(II).CODD rate constant of fluorescence quenching an average of three, n=3 spectra across two separate enzyme batches. All fluorescence curves reported here were fit with three separate single exponential functions, reflecting three apparent separate quenching steps, resulting in three fluorescence rate constants (for example see the annotated fluorescence quenching spectrum, Fig 6, **pink** line).

The first fluorescence curve to be discussed here is that of the PHD2 W334F/W367F.2OG.Fe(II).CODD active complex. The fluorescence pattern of the PHD 2 W334F/W364F catalytically active variant was monitored during catalysis – that is during the conversion of CODD to CODD-OH. The fluorescence curve generated was fit with three exponential functions, reflecting three apparent separate quenching steps, resulting in three rates of fluorescence quenching: k_1 = 0.00207 ± 0.00196 s^{-1} (~0 - 10 s),

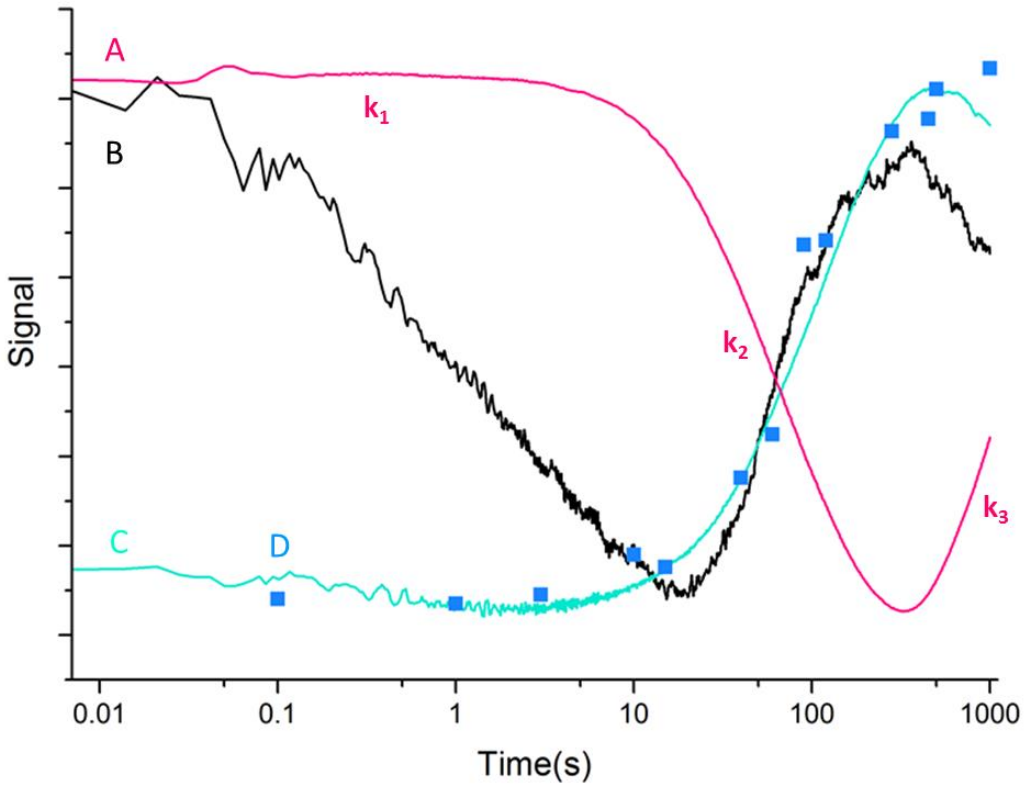

Figure 6: *A) Fluorescence quenching of PHD 2W334F/W367F in the presence of Fe, 2OG and CODD by O_2 in pink (with the fluorescence signal ranging from ~0.95 V to -0.25 V), **B**) the 520 nm shift for the consumption of PHD2.Fe(II).2OG.CODD complex and/or formation of PHD2.Fe(II).Succinate.CODD-OH complex in **black** [6] (with the negative absorption of the 520 nm species ranging from ~0.000 to 0.027 AU) C) the 310 nm iron oxidation, likely Fe(II) to Fe(III) subsequent to the productive reaction in green [6] (with the absorption of the 310 nm species ranging from ~0.00 to 0.25 AU) and D) the rate of CODD hydroxylation by PHD2 under pre-steady state conditions in blue (with CODD hydroxylation ranging from ~16% to 80%).* [3]

k_2 = 0.0127 ± 0.008 s^{-1} (~100 - 300 s) and k_3 = 0.00180 ± 0.00171 s^{-1} (300 – 1000 s), Fig 6, **pink** line. The first rate constant of fluorescence quenching, k_1, is small and appears on the curve to be part of a fluorescence quenching 'delay' –supportive of slow PHD 2 O_2 kinetics. The third rate constant (k_3), where fluorescence begins to increase after decay, correlates with PHD 2's final absorbance decay at 520 nm for the consumption of the PHD2WT.Fe(II).2OG.CODD complex and/or the formation of the PHD2WT.Fe(II).2OG.Succinate complex [3] (Fig 6, **black** line Fig 7, **B**). This increase in fluorescence observed in the 300 – 1000 s range also correlates with the formation of a 310

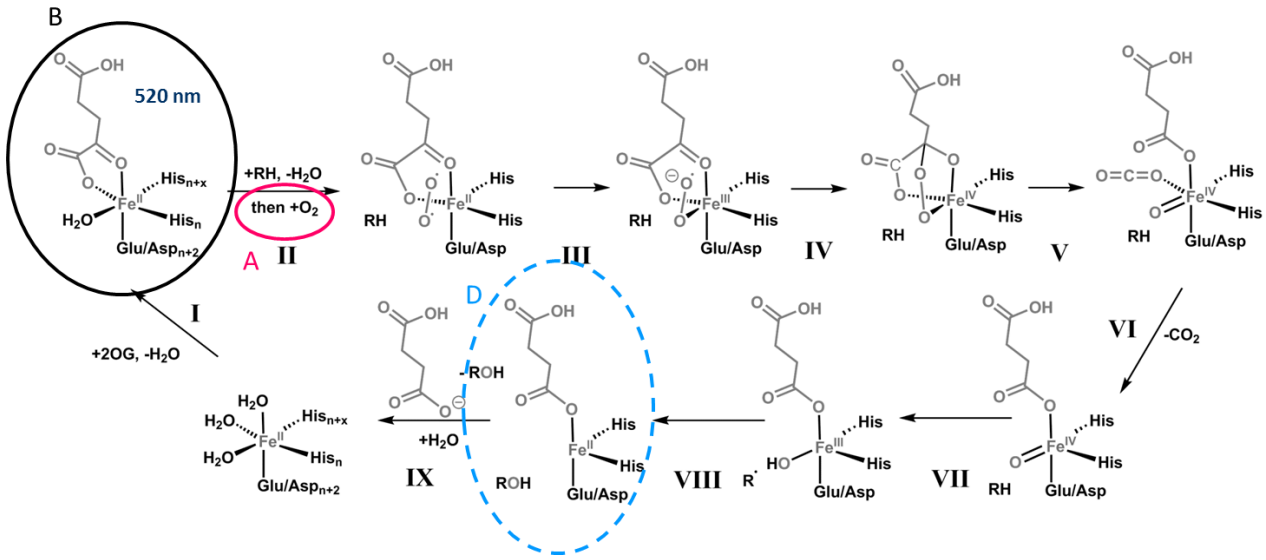

Figure 7: *Outline of the proposed mechanism of Fe(II)/2OG dependent oxygenases. Highlighted here are three of the four species and/or mechanisms reported in Fig 6.* ***A****) highlights* O_2 *entry to the active site, the propsoed source of tryptophan fluroescence quenching in the PHD 2W334F/W367F complex seen in Fig 6,* ***pink*** *line.* ***B****) Represents the absorbance decay feature at 520 nm for the consumption of the PHD2WT.Fe(II).2OG.CODD complex and/or the formation of the PHD2WT.Fe(II).2OG.Succinate complex* [3] *Fig 6,* ***black*** *line.* ***D****) Highlights the formation of hydroxylated CODD product as illustrated in Fig 6,* ***blue*** *data points. The fourth spectrum on Fig 6,* ***green*** *line, representing the 310 nm absorbance feature is not highlighted here, as it has not been fully elucidated as to which species formation it represents. It has been proposed to be the oxidation of Fe(II) to Fe(III) as it corresponds with the 520 nm absorbance decay of species* ***B****.*

nm species proposed to be the oxidation of Fe(II) to Fe(III) subsequent to the productive reaction [3] (Fig 7, **green** line) – i.e. *not* part of the catalytic pathway. The second rate constant is believed to reflect the productive catalysis in the active PHD2 W334F/W367F.2OG.Fe.CODD complex – that is the conversion of CODD to CODD-OH. This is supported by comparing the rate constant of fluorescence quenching generated here, k_2 = 0.0127 ± 0.008 s^{-1}, to the rate of CODD hydroxylation by PHD2 WT under similar pre-steady state conditions; 0.0095 ± 0.0012 s^{-1} [3] (Fig 6, **blue** data points and Fig 7, **D**). The k_2 rate constant value, therefore, was chosen to compare fluorescence quenching rate constants across the various complexes to be reported later.

The fluorescence quenching rate constant, k_2, generated for the PHD2W334F/W367F.2OG.Fe(II).CODD active complex indicates a quenching reagent comes

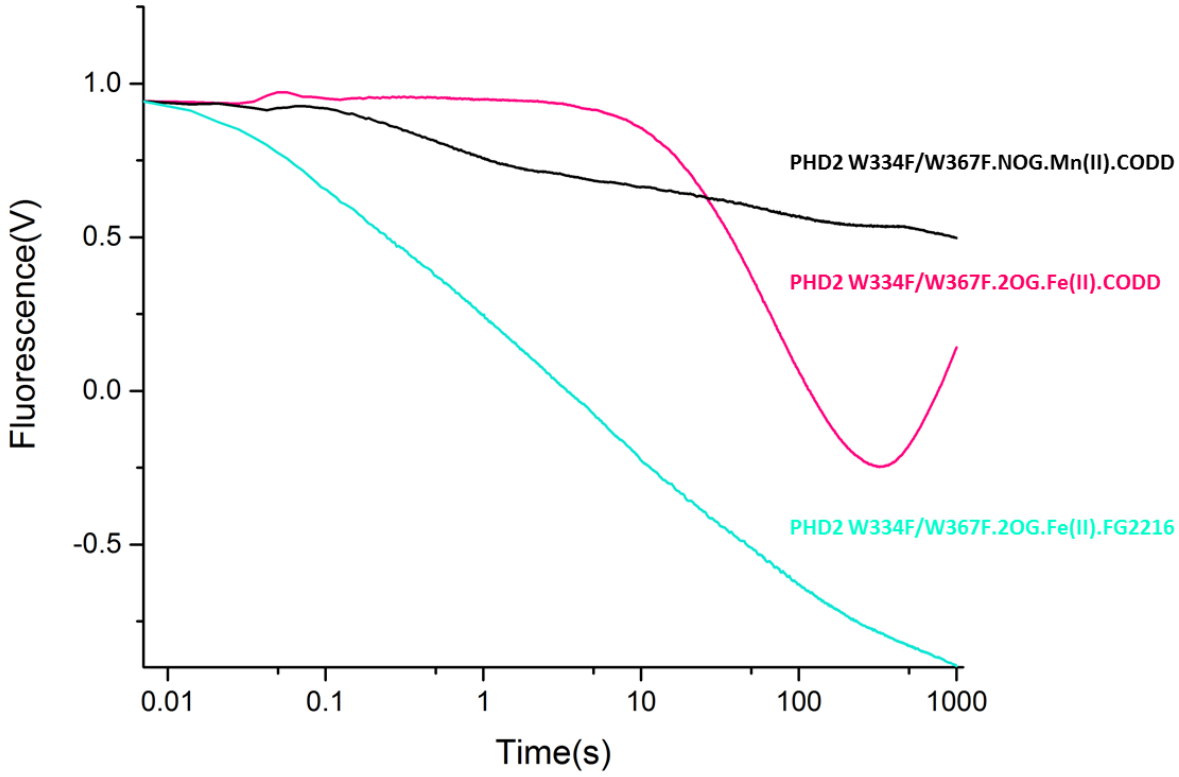

Figure 8: *Fluorescence quenching of PHD 2W334F/W367F in the presence of Fe, 2OG and CODD by O_2 in **pink,** PHD 2W334F/W367F in the presence of Fe, 2OG and FG-2216 in **green** and PHD 2W334F/W367F in the presence of Mn(II), NOG and CODD in **black**. The FG-2216 and Mn(II).NOG quenching patterns differ significantly from that of the active complex. Measured using SX20 Stopped-flow, at 5°C, under anaerobic conditions (<60 ppm O_2).*

into close proximity to tryptophan residues 258 and 289 during the course of PHD 2 W334F/W367F catalysis. Overall, this data is supportive of the presence of tryptophan 258 and 389 along PHD2's O_2 uptake pathway, but suggests that the delayed O_2 kinetics of the PHD2 reaction occurs prior to tryptophan fluorescence quenching. As tryptophans 258 and 389 are part of the proposed E-cluster, these results suggest the E-cluster may not kinetically hinder the reaction with O_2. It is acknowledged that succinate release could induce tryptophan fluorescence quenching. To eliminate this possibility, another control mechanism using succinate saturated solvent would have to be conducted.

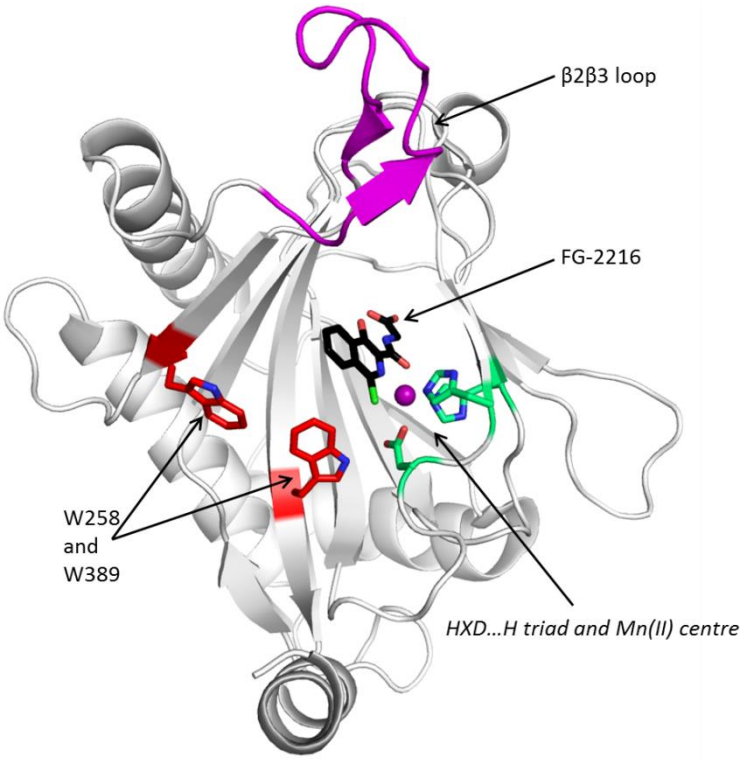

Figure 10: *PHD2 bound to FG-2216, a known CODD inhibitor. with tryptophan 258 and 389 shown in **red**, the β2β3 loop in **pink**, CODD substrate in black and the PHD2 in grey. The Mn(II) metal centre is depicted here in **purple**, coordinated by the HXD…H triad in **green**. This illustrates the different, β2β3 loo conformation upon FG-2216 binding, a direct contrast of the "fixed" CODD binding position.PDB ID: 4BQX* [2]

To verify that the tryptophan fluorescence quenching observed for the PHD2W334F/W367F.2OG.Fe(II).CODD complex was related to the possible catalytically relevant reaction with O_2, Fe(II), 2OG and CODD were replaced with other metals or 2OG and CODD analogues, respectively, to render the complex catalytically inactive (Fig 8 and 10). The first inactive analogue to be studied was the PHD2 W334F/W367F.**NOG**.**Mn(II)**.CODD complex. NOG is a known inhibitor of PHD2 [26, 27] (Fig 11, B) and analogue of 2OG (Fig 11, A). NOG, together with Mn(II), are the cofactors used in the PHD2-CODD crystal structure. [28] As the molecular modelling studies - in which the E-cluster theory is rooted - are based upon this crystal structure, it was thought prudent to try and observe the interaction of O_2 with the PHD2 W334F/W367F.**NOG**.**Mn(II)**.CODD complex (Fig

8, **black** line). The fluorescence curve was, once again, fit with three exponential functions resulting in three fluorescence rate constants: k_1 = 1.3723 ± 0.0133 s^{-1} (0-5 s),

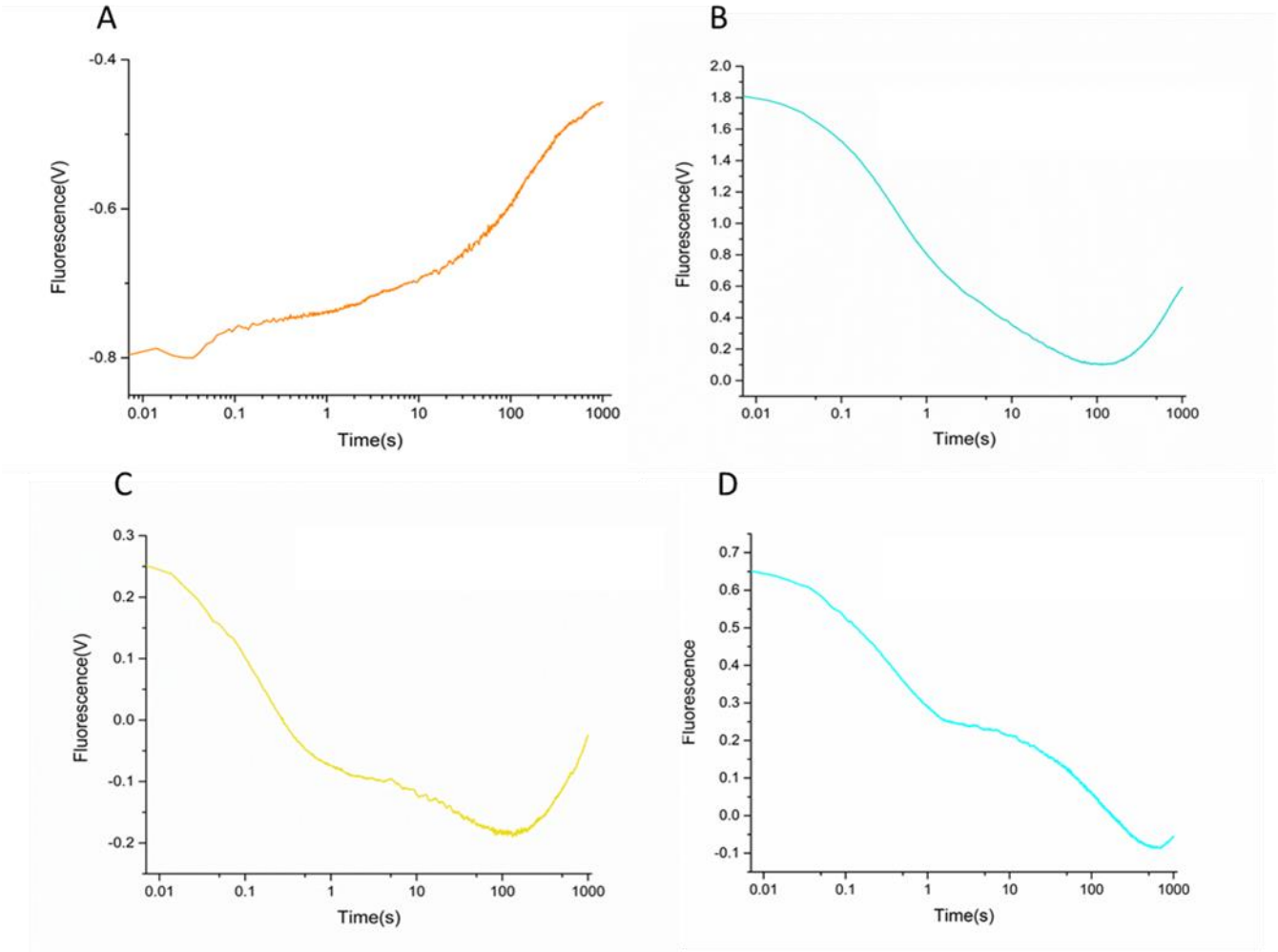

Figure 11: *Fluorescence quenching of A) the inactive PHD 2W334F/W367F.2OG.Zn(II).CODD complex in* ***orange****, B) the inactive PHD 2W334F/W367F.2OG.Mn(II).CODD complex in* ***green****, C) the inactive PHD 2W334F/W367F.NOG.Zn(II).CODD complex in* ***yellow*** *and D) the inactive PHD 2W334F/W367F.NOG.Fe(II).CODD complex in* ***blue****. Measured using SX20 Stopped-flow, at 5°C, under anaerobic conditions (<60 ppm* O_2*).*

k_2 = 0.0251 ± 0.004 s^{-1} (5-300 s) and k_3 = 0.00028 ± 0.00011 s^{-1} (300-1000 s). Both the k_1 and k_2 values are larger than that of the active complex, with a gradual fluorescence quenching commencing ~10 s earlier than that which was observed for the active complex. The reduced amplitude of fluorescence quenching likely reflects O_2 passage towards the active

site but suggests there is less direct interaction with the tryptophans than in the active complex.

The third inactive analogue of interest was the PHD2 W334F/W367F.2OG.Fe(II).**FG2216** complex. FG-2216 is a known inhibitor of PHD2, preventing CODD peptide binding [29] to PHD2, stabilizing the β2β3 loop in an open confirmation [2] (Fig 9) - a contrast to the "fold" structural change observed upon the binding of CODD to PHD2 (Chapter 3, Fig 1). The tryptophan fluorescence quenching curve observed for a PHD2 W334F/W367F.2OG.Fe(II).**FG2216** complex was again fit with three exponential functions, k_1 = 2.5319 ± 0.0556 s^{-1} (0-1 s), k_2 = 0.141 ± 0.0025 s^{-1} (1-500 s) and k_3 = 0.0079 ± 0.0001 s^{-1} (500-1000 s). This complex demonstrated significant fluorescence quenching upon the introduction of O_2 (Fig 8, **green** line), with a k_1 and k_2 and amplitude much greater than those reported for either the PHD2 W334F/W367F.2OG.Fe(II).CODD or PHD2 W334F/W367F.**NOG**.**Mn(II)**.CODD complexes. This is consistent with the PHD2.FG-2216 crystallographic information (Fig 9), where the β2β3 loop is stabilized in the "mobile" position upon the binding of FG-2216. This exposes the tryptophans to the bulk O_2 saturated solvent and therefore potentially an increased number of quenching O_2 molecules compared with the "folded" position of the β2β3 loop in the PHD2 W334F/W367F.2OG.Fe(II).CODD and PHD2.**NOG**.**Mn(II)**.CODD complexes. The spectra in Fig 8 show not only the

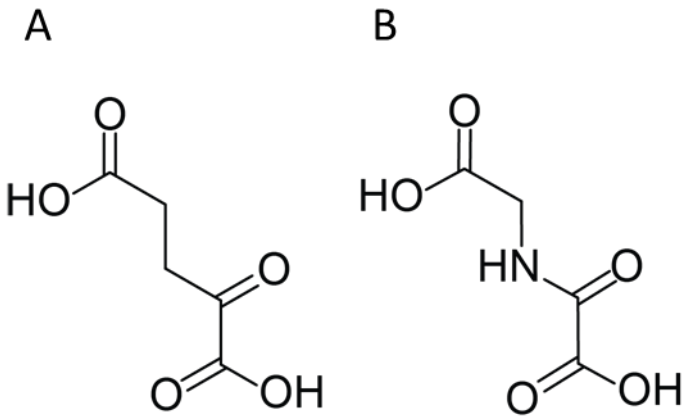

Figure 12: *A) PHD2 co-factor: 2-oxoglutarate and B) known PHD2 inhibitor: N-oxalylglycine*

fluorescence quenching pattern for the active PHD2W334F/W367F.2OG.Fe(II).CODD complex is unique, it illustrates how certain structural features can be inferred from fluorescence quenching patterns. For example the PHD2W334F/W367F.FG-2216 complex was expected to have a high amplitude of fluorescence quenching due to the "mobile" positioning of the β2β3 loop exposing tryptophans 258 and 289 to more quenching species. This observation was nicely reflected by the measured fluorescence quenching pattern.

To ensure no one particular co-factor was responsible for the various quenching patterns observed for the inactive complexes, and to see if a similar quenching pattern for the inactive PHD2.2OG.**Zn(II)**.CODD complex chosen for singlet state O_2 experiments (next section) could be observed, a further series of controls were conducted (Fig 10). Interestingly, the PHD2W334F/W367F.2OG.**Zn(II)**.CODD complex yielded an increase in fluorescence upon the introduction of O_2 suggesting the tryptophans are not exposed to bulk solvent in the complex (Fig 10, A). The PHD2W334F/W367F.**NOG.Zn(II)**.CODD complex, however, exhibited clear fluorescence quenching upon the introduction of O_2 (Fig 10, C). This implies two possibilities: experimental error or the relative combinations of NOG, 2OG and Zn(II) facilitate or restrict tryptophan accessibility. In contrast, both the PHD2W334F/W367F.2OG.**Mn(II)**.CODD and PHD2W334F/W367F.**NOG**.Fe(II).CODD complexes (Fig 10, B and D respectively) are comparable to the PHD2W334F/W367F.**NOG**.**Mn(II)**.CODD complex quenching pattern (Fig 8, **black** line).

4.2.3 Laser-excitation of molecular O_2 to covalently modify amino acids present at the E-cluster

Further to tryptophan fluorescence studies, it was thought that singlet state O_2 could be used to react with and confirm residues in regions of local O_2 stability in PHD2 and thus confirm the existence of the E-cluster. Molecular O_2 can undergo excitation, transitioning from its ground triplet state to its excited singlet state. Molecular O_2 has the $(1\pi g)^2$ configuration with two unpaired electrons in the π^* orbitals. Hence, the ground state of the O_2 molecule is a triplet state. Excitation of molecular O_2 results in an intersystem crossing transition from ground state T_1, to an excited S_1, or O_2^* state. As the T-S transition and spin states are strictly forbidden (or *vice versa*), singlet state O_2 is highly reactive and as such has been reported as a tool to probe enzyme structure and identify important residues involved in reactivity. [30]

Sensitizers such as fluorescein dyes, methylene blue, and polycyclic aromatic hydrocarbons, are compounds which are able to absorb light transitioning from a ground to an excited state and then transfer that energy to molecular O_2, inducing a photooxidation process. The use of light has been reported to excite O_2 with, [7, 31] and without [4, 5, 32] the use of a sensitizer. The no-sensitizer approach was favoured as a starting point as it negates the use of another reagent in the system. It is acknowledged that a sensitizer is unlikely to affect the PHD2.Metal.2OG.CODD complex, but in the absence of certainty, caution was exercised. Therefore laser excitation of O_2 with and without the use of a sensitizer in the presence of a PHD2.Metal.2OG.CODD complex was attempted. Neodymium-yttrium-aluminium garnet

(Nd-YAG) and dye lasers have been reported as means by which to produce singlet O_2 at a wavelength of 1064 nm. [5, 7]

An alternative metal to Fe(II) was used so as to avoid product turnover and maintain a stable PHD2.Metal.2OG.CODD complex. Zinc was chosen as the metal centre for the PHD2.Metal.2OG.CODD complex as it is known to form a stable inactive complex with PHD2 and 2OG (I. Leung, personal communication).

The complex was exposed to a range of laser intensities and frequencies in an effort to oxidize residues local to regions of O_2 stability in the PHD2.Zn.2OG.CODD complex (see Materials and Methods). The experiment was followed by analysis of CODD by MALDI-MS and analysis of PHD2 by LC-MS to look for oxidative modifications. Should the LC-MS results have revealed oxidation events in PHD2, it was anticipated the identity of the oxidized amino acids could then be revealed by trypsin digestion and LC-MS/MS. Alongside the PHD2.Zn.2OG.CODD complex, a series of control complexes were also analysed, namely "no-enzyme", "no-O_2", "no CODD" and "no laser". This was to ensure any observed oxidation events were as a result of photo oxidation. Lasers were provided by Prof Claire Vallance, with technical help gratefully received from Dr Simon-John King and Mr Dean James.

4.2.3.1 Experiment 1.0

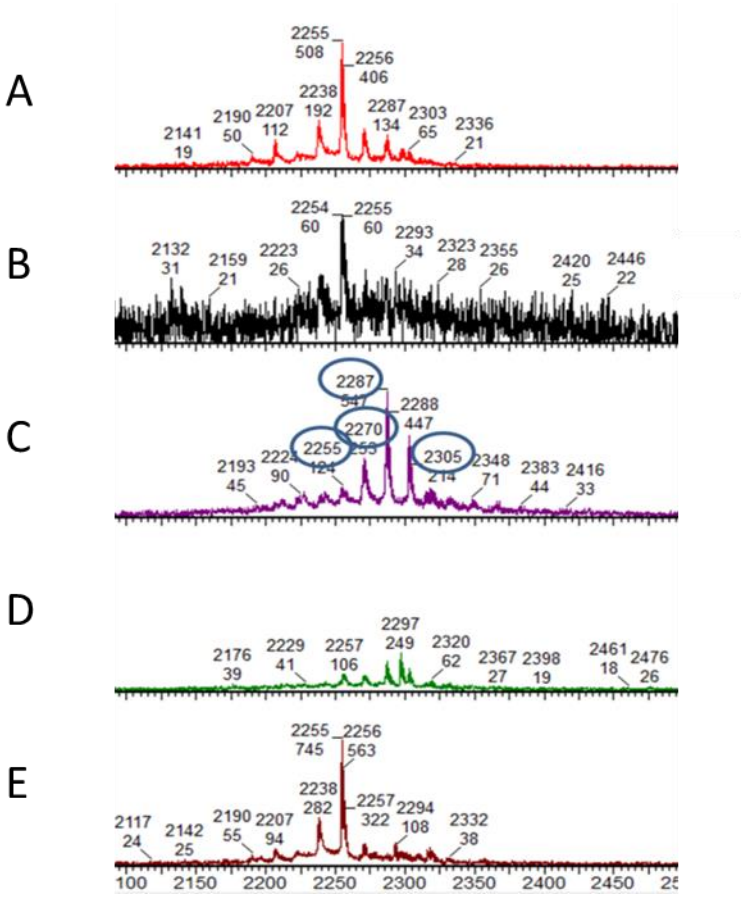

Figure 13: *MALDI-TOF spectra of CODD for laser experiment 1.0 with, A) No laser, B) No O_2, C) No enzyme, D) No CODD and E) the PHD2.Zn.2OG.CODD sample. All samples, with the exception of the "No laser" contol, were exposed to 500 Hz for 10 s at 2 mJ pulse^{-1} at 1064 nm. exposed to 500 Hz for 10 s at 2 mJ pulse^{-1} at 1064 nm.*

In experiment 1.0 (see MM), complexes were subjected to 500 Hz for 10 s at 2 mJ pulse^{-1} at 1064 nm [4] using an NL 202 Nd-YAG laser source. Each control and the PHD2.2OG.Zn(II).CODD complex were subsequently analysed by MALDI-TOF and LC-MS. Fig 11 shows resulting MALDI-MS spectra of CODD; $CODD_{19mer}$ peptide has a MW of 2255 Da, with +16, +32 and +48 Da modifications presenting as 2271, 2287 and 2305 Da respectively. Interestingly, in the 'no-enzyme' control, CODD species +16, +32 and +48 Da peaks were observed indicating oxidation of some CODD residues. It is possible these oxidation events correspond to the oxidation of CODD's two methionine residues to methionine sulfoxide and methionine sulfone. No other CODD oxidation events were observed in this experiment. The lack of oxidation of CODD in the presence of enzyme (Fig 11, E) suggests the protein may "shield" CODD from modification and/or the CODD substrate is still bound to the enzyme and therefore unobservable by

MALDI-TOF MS. The enzyme-containing samples exhibited significant oxidation in LC-MS analysis (Fig 12 and Fig 13), with the exception of the “No-laser” control. The oxidation events observed are consistent with the oxidation of 4 cysteine and 7 methionine residues present in the $PHD2_{181-426}$ catalytic domain (Fig 13, A). This result was never repeated throughout the various laser experiments. The laser experiment was repeated using alternative energies and frequencies in an effort to oxidize PHD2.

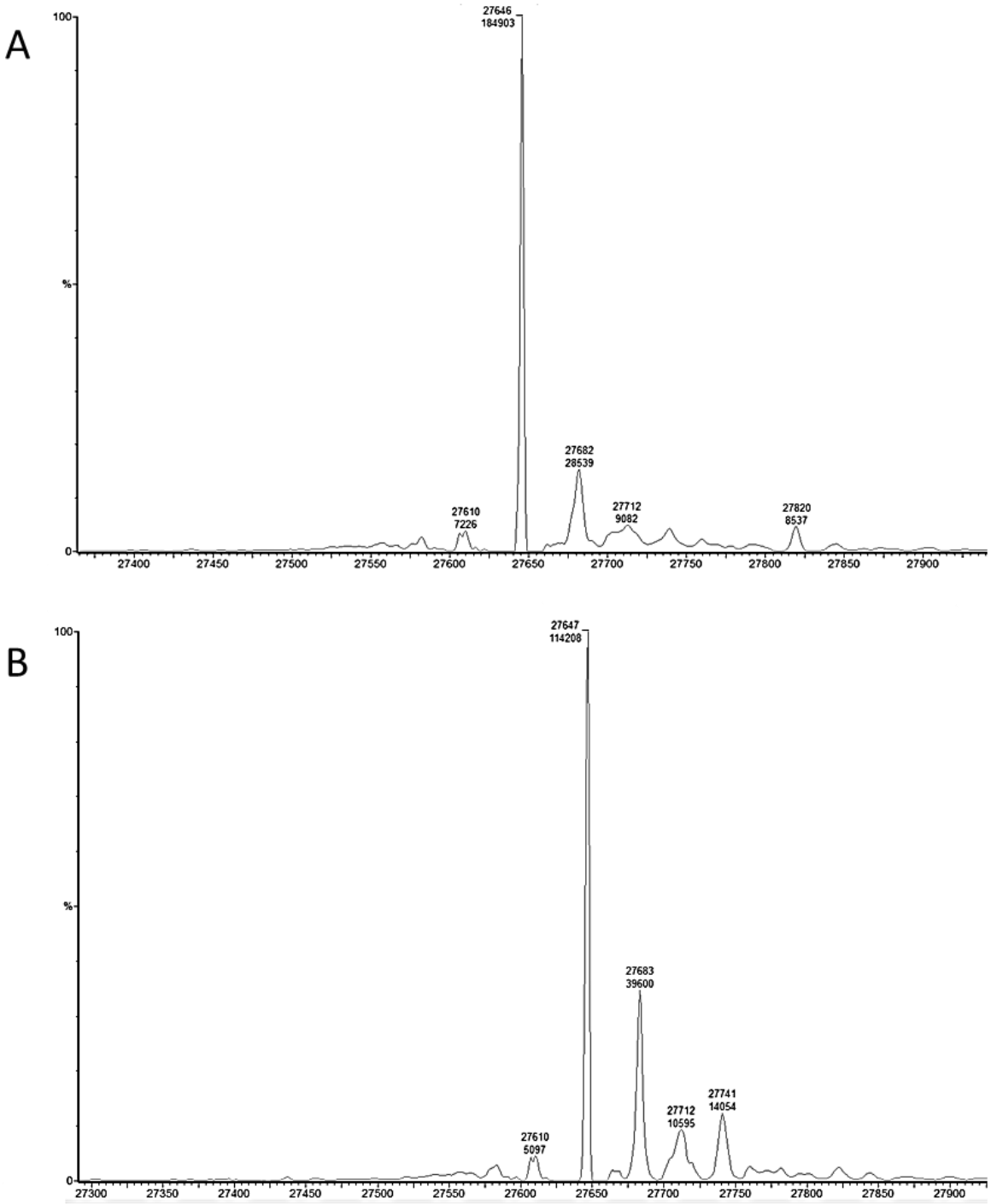

Figure 14: *LC-MS spectra of PHD2 from experiment 1.0. A) PHD2.2OG.Zn(II) (No CODD) and B) PHD2.2OG.Zn(II).CODD (No O_2) controls. Each sample was exposed to 500 Hz for 10 s at 2 mJ pulse^{-1} at 1064 nm using an NL 202 Nd-YAG laser source.* [4] *The expected molecular weight of PHD2 is 27.64 kDa.*

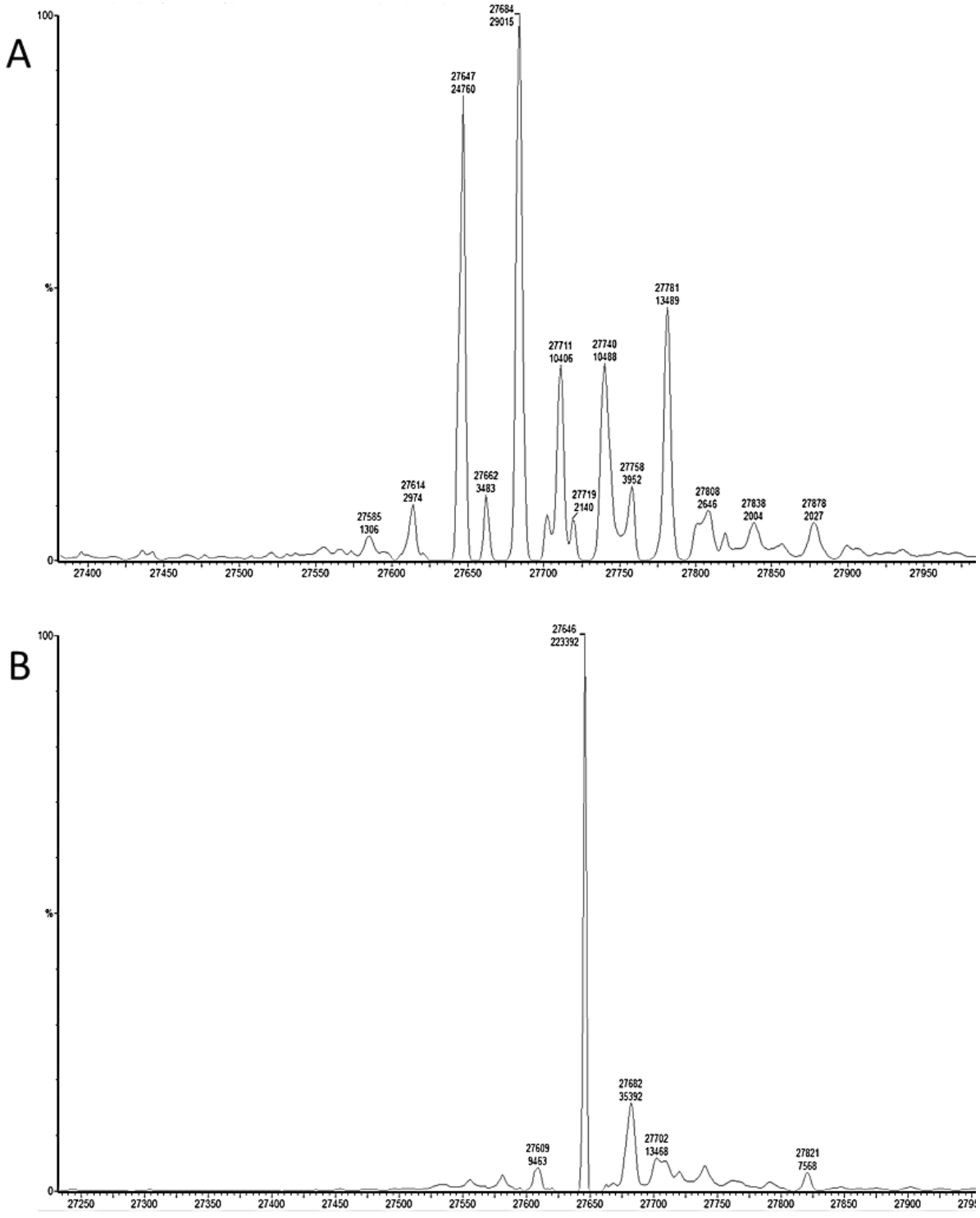

Figure 15: *LC-MS spectra of PHD2 from experiment 1.0. A) PHD2.2OG.Zn(II).CODD (No laser control) and B) the PHD2.Zn(II).CODD.2OG complex. Each sample, with the exception of the "no-laser" control, was exposed to 500 Hz for 10 s at 2 mJ pulse^{-1} at 1064 nm using an NL 202 Nd-YAG laser source.* [4] *The expected molecular weight of PHD2 is 27.64 kDa.*

4.2.3.2 Experiment 1.1

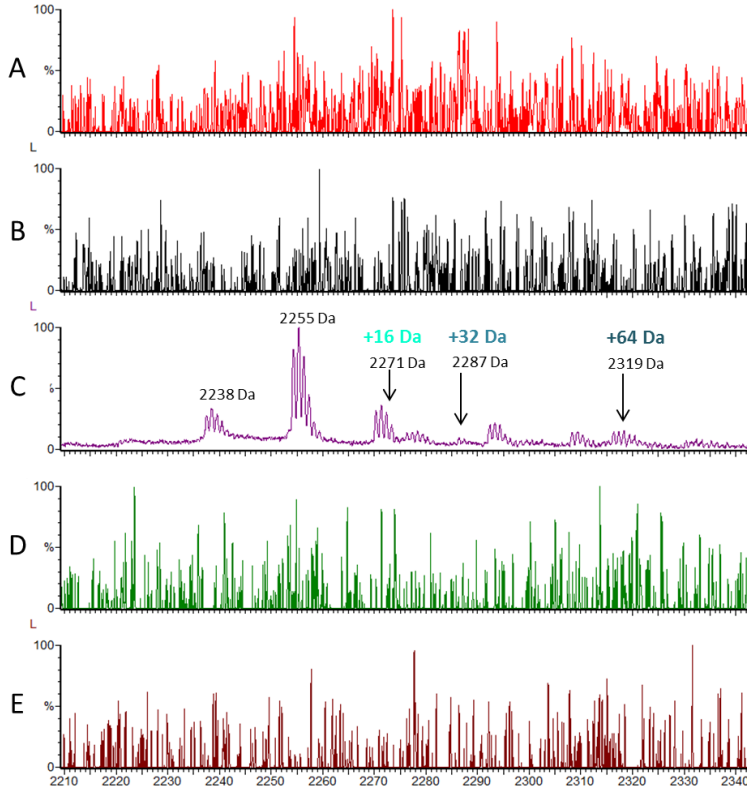

Figure 16: *MALDI-TOF spectra of CODD for laser experiment 1.1 with, A) No laser, B) No O_2, C) No enzyme, D) No CODD and E) the PHD2.Zn.2OG.CODD sample. All samples, with the exception of the "No laser" contol, were exposed to 1000 Hz for 10 s at 2 mJ pulse^{-1} at 1064 nm.*

For experiment 1.1 (see Materials and Methods), the PHD2.Zn.2OG.CODD complex underwent prolonged exposure at a higher frequency (1000 Hz for 10 min at 2 mJ pulse^{-1}) using the same NL202 Nd-YAG, 1064 nm source as in experiment 1.0. The MALDI-TOF spectra of CODD revealed a similar oxidation pattern for the "no-enzyme" control, with no CODD at all observed in the other spectra (Fig 14). This lends credence to the hypothesis that the majority of CODD remains bound to PHD2 during MALDI-TOF analysis - possibly due to the stability of the inactive PHD2.Zn.2OG.CODD complex.

To rule-out this possibility a series of separation techniques were attempted in an effort to separate CODD from PHD2. This was done using i) 500 mM NaCl to try and unfold PHD2 and release CODD ii) heating at 180 °C for 3 min to thermally denature PHD2 iii) mixing with 1:1 1% trifluoroacetic acid again, to denature PHD2 and iv) mixing with 500 mM NaCl and filtered in a 10k MWCO tube to separate denatured PHD2 from CODD with the "no-enzyme" sample used as a control. None of the techniques yielded observable CODD via subsequent

MALDI-TOF analysis (results not shown). No protein oxidation events were observed via LC-MS (Fig 15 and 16).

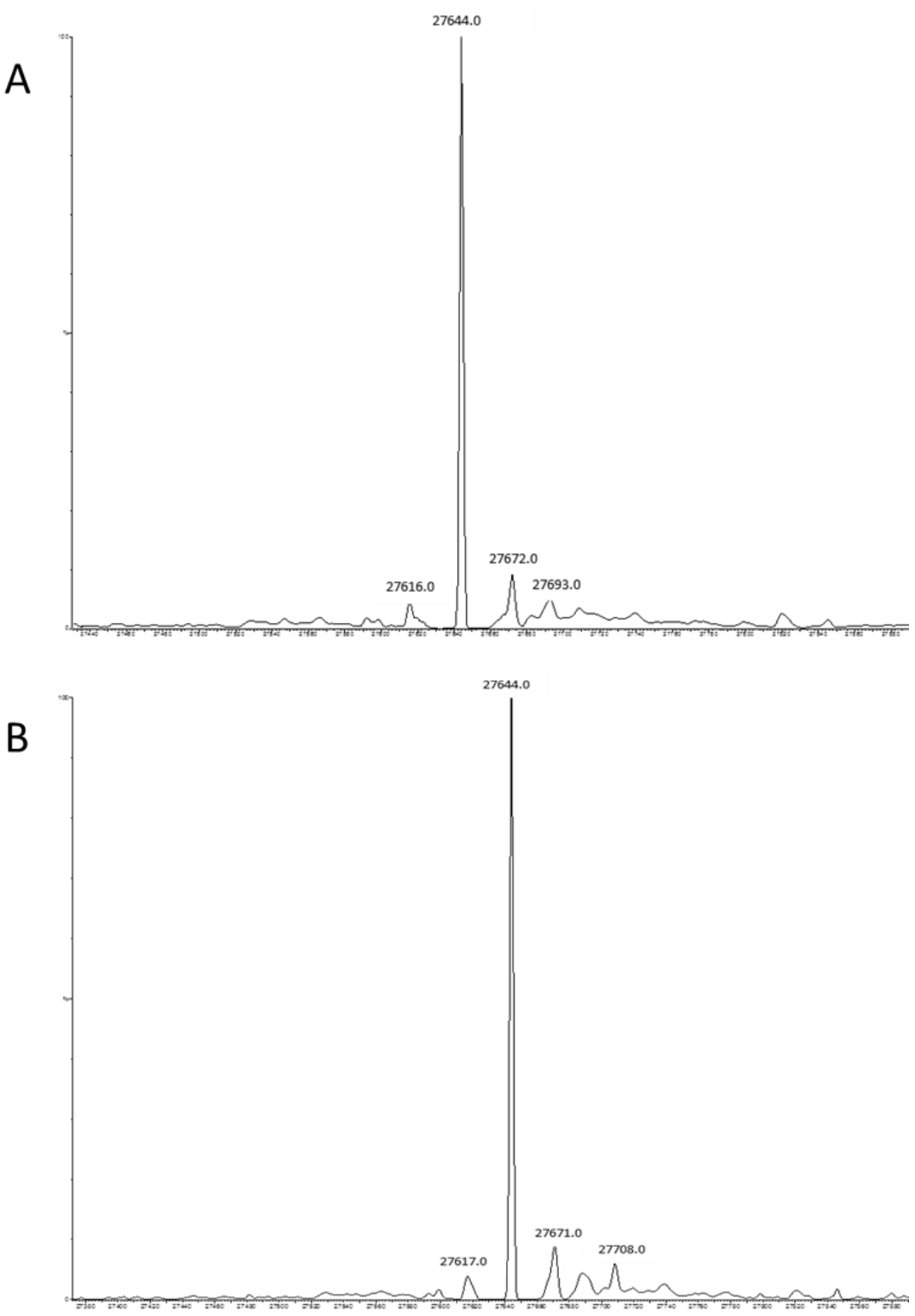

Figure 17: *LC-MS spectra of PHD2 from experiment 1.1. A) PHD2.2OG.Zn(II) (No CODD) and B) PHD2.2OG.Zn(II).CODD (No O_2) controls. Each sample was exposed to 500 Hz for 10 min at 2 mJ pulse^{-1} at 1064 nm using an NL 202 Nd-YAG laser source.* [4] *The expected molecular weight of PHD2 is 27.64 kDa.*

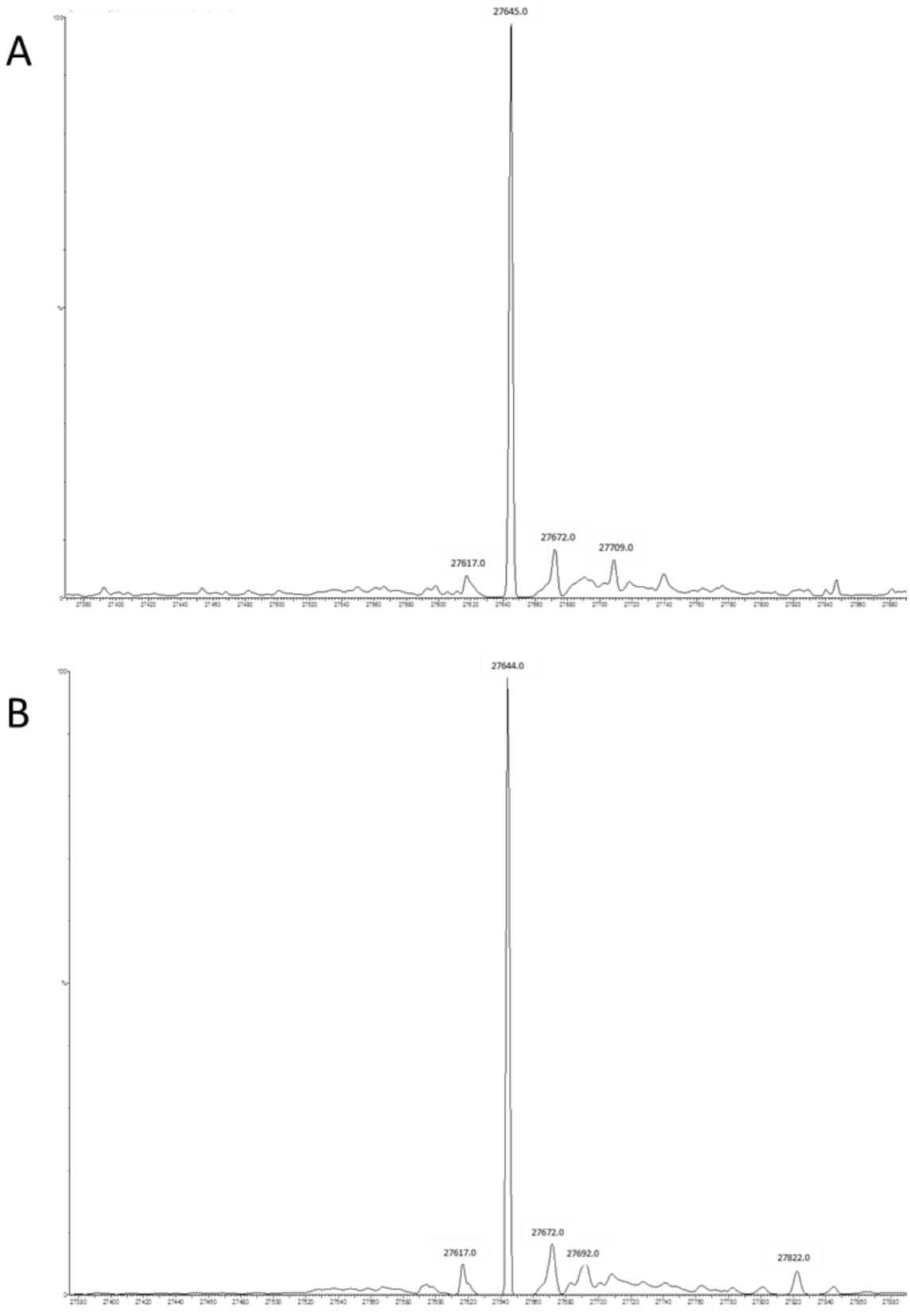

Figure 18: *LC-MS spectra of PHD2 from experiment 1.1. A) PHD2.2OG.Zn(II).CODD (No laser control) and B) the PHD2.Zn(II).CODD.2OG complex. Each sample, with the exception of the "no-laser" control, was exposed to 500 Hz for 10 min at 2 mJ pulse^{-1} at 1064 nm using an NL 202 Nd-YAG laser source. [4] The expected molecular weight of PHD2 is 27.64 kDa.*

4.2.3.3 Experiment 2.0

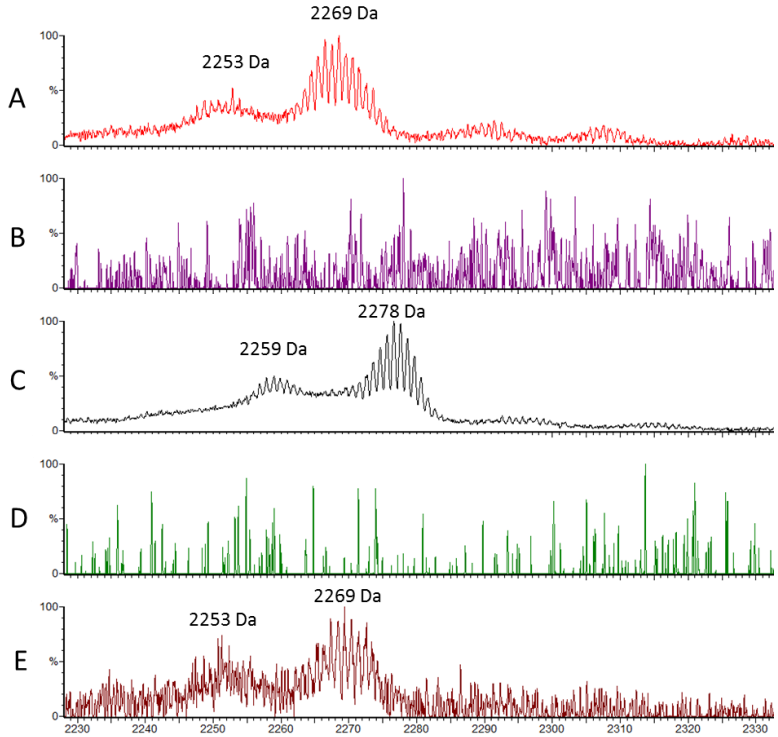

Figure 19: *MALDI-TOF spectra of CODD for laser experiment 2.0 with, A) No laser, B) No O_2, C) No enzyme, D) No CODD and E) the PHD2.Zn.2OG.CODD sample. All samples, with the exception of the "No laser" contol, were exposed to 10 Hz for 26 min 40 s at 0.376 J pulse^{-1}.*

To further attempt to promote oxidation of PHD2 by laser excitation of O_2, the solvent was adjusted to include D_2O as it is reported to prolong the lifetime of O_2*. [5, 31, 32] The complex was exposed to 10 Hz for 26 min 40 s at 0.376 J pulse^{-1}. The total energy input was increased in accordance with experiments carried-out by Singh *et al,* [5] increasing the total energy input to 6016 J, at 10 Hz. The total energy input and frequency used here is slightly lower than that recommended by Singh *at al* due to instrument hardware restrictions changing the frequency and energy measurement error. The experiment yielded inconclusive results for oxidation events on CODD due to the complex isotope distribution (Fig 17), however LC-MS indicated a small proportion of PHD2 appeared to be oxidized in both the controls and the PHD2.Zn.2OG.CODD "sample" (Fig 18 and 19). Unfortunately the mass increases were present in all the controls as well as the sample. The mass increases ranged from +64 to +176 Da; consistent with the oxidation of 4 methionine and 7 cysteine

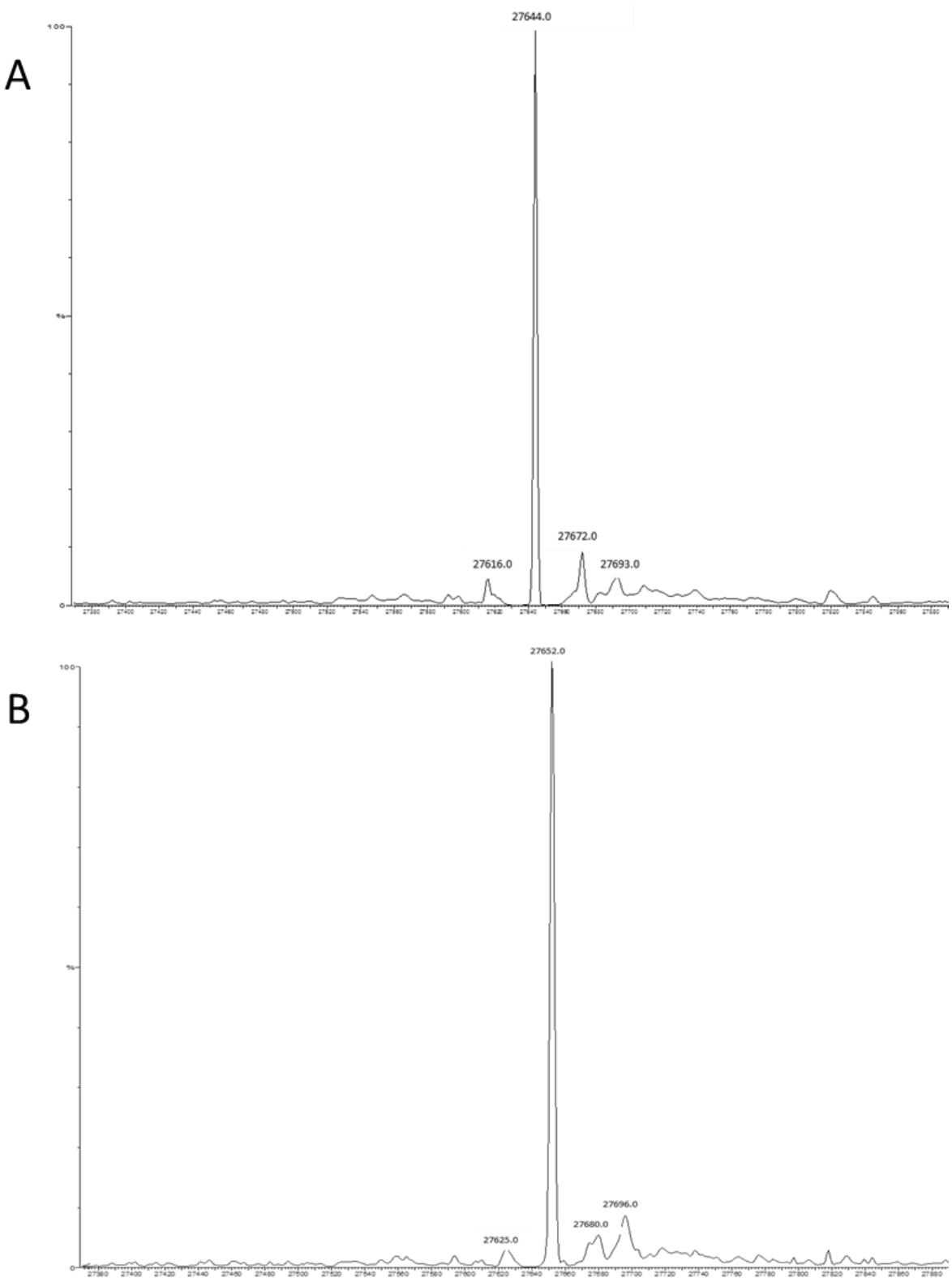

Figure 20: *LC-MS spectra of PHD2 from experiment 2.0. A) No CODD and B) No O_2 controls.. LC-MS spectra of PHD2 from experiment 1.1. A) PHD2.2OG.Zn(II) (No CODD) and B) PHD2.2OG.Zn(II).CODD (No O_2) controls. Each sample was exposed to 10 Hz for 26 min 40 s at 0.376 mJ pulse^{-1} at 1064 nm using a Sirah Cobrah Stretch, 300 mJ/~5 ns pulse using Coumarin 450 laser dye pumped by a third harmonic of a Nd-YAG laser (continuum Surelite II).* [7] *The expected molecular weight of PHD2 is 27.64 kDa.*

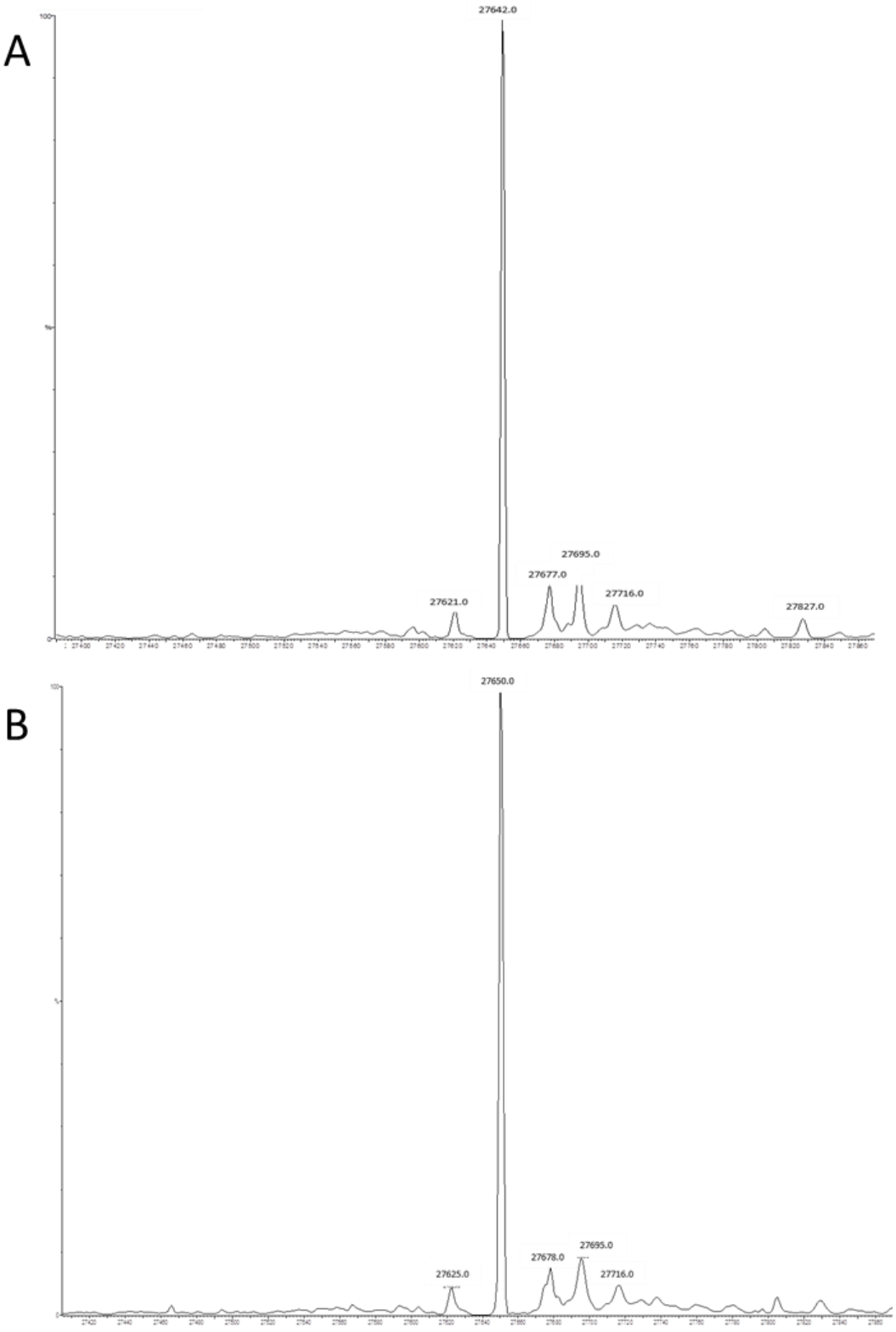

Figure 21: *LC-MS spectra of PHD2 from experiment 2.0. A) PHD2.2OG.Zn(II).CODD (No laser control) and B) the PHD2.Zn(II).CODD.2OG complex. Each sample, with the exception of the "no laser" control, was exposed to 10 Hz for 26 min 40 s at 0.376 J pulse^{-1} using a Sirah Cobrah Stretch, 300 mJ/~5 ns pulse using Coumarin 450 laser dye pumped by a third harmonic of a Nd-YAG laser (continuum Surelite II).* [7] *The expected molecular weight of PHD2 is 27.64 kDa.*

residues present in $PHD2_{181-426}$ catalytic domain. While there is a methionine present at the e-cluster it would be difficult to associate its oxidation here specifically with modification due to its interaction with singlet O_2. Furthermore, the proportion of oxidised enzyme was too low for subsequent trypsin digestion analysis, to identify the modified amino acid residues.

4.2.3.4 Experiment 3.0

A final attempt was made to use this technique to activate O_2 and promote specific oxidation of PHD2 by using a sensitizer, Rose Bengal. Sensitizers are compounds which absorb light incurring a transition from its ground to its excited state. The sensitizer then transfers that energy to molecular O_2, inducing a photooxidation process. The experimental design was based upon work done by Lambert *et al* [7], lowering the total energy input significantly, to 7J. The recommended frequency once again had to be changed from 5 to 10 Hz due to hardware restrictions. The type of laser was also changed to facilitate the lower energy per pulse required. The laser was a Sirah Cobrah Stretch, 300 mJ/~5 ns pulse using Coumarin 450 laser dye pumped by a third harmonic of a Nd-YAG laser (continuum Surelite II).

The concentrations of reagents were lowered significantly (see MM), in accordance with those used by Lambert *et al.* The LC-MS chromatograms indicated that the samples contained enzyme (Fig 20). However in the corresponding spectra there were no peaks at 27.64 kDa to indicate the presence of PHD2 (Fig 21, 22 and 23). As peaks close to this mass range had been seen previously the LC-MS spectra of samples analysed under the conditions outlined in Experiment 2.0 - using D_2O as a solvent - peaks between 27.64 and 27.65 kDa MW were expected (Fig 18 and Fig 19).

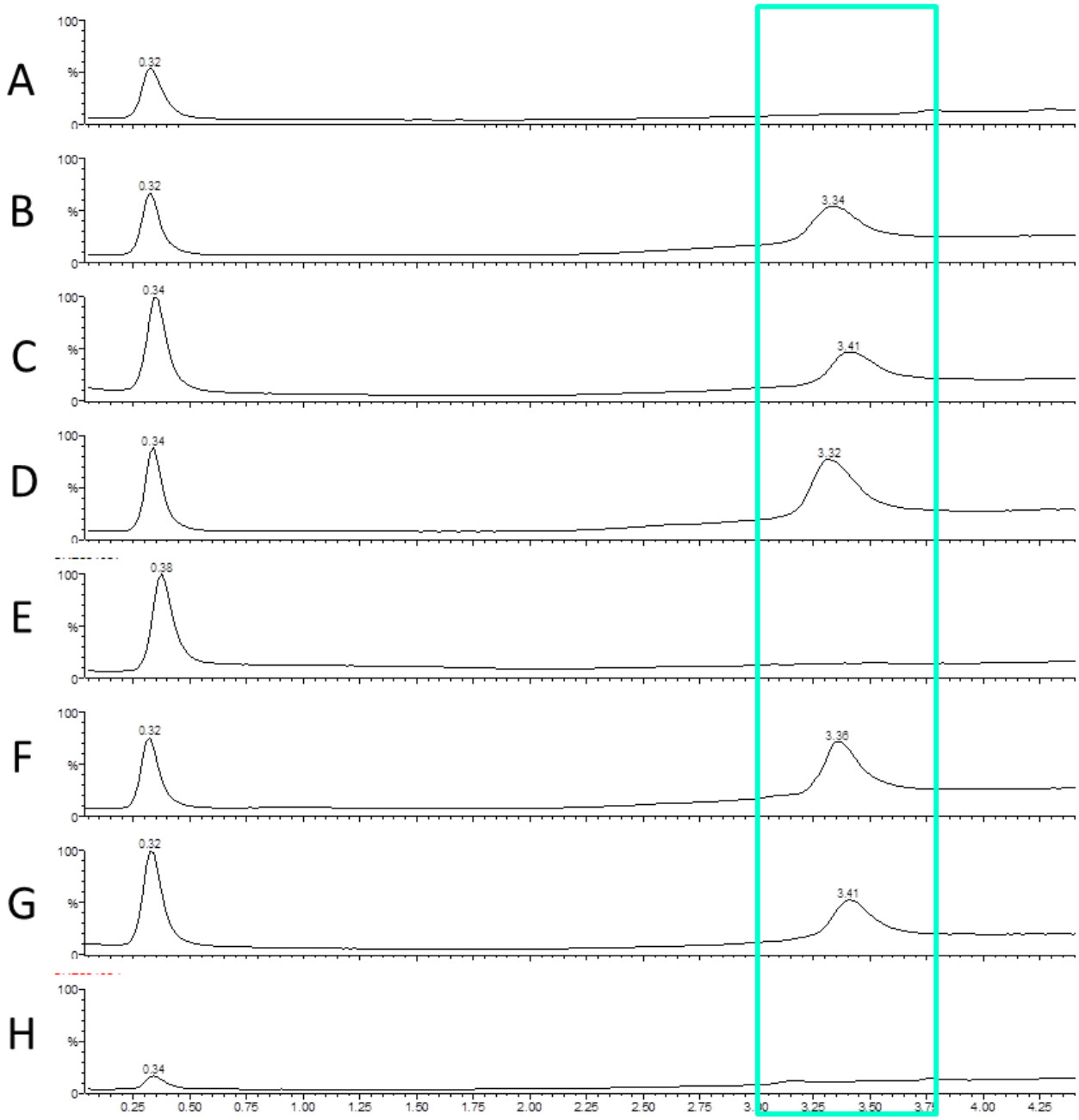

Figure 22: *Chromatograms of the assays conducted in experiment 3.0. A) IPA, B) the "No CODD" control, C) the "No Laser" control, D) the "No O_2" control, E) the "No Enzyme" control, F) the "No Rose Bengal" control, G) the PHD2.Zn.2OG.CODD sample and H) IPA. All samples with the exception of the IPA blanks and the "No Laser" control were exposed to 10 Hz for 3 min 51 s at 3 mJ pulse^{-1} at 532 nm. The enzyme-containing peaks between 3.31 and 3.41 min are highlighted in* ***green****, with the non-enzyme containing control (E)and IPA blanks (A and H) exhibiting no observeable peak in that region.*

This could indicate the PHD2 spectra are obscured by the high concentration of Rose Bengal-Na_2 salt, with residual salt carrying-over from the other samples into the 'No Rose

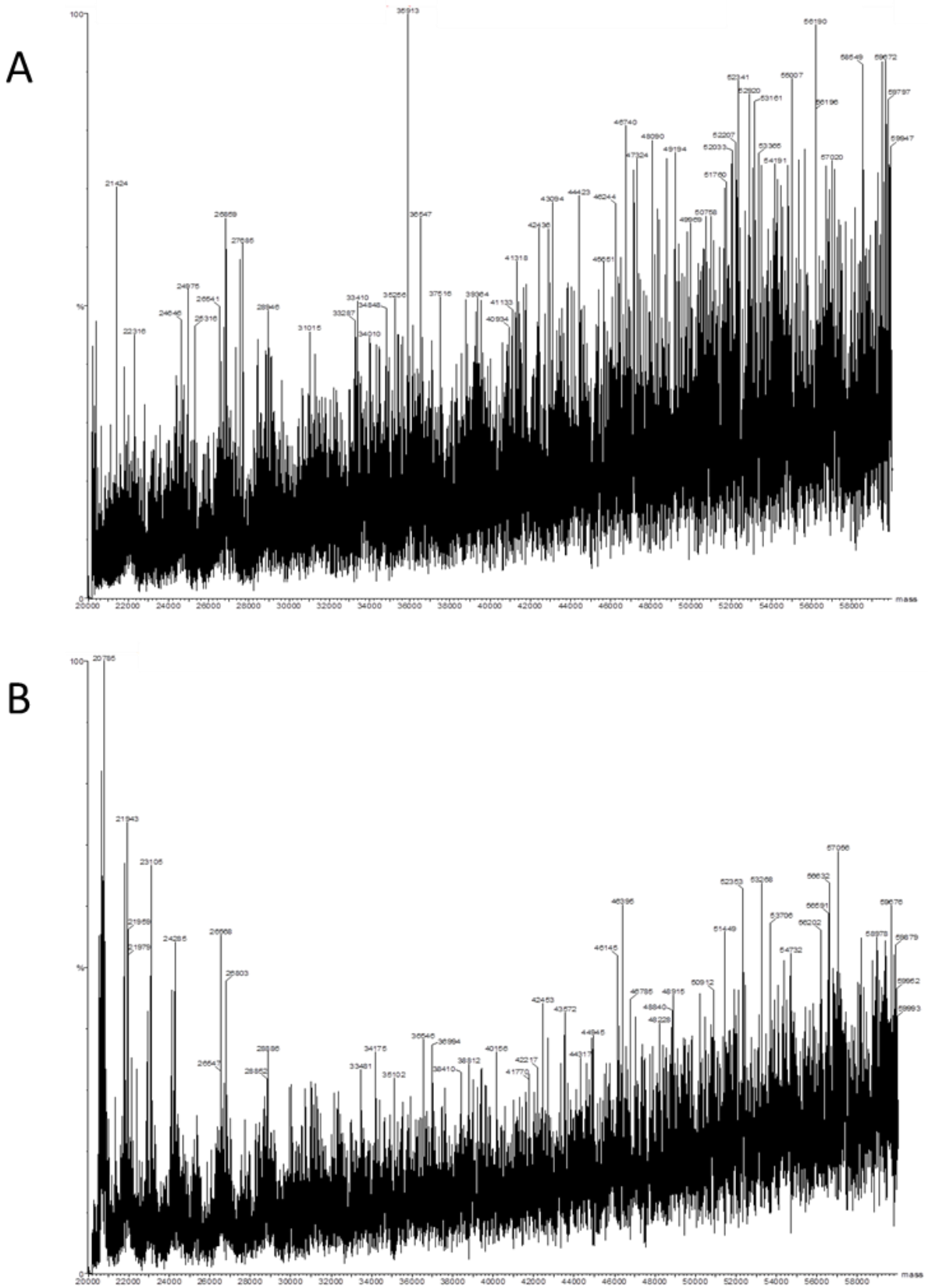

Figure 23: *LC-MS spectra of PHD2 from experiment 3.0. A) PHD2.2OG.Zn(II) (No CODD) and B) PHD2.2OG.Zn(II).CODD (No O_2) controls. Each sample was exposed to samples were exposed to 10 Hz for 3 min 51 s at 3 mJ pulse^{-1} at 532 nm using a Sirah Cobrah Stretch, 300 mJ/~5 ns pulse using Coumarin 450 laser dye pumped by a third harmonic of a Nd-YAG laser (continuum Surelite II) [7] in the presence of rose bengal and D_2O.The expected molecular weight of PHD2 is 27.64 kDa.*

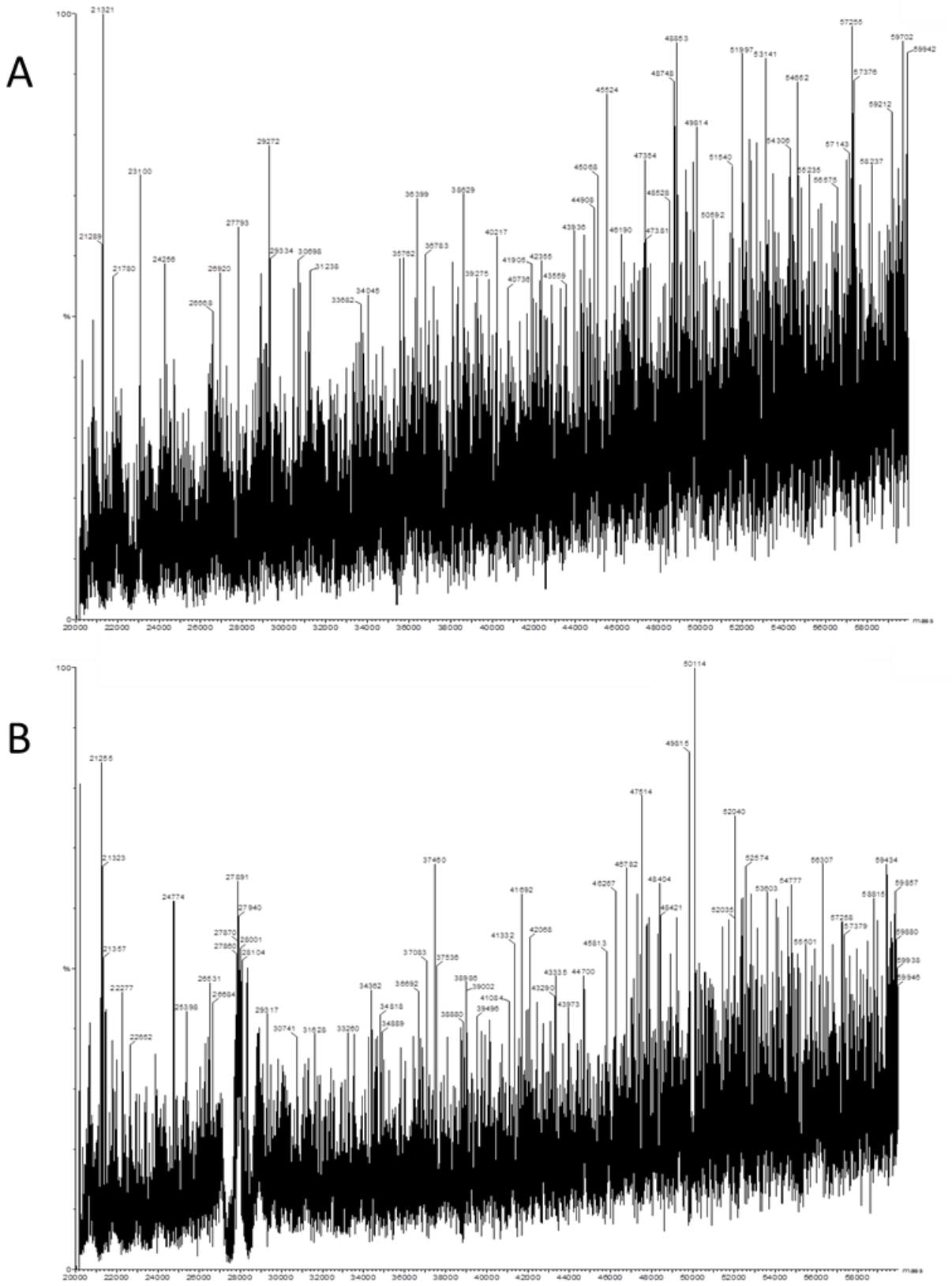

Figure 24: *LC-MS spectra of PHD2 from experiment 3.0. A) the PHD2.2OG.Zn(II).CODD (No laser) and B) the PHD2.Zn(II).CODD.2OG "No Rose Bengal" controls. Each sample, with the exception of the "no laser" control, was exposed to 10 Hz for 3 min 51 s at 3 mJ pulse^{-1} at 532 nm using a Sirah Cobrah Stretch, 300 mJ/~5 ns pulse using Coumarin 450 laser dye pumped by a third harmonic of a Nd-YAG laser (continuum Surelite II)* [7] *in the presence of rose bengal (with the exception of the "No Rose Bangal control") and D_2O.*

Bengal' sample, thus obscuring the spectra for this control too. This will therefore require an experimental adjustment to include a washing step, removing the Na(II). The use of MALDI was ruled-out as the peptide concentration was far below the limit of MALDI detection.

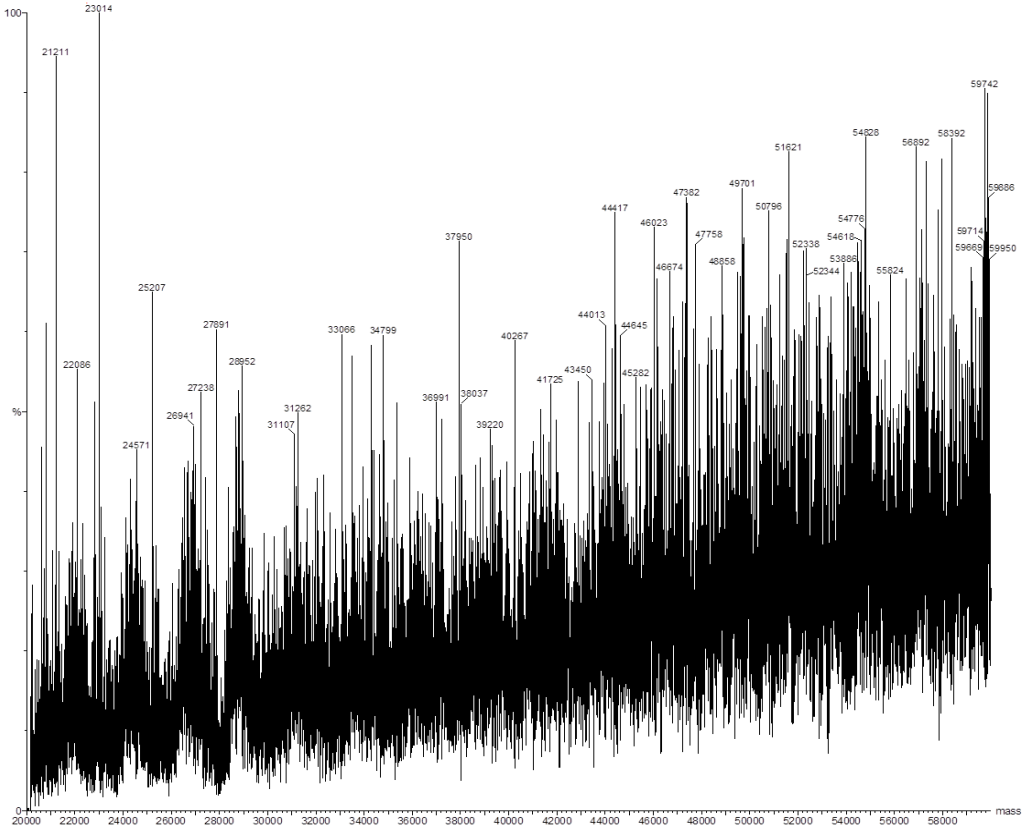

Figure 25: *LC-MS spectra of PHD2 from experiment 3.0. The sample inlcudes PHD2.Zn(II).CODD.2OG in the presence of rose bengal and D_2O. The sample was exposed to 10 Hz for 3 min 51 s at 3 mJ pulse^{-1} at 532 nm using a Sirah Cobrah Stretch, 300 mJ/~5 ns pulse using Coumarin 450 laser dye pumped by a third harmonic of a Nd-YAG laser (continuum Surelite II)* [7]

4.3 Conclusions

The purpose of the experiments conducted in this Chapter was to experimentally prove the existence of a stable "E-cluster" in which O_2 is proposed to interact non-covalently prior to entry to PHD2's active site, as proposed according to modelling studies by Jorgensen *et al*. The steady state kinetic studies with the M299H variant did not reveal any changes in O_2 kinetics compared to PHD2 WT. If M299H did alter any interactions with O_2, this implies the characteristics of the E-cluster are not responsible for the slow kinetics of PHD2 with respect to O_2. Rather, that events involved in O_2 delivery to the E-cluster may be limiting. This is further supported by the kinetic studies of the PHD2.1 and PHD2.3 loop variants, whereby changing the β2β3 loop sequence to that of PHD 1 or 3 yielded altered kinetics with respect to O_2.

The tryptophan fluorescence quenching studies verify the presence of W258 and W389 along the proposed O_2 entry route to the active site in PHD2. Furthermore, the active PHD2 W334F/W367F.2OG.Fe.CODD complex was determined to have an average rate constant of fluorescence quenching, 0.0127 ± 0.008 s^{-1} (Fig 7, pink line), comparable to the rate of CODD hydroxylation by PHD2 WT: 0.0095 ± 0.0012 s^{-1} [3] and 0.0155 ± 0.0012 s^{-1}. [33] The observed quenching pattern is thus reminiscent of the slow reaction of PHD2 with O_2 under pre-steady state conditions. The tryptophans, however, are proposed to be part of the E-cluster. The "delayed" quenching observed therefore suggests the stabilization of the E-cluster is not rate limiting with respect to O_2, rather that PHD2's slow reaction with O_2 could be attributed to restricted O_2 access *via* the PHD2:substrate interface.

The laser experiments were unable to identify laser-induced oxidation of PHD2 residues local to regions of O_2 stability. The technique itself is challenging and requires substantial optimization. In light of the fluorescence quenching studies of both the PHD2W334F/W367F.2OG.Fe(II).CODD and PHD2W334F/W367F.2OG.Zn(II).CODD complexes, whereby the active PHD2W334F/W367F.2OG.Fe(II).CODD complex had a unique interaction with O_2 by comparison to the other inactive complexes studied and the PHD2W334F/W367F.2OG.Zn(II).CODD complex appeared to "shield" tryptophans 258 and 389 from the bulk solvent- perhaps an active complex would yield oxidation events on PHD2 using O_2*.

4.4 Materials and Methods

Kinetic analysis of PHD2 M299H variant reaction with O_2

PHD2 M299H was produced as outlined in Chapter 2. The $K_m^{app}(O_2)$ determined in accordance with those described in Chapter 3, with a saturating concentration of 100 µM CODD chosen for PHD2 M299H (>2*K_m^{app}PHD2).

Stopped-flow intrinsic fluorescence quenching studies of PHD2 W334F/W367F

Experiments were performed under anaerobic conditions (<60 ppm O_2) on an Applied Photophysics SX20 Stopped Flow system fitted with a photomultiplier tube (320 nm wavelength cut-off filter) and a monochromator (excitation and emission slit width 4 mm). Reagents were mixed in the anaerobic chamber prior to mixing with buffer to a concentration of; 160 µM PHD2 W334F/W367F, 100 µM Fe(II)/Mn(II)(II)/Zn(II), 1000 µM 2OG/NOG and 200 µM CODD/FG-2216. The reagents were loaded into one of the two 2.5 mL loading syringes, with O_2 saturated or deoxygenated buffer in the other syringe. The complex and buffer were mixed in a 1:1 ratio, initiating the reaction and halving the

concentration of the reagents. The fluorescence signal (λ_{exc}=295 nm, λ_{em}>320 nm) was measured over 1000 s after mixing (1 s sample time). The temperature of the mixing and reaction chambers was at 5 °C. Buffer that had undergone treatment with vaccum and argon to remove O_2 (deoxygenated buffer) was used as a baseline – removing any non-specific background interference to fluorescence signal.

Laser excitation of molecular O_2 using Nd-YAG and dye lasers

$ZnCl_2$ and 2OG were allowed to equilibrate for a minimum of 5 min prior to enzyme and CODD addition, due to $ZnCl_2$ Lewis acid properties. The final volume was 1 mL, with reagent concentrations as per Tables 1 - 4. The solution was allowed to equilibrate for 15 min prior to incubation with 80% O_2. The solution was equilibrated in 80% O_2 for 5 min using mass-flow controllers (Brooks Instrument) in a sealed quartz 1 cm^3 cuvette. Once equilibrated, the cuvette was exposed to a beam from an NL 202 Nd-YAG, Surelite I-10 1064 nm dye laser or Sirah Cobrah Stretch, 300 mJ/~5 ns pulse using Coumarin 450 laser dye pumped by a third harmonic of a Nd-YAG laser (continuum Surelite II) for various intensities and exposure times. Modifications to suggested intensities and frequencies in the literature had to be made due to hardware restrictions. Exp. 2.0 and 3.0 were conducted In in D_2O, as deuterium oxide is said to prolong the lifetime of singlet state O_2. Following laser exposure, the samples were frozen at – 20 °C. Subsequent analysis was carried-out using MALDI-TOF and LC-MS.

Reagent	[Stock] (mM)	[Final] (µM)
PHD2	1	40
CODD	1	30
$ZnCl_2$	50	100
2OG	100	200

Table 1: *Experiment 1.0:* 500 Hz for 10 s at 2 mJ $pulse^{-1}$ [4]

Reagent	[Stock] (mM)	[Final] (µM)
PHD2	1	15
CODD	1	12.5
$ZnCl_2$	50	50
2OG	100	100

Table 2: *Experiment 1.1:* 1000 Hz for 10 min at 2 mJ $pulse^{-1}$

Reagent	[Stock] (mM)	[Final] (µM)
PHD2	1	40
CODD	1	30
$ZnCl_2$	50	100
2OG	100	50

Table 3: *Experiment 2.*0: 10 Hz for 26 min 40 s at 0.376 J $pulse^{-1}$ [5]

Reagent	[Stock] (mM)	[Final] (µM)
PHD2	1	1.8
CODD	1	1.7
$ZnCl_2$	50	3.6
2OG	100	7.2
Rose Bengal	1	5

Table 4: *Experiment 3*.0: 532nm, 10 Hz for 3 min 51 s at 3 mJ pulse^{-1} [7]

4.5 References

1. R. Chowdhury, M. A. McDonough, J. Mecinovic, C. Loenarz, E. Flashman, K. S. Hewitson, C. Domene and C. J. Schofield, *Structure*, 2009, **17**, 981-989.
2. R. Chowdhury, J. I. Candela-Lena, M. C. Chan, D. J. Greenald, K. K. Yeoh, Y. M. Tian, M. A. McDonough, A. Tumber, N. R. Rose, A. Conejo-Garcia, M. Demetriades, S. Mathavan, A. Kawamura, M. K. Lee, F. van Eeden, C. W. Pugh, P. J. Ratcliffe and C. J. Schofield, *ACS chemical biology*, 2013, **8**, 1488-1496.
3. H. Tarhonskaya, R. Chowdhury, I. K. H. Leung, N. D. Loik, J. S. O. McCullagh, T. D. W. Claridge, C. J. Schofield and E. Flashman, *Biochem J*, 2014, **463**, 363-372.
4. I. B. C. Matheson, *Photochemistry and Photobiology*, 1979, **29**, 875-878.
5. A. Singh, G. W. Koroll and S. A. Antonsen, *J Photochem*, 1984, **25**, 99-104.
6. H. Tarhonskaya, A. Szöllössi, I. K. H. Leung, J. T. Bush, L. Henry, R. Chowdhury, A. Iqbal, T. D. W. Claridge, C. J. Schofield and E. Flashman, *Biochemistry-Us*, 2014, **53**, 2483-2493.
7. C. R. Lambert, H. Stiel, D. Leupold, M. C. Lynch and I. E. Kochevar, *Photochemistry and Photobiology*, 1996, **63**, 154-160.
8. J. S. Scotti, I. K. H. Leung, W. Ge, M. A. Bentley, J. Paps, H. B. Kramer, J. Lee, W. Aik, H. Choi, S. M. Paulsen, L. A. H. Bowman, N. D. Loik, S. Horita, C. H. Ho, N. J. Kershaw, C. M. Tang, T. D. W. Claridge, G. M. Preston, M. A. McDonough and C. J. Schofield, *P Natl Acad Sci USA*, 2014, **111**, 13331-13336.
9. E. Flashman, L. M. Hoffart, R. B. Hamed, J. M. Bollinger, C. Krebs and C. J. Schofield, *Febs J*, 2010, **277**, 4089-4099.
10. E. Flashman, E. A. L. Bagg, R. Chowdhury, J. Mecinovic, C. Loenarz, M. A. McDonough, K. S. Hewitson and C. J. Schofield, *J Biol Chem*, 2008, **283**, 3808-3815.
11. D. Ehrismann, E. Flashman, D. N. Genn, N. Mathioudakis, K. S. Hewitson, P. J. Ratcliffe and C. J. Schofield, *Biochem J*, 2007, **401**, 227-234.
12. R. P. Hausinger and F. Fukumori, *Environ Health Persp*, 1995, **103**, 37-39.
13. J. C. Dunning Hotopp, T. A. Auchtung, D. A. Hogan and R. P. Hausinger, *J Inorg Biochem*, 2003, **93**, 66-70.

14. R. F. Chen, *Anal Letters*, 1967, **1(1)**, p. 35-42.
15. D. E. Epps, T. J. Raub, V. Caiolfa, A. Chiari and M. Zamai, *Journal of pharmacy and pharmacology*, 1999, **51**, 41-48.
16. F. Gao, N. Bren, T. P. Burghardt, S. Hansen, R. H. Henchman, P. Taylor, J. A. McCammon and S. M. Sine, *J Biol Chem*, 2005, **280**, 8443-8451.
17. A. Dusa, J. Kaylor, S. Edridge, N. Bodner, D.-P. Hong and A. L. Fink, *Biochemistry-Us*, 2006, **45**, 2752-2760.
18. S. B. Hansen, Z. Radić, T. T. Talley, B. E. Molles, T. Deerinck, I. Tsigelny and P. Taylor, *J Biol Chem*, 2002, **277**, 41299-41302.
19. A. I. De Kroon, M. W. Soekarjo, J. De Gier and B. De Kruijff, *Biochemistry-Us*, 1990, **29**, 8229-8240.
20. J. S. Johansson, *J Biol Chem*, 1997, **272**, 17961-17965.
21. M. E. Cockman, J. D. Webb, H. B. Kramer, B. M. Kessler and P. J. Ratcliffe, *Mol Cell Proteomics*, 2009, **8**, 535-546.
22. J. R. Lakowicz, *Principles of Fluorescence Spectroscopy* Springer Science & Business Media, New York, 2006.
23. M. P. Brown and C. Royer, *Current Opinion in Biotechnology*, 1997, **8**, 45-49.
24. J. R. Lakowicz, *Principles of Fluorescence Spectroscopy* 3rd edn., Springer Science & Business Media, New York, 2006.
25. J. R. Lakowicz and G. Weber, *Biochemistry-Us*, 1973, **12**, 4161-4170.
26. M. A. McDonough, L. A. McNeill, M. Tilliet, C. A. Papamicaël, Q.-Y. Chen, B. Banerji, K. S. Hewitson and C. J. Schofield, *Journal of the American Chemical Society*, 2005, **127**, 7680-7681.
27. K. S. Hewitson and C. J. Schofield, *Drug Discov Today*, 2004, **9**, 704-711.
28. R. Chowdhury, M. A. McDonough, J. Mecinović, C. Loenarz, E. Flashman, K. S. Hewitson, C. Domene and C. J. Schofield, *Structure*, 2009, **17**, 981-989.
29. W. M. Bernhardt, M. S. Wiesener, P. Scigalla, J. Chou, R. E. Schmieder, V. Günzler and K.-U. Eckardt, *Journal of the American Society of Nephrology : JASN*, 2010, **21**, 2151-2156.
30. L. Weil, W. G. Gordon and A. R. Buchert, *Archives of biochemistry and biophysics*, 1951, **33**, 90-109.
31. F. Wilkinson, W. P. Helman and A. B. Ross, *J Phys Chem Ref Data*, 1995, **24**, 663-1021.
32. G. W. Koroll and A. Singh, *Photochemistry and Photobiology*, 1978, **28**, 611-613.
33. H. Tarhonskaya, A. P. Hardy, E. A. Howe, N. D. Loik, H. B. Kramer, J. S. O. McCullagh, C. J. Schofield and E. Flashman, *J Biol Chem*, 2015.

Chapter 5: Investigating the kinetics of PHD2 in the presence of a 3C peptide

5.1 Introduction

Hypoxia-inducible factor (HIF) is an α,β-heterodimeric transcription factor that mediates cellular responses to low oxygen concentrations via the transcriptional activation of specific genes involved in both tumorigenesis and angiogenesis. [2] As such there is an active interest in developing therapeutics that can selectively alter the HIF-system *via* the activation or inhibition of the HIF-hydroxylases.

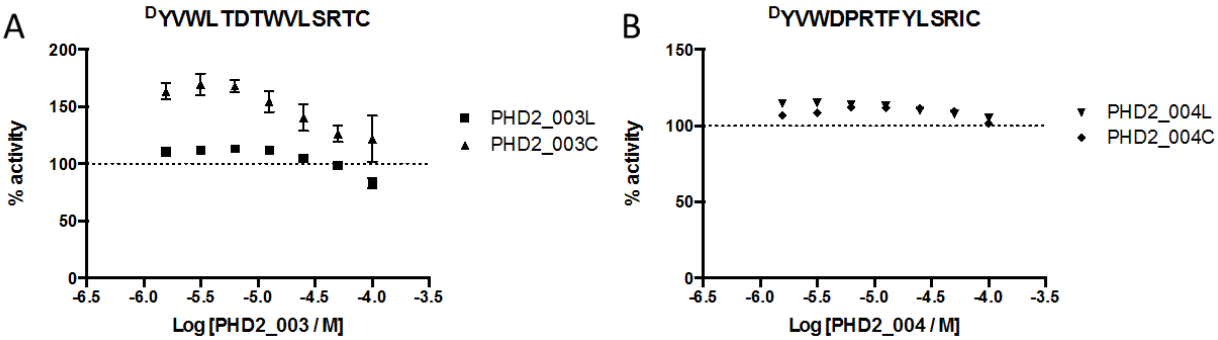

Figure 1: *RapidFire MS of A) PHD2 in the presence of the cyclic and linear 14-mer peptide, 3C and 3L respectively and B) PHD2 in the presence of the cyclic and linear 14-mer peptide, 4C and 4L respectively. Activation of CODD hydroxylation in the presence of 3C is clearly visible by comparison with 3L, 4C and 4L, with the dashed line lending reference to the graphs (Kawamura et al, unpublished)*

Recent RapidFire MS studies carried-out by Kawamura *et al* (unpublished), found that PHD2 hydroxylation of the 19-mer HIF-1α-CODD peptide appeared to be enhanced in the presence of a cyclic-14-mer peptide, known as 3C (Fig 1, A and Fig 2). The 3C peptide-PHD 2 interaction was identified during an unbiased mRNA display to identify cyclic peptides that bind PHD 2. This involved the use of a ribosome-expressed *de novo* cyclic peptide library with over 10^{12} permutations of cyclic peptides, with inserts varying from 4 – 12 mer. [3, 4] This work was carried-out by Kawamura *et al* in collaboration with the Suga group at the

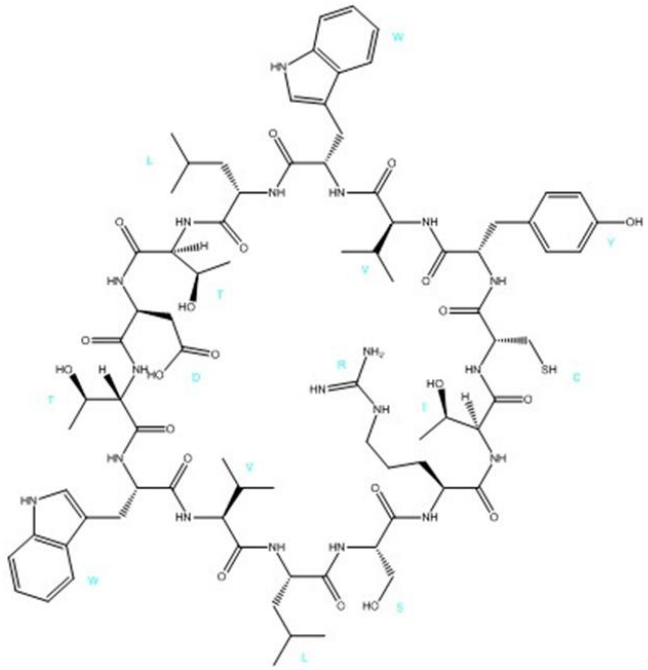

Figure 2: *Sequence and structure of the 3C peptide.*

University of Tokyo. Preliminary cell data by Kawamura *et al* suggests 3C may be cell permeable, but further studies will have to be carried-out to confirm.

NMR studies of ^{15}N-labelled *apo* $PHD2_{181–402}$ in the presence of the 3C peptide (Kawamura *et al*, unpublished) indicated the peptide binds in an allosteric position (Fig 3, B), with all significant Δδ shifts in PHD2's alpha-1-helix region (Fig 3, B). Surface analysis of the PHD2.Mn(II).NOG.CODD crystal structure "mapped" with the significant Δδ shifts, reveals structural changes in close proximity to both CODD and the proposed O_2 uptake pathway (Fig 3, A) - changes that could have implications with respect to the O_2 kinetics of the reaction of PHD2 with O_2. While the ^{15}N NMR of PHD2 in the presence of other, very similar cyclic peptides reveals a similar binding region, kinetic studies reveal no significant increases in apparent CODD hydroxylation levels (Fig 1, B). Therefore the aim of the work described in this Chapter was to confirm the proposed activation of CODD hydroxylation in the presence of PHD2 and 3C and to determine the effect on the reaction with respect to O_2. Should the O_2 kinetics of PHD2 be affected in the presence of the 3C peptide, it may be as a result of the disruption of O_2 stabilization features in PHD2 (See Chapter 4). This hypothesis is supported by the ^{15}N NMR data of PHD2, whereby significant Δδ shifts are apparent close to the proposed E-cluster.

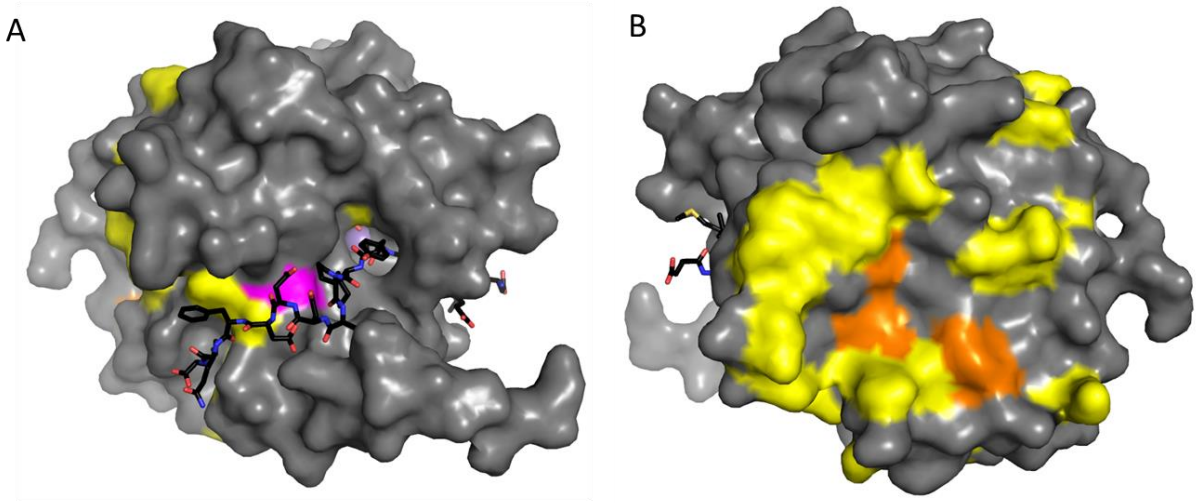

Figure 3: *Crystal structure of PHD2 (**grey**) in the presence of NOG, Mn(II) (purple) and CODD (**black,** sticks). The surface is mapped with the significant changes observed upon binding of 3C to PHD2$_{181–402.}$ Changes are coloured in accordance with significance, ranging from 0.05-0.10 ppm (in yellow), 0.10-0.15 ppm (in orange), 0.15-0.20 ppm (in pink) and >0.20 ppm (in white).* ***A)*** *Is the 'front' of the PHD 2 crystal structure with bound CODD peptide.* ***B)*** *Is the rotated PHD 2 crystal structure with bound CODD peptide, showing the 'back' region at which 3C is proposed to bind allosterically. ^{15}N NMR conditions include; 300 µM Zn^{II}, 500 µM 2OG, 50 mM Tris-D11 pH 6.6, 0.02% NaN_3, 10% D_2O + 90% H_2O, T = 310 K. (Kawamura et al, unpublished) PDB ID: 3HQR* [1]

5.2 Results and Discussion

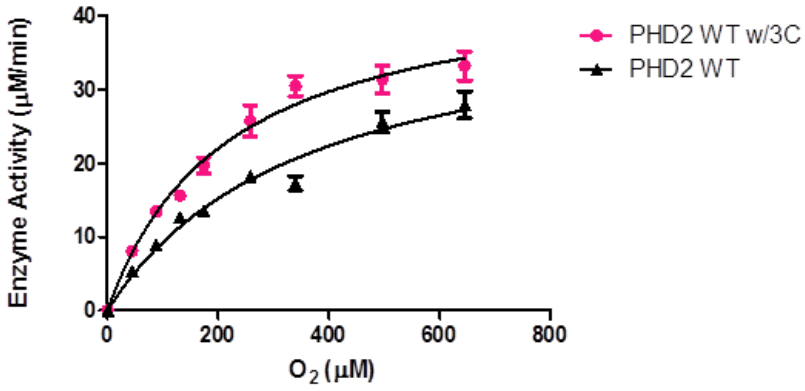

Figure 4: *$K_m(O_2)$ graphs for PHD2 in the presence (**pink** data points) and absence (**black** data points) of 3C peptide. All time courses were performed under the conditions; 4 µM PHD2, 50 µM Fe(II), 4 mM L-ascorbate, 300 µM 2OG, 100 µM HIF-1α CODD 19-mer peptide, at 37 °C in Tris·HCl 50 mM, pH 7.5.O_2 concentrations were varied from 5 to 80%.*

The $K_m^{app}(O_2)$ for PHD2 in the presence of CODD and 3C was conducted in accordance with procedures outlined in Materials and Methods (MM). Interestingly, the $K_m^{app}(O_2)$ for PHD2 in the presence of 3C was 216 ± 30 µM, by

comparison to PHD2 in the absence of 3C, 355 ± 80 µM (Fig 4). The V_{max} in the presence of 3C was also found to be higher, 44 µM/min by comparison to that of PHD2 in the absence of 3C, 40 µM/min. While activation in the presence of 3C in terms of O_2 is apparent, it is imperative to ensure the observed activation is due to increased CODD Pro564 hydroxylation and not increased Met561 or Met568 oxidation as increases in these species would be reflected by an overall increase in +16 Da (See materials and methods, Chapter 3,

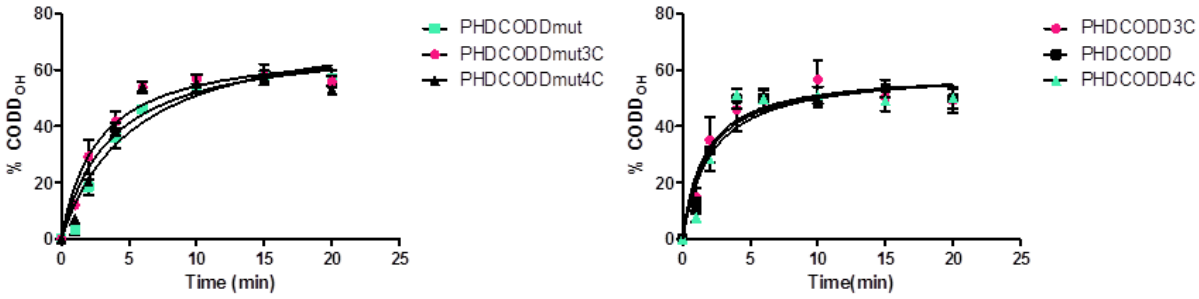

Figure 5: *Controls conducted in the presence of A) $CODD_{mut}$ and B) CODD with 3C, 4C and PHD2 included where applicable. All time courses were performed under the conditions; 4 µM PHD2, 50 µM Fe(II), 4 mM L-ascorbate, 300 µM 2OG, 100 µM HIF-1α CODD 19-mer peptide, at 37 °C in Tris·HCl 50 mM, pH 7.5.*

for $K_m^{app}(O_2)$ experimental outline).

To investigate this possibility, a series of controls were conducted as outlined in materials and methods. A CODD peptide variant, whereby methionines 561 and 568 were replaced with alanines, was used alongside CODD as a control. 4C, a cyclic peptide known to bind PHD2 in a similar region without any observed kinetic activation, was used as a negative control as 4C is structurally and chemically similar to 3C. The following reactions were conducted; 1) CODD + PHD2, 2) $CODD_{mut}$ + PHD2, 3) CODD + 3C, 4) $CODD_{mut}$ + 3C, 5) CODD + PHD2 + 3C, 6) $CODD_{mut}$ + PHD2 + 3C, 7) PHD2 + CODD + 4C, 8) $CODD_{mut}$ + PHD2 + 4C and 9) CODD. All controls contained 50 µM Fe(II), 100 µM CODD, 300 µM 2OG, 4 mM ascorbate, 4

μM PHD2 and 4 μM 3C where relevant. PHD2 and 3C/4C were incubated on ice for a minimum of 15 min prior to the initiation of the reaction, as per the experiments conducted previously.

Initial results (not shown) revealed activation in the presence of PHD2 + CODD + 3C compared to that of PHD2 + CODD and PHD + CODD + 4C. Conversely, the PHD2 + $CODD_{mut}$ + 3C appeared to be inhibited compared to PHD2 + $CODD_{mut}$ and PHD + $CODD_{mut}$ + 4C. These results suggest the apparent activation for PHD2 in the presence of 3C may be due to methionine oxidation. The commercial CODD peptide batch used for this series of controls, however, revealed high background oxidation (~26%), likely attributed to background methionine oxidation as a result of the peptide synthesis/purification process.

To avoid a false-positive result, a second series of controls were therefore conducted with CODD peptide purchased from a trusted supplier, where background methionine oxidation was known to be lower, and confirmed via MALDI-TOF analysis to be ~10%. All assays contained 50 μM Fe(II), 100 μM CODD, 300 μM 2OG, 4 mM ascorbate and 4 μM PHD2/3C. PHD2 and 3C/4C were incubated on ice for a minimum of 15 min prior to the initiation of the reaction. The second set of experiments reveals no significant activation in the presence of 3C for the PHD2 + CODD + 3C or PHD2 + $CODD_{mut}$ + 3C controls (Fig 5).

5.3 Conclusions

While $K_m^{app}(O_2)$ results revealed activation in the presence of 3C peptide, control time-course experiments using CODD, $CODD_{mut,}$ 3C and 4C show conflicting results. It is likely the activation seen in the first set of data for the PHD2 + CODD + 3C control was due to

experimental error and not true activation. Thus 3C is not likely a PHD2-activating peptide, and further opportunities to 'activate' PHD2 should be pursued.

5.4 References

1. R. Chowdhury, M. A. McDonough, J. Mecinovic, C. Loenarz, E. Flashman, K. S. Hewitson, C. Domene and C. J. Schofield, *Structure*, 2009, **17**, 981-989.
2. K. S. Hewitson and C. J. Schofield, *Drug Discov Today*, 2004, **9**, 704-711.
3. Y. Yamagishi, I. Shoji, S. Miyagawa, T. Kawakami, T. Katoh, Y. Goto and H. Suga, *Chemistry & Biology*, 2011, **18**, 1562-1570.
4. Y. Hayashi, J. Morimoto and H. Suga, *ACS chemical biology*, 2012, **7**, 607-613.

Chapter 6: Conclusions and future plans

PHD2 is reported to be the key O_2 sensor regulating the hypoxic response. [1] It has also been reported to have a high $K_m^{app}(O_2)$ value [1-6] and a slow reaction with O_2 in pre-steady state studies, kinetic features that are proposed to be related to its role as an O_2-sensor. [1, 3] We are interested in the molecular features that enable this O_2-sensing role, when other Fe(II)/2OG oxygenases react ~100-fold more rapidly with O_2. This study, coupled with molecular dynamic studies by our collaborators Dr C. Domene and C. Jorgensen (KCL), addressed the molecular features of PHD2 responsible for its O_2 sensing role.

Molecular dynamic studies carried out by Jorgensen et al (unpublished) identified a single O_2-entry pathway in PHD2 via the interface between HIF-α and the β2β3 loop. Coupled with studies conducted by Flashman *et al* [7], which proposed that the β2β3 loop of PHD2 was responsible for substrate recognition, with PHD2 β2β3 loop variants displaying different substrate affinities, [7] it was therefore thought important to understand whether or not the β2β3 loop had a role in the reaction of PHD2 with O_2. O_2 kinetic analysis of the same PHD2 β2β3 loop variants, whereby the loop region of PHD2 was replaced with the loop sequences from both PHD1 and PHD3 (PHD2.1 and PHD2.3 respectively), [7] was conducted.

Studies presented here revealed a dependence of PHD2's O_2 kinetics on the β2β3 loop sequence – with the PHD loop variants yielding distinctly different $K_m^{app}(O_2)$ values, with PHD2.3 yielding a $K_m^{app}(O_2)$ value six-fold lower than PHD2WT, followed by PHD2.1 with a value 2 fold lower than WT. The findings reflect large differences in sensitivity for O_2 between the isoforms, suggesting the O_2-sensing characteristics of different isoforms are

therefore worth investigating. The three PHD isoforms are found to manifest distinct patterns of cellular expression. [4, 8-11] For example PHD1 distribution is highest in the testes whereas PHD3 is the highest in the heart. [12] Therefore in different cell types, isoform-specific patterns of PHD expression alter both the relative abundance of the PHDs and their relative contribution to the regulation of HIF – which may depend on their individual reactivity with O_2. This has the potential to give some insight into how certain cell types may therefore have different O_2-sensing 'thresholds'.

The molecular dynamic studies also proposed a stabilizing internal "pocket" of amino acids termed the "E-cluster" in which O_2 interacts non-covalently prior to active site-entry. Should this E-cluster be validated, it could provide a platform from which we could begin to understand slowed PHD2 kinetics with respect to O_2. A major part of this study addressed the experimental realisation of this stabilizing "pocket" using site directed mutagenesis and subsequent kinetic studies, laser-induced excitation of molecular O_2 to modify local, stabilizing amino acids and tryptophan fluorescence quenching studies to confirm the presence of tryptophan residues local to the proposed E-cluster.

Laser-induced excitation of molecular O_2 to O_2* was used to attempt to modify and thus identify amino acid residues in regions where O_2 was stably bound, i.e. the E-cluster. This approach was technically challenging, and results obtained were inconclusive. Further investigations using this method would require substantial optimization, e.g. the implementation of various laser intensities, exposure times and frequencies. This, in turn, demands the optimization of laser hardware to accommodate the experimental requirements. Furthermore, a new complex, other than the PHD2.Zn(II).2OG.CODD complex

chosen, may yield more conclusive results as fluorescence studies revealed E-cluster access may be restricted in the PHD2.Zn(II).2OG.CODD complex.

The difference in $K_m^{app}(O_2)$ between PHD2 WT and PHD2M299H is not thought to be significant suggesting either methionine 299 does not alter the O_2 'stabilizing' characteristics of the E-cluster or the E-cluster is not significant in O_2 kinetics. Site directed mutagenesis of different amino acids proposed to be part of the E-cluster, e.g. W258, I258, R252 (PHD2 residues) or I566, Y565 or Q239 (CODD residues) and subsequent kinetic analysis would help validate whether or not the E-cluster exists. Should their O_2 kinetics vary, it would suggest a disruption of a stabilizing feature of PHD2 enabling altered O_2 uptake.

The observation of tryptophan fluorescence quenching by O_2 validated crystallographic and molecular modelling (Jorgensen *et al*, unpublished) observations, suggesting tryptophans 258 and 389 (proposed to be part of the proposed E-cluster) encounter O_2 as it enters the active site. Interestingly, the rate of fluorescence quenching by O_2 for PHD2 W334F/W367F is very similar to the rate of CODD hydroxylation by PHD2 WT under equivalent conditions, i.e. slow (~0.01 s^{-1}). This result suggests the observed fluorescence quenching is synonymous with PHD2 catalysis. These findings do not validate the proposal that O_2 resides stably in the E cluster before moving to the active site. It is implied that the rate limiting step is elsewhere in the O_2 delivery mechanism.

Overall, this study made strides towards realising the molecular features that enable PHD2's characteristic O_2 sensing capabilities. The kinetics of the PHD2 variants revealed a dependence on the β2β3 loop sequence, suggesting the loop is an important feature in O_2 uptake. The E-cluster remains unresolved, with further studies required to validate it directly. Fluorescence quenching studies suggest, should the E-cluster exist, is not the rate-

limiting step in O_2 uptake. It would appear from the fluorescence quenching studies the rate limiting step with respect to O_2 occurs prior to interacting with tryptophans 258 and 389, suggesting the β2β3 loop/HIF-α interface may be responsible.

Finally, studies reported here with PHD2 and 3C peptide, a proposed CODD hydroxylation "enhancer", suggest the peptide did not enhance PHD2 CODD hydroxylation and thus nor reduce the $K_m^{app}(O_2)$. Whether or not PHD2 activity can be improved using a peptide remains inconclusive. These results suggest that the precise rate limiting step of O_2 uptake in PHD2 would first have to be identified and a suitable intervention developed.

As high HIF levels are directly correlated with aggressive tumour phenotypes, [13] there is an active interest in developing both PHD2 inhibitors and activators. Should a suitable small molecule artificially reduce PHD2's $K_m(O_2)$, then the HIF upregulation in cancers may also be reduced. Conversely, should PHD1 and PHD3 turn out to have lower $K_m(O_2)$ values, selectively inhibiting PHD2 over PHD1 or PHD3 could be a way of rendering PHD1 and PHD3 as HIF regulators in cells. Their lower $K_m(O_2)$ values would effectively lower cellular HIF levels. The kinetic data of the PHD2.1 and PHD2.3 variants presented here would suggest the investigation of PHD1 and PHD3 O_2 kinetics as a viable avenue of research. Future research could focus on such kinetic studies and the development of specific small molecule activators or inhibitors of PHD2.

In light of the data presented here, it would be of interest to see how PHD1 and 3 β2β3 loop variants behave. That is, to create loop variants analogous to those studied here, taking PHD 1 and 3, the loops of PHD2, 1 and 3 and creating PHD3.1/3.2/1.2 and 1.3 variants with a view to characterising their O_2 kinetics. Such studies could be very insightful in terms of the role of the β2β3 loop in O_2 uptake across the PHDs.

Should such structural studies, as those outlined here, identify certain structural “cues” dictating increased or decreased oxygen sensitivity, it may be possible by simple sequence analysis to predict the O_2 sensitivity of certain O_2-dependent enzymes.

References

1. H. Tarhonskaya, A. P. Hardy, E. A. Howe, N. D. Loik, H. B. Kramer, J. S. O. McCullagh, C. J. Schofield and E. Flashman, *J Biol Chem*, 2015.
2. E. Flashman, L. M. Hoffart, R. B. Hamed, J. M. Bollinger, C. Krebs and C. J. Schofield, *Febs J*, 2010, **277**, 4089-4099.
3. H. Tarhonskaya, R. Chowdhury, I. K. H. Leung, N. D. Loik, J. S. O. McCullagh, T. D. W. Claridge, C. J. Schofield and E. Flashman, *Biochem J*, 2014, **463**, 363-372.
4. M. Hirsilä, P. Koivunen, V. Günzler, K. I. Kivirikko and J. Myllyharju, *J Biol Chem*, 2003, **278**, 30772-30780.
5. J. H. Dao, R. J. M. Kurzeja, J. M. Morachis, H. Veith, J. Lewis, V. Yu, C. M. Tegley and P. Tagari, *Anal Biochem*, 2009, **384**, 213-223.
6. D. Ehrismann, E. Flashman, D. N. Genn, N. Mathioudakis, K. S. Hewitson, P. J. Ratcliffe and C. J. Schofield, *Biochem J*, 2007, **401**, 227-234.
7. E. Flashman, E. A. L. Bagg, R. Chowdhury, J. Mecinovic, C. Loenarz, M. A. McDonough, K. S. Hewitson and C. J. Schofield, *J Biol Chem*, 2008, **283**, 3808-3815.
8. D. Dupuy, I. Aubert, V. G. Dupérat, J. Petit, L. Taine, M. Stef, B. Bloch and B. t. Arveiler, *Genomics*, 2000, **69**, 348-354.
9. N. Erez, M. Milyavsky, N. Goldfinger, E. Peles, A. V. Gudkov and V. Rotter, *Oncogene*, 2002, **21**, 6713-6721.
10. C. L. Cioffi, X. Qin Liu, P. A. Kosinski, M. Garay and B. R. Bowen, *Biochem Bioph Res Co*, 2003, **303**, 947-953.
11. F. Oehme, P. Ellinghaus, P. Kolkhof, T. J. Smith, S. Ramakrishnan, J. Hutter, M. Schramm and I. Flamme, *Biochem Biophys Res Commun*, 2002, **296**, 343-349.
12. C. Willam, P. H. Maxwell, L. Nichols, C. Lygate, Y. M. Tian, W. Bernhardt, M. Wiesener, P. J. Ratcliffe, K.-U. Eckardt and C. W. Pugh, *Journal of Molecular and Cellular Cardiology*, 2006, **41**, 68-77.
13. E. Rankin and A. Giaccia, *Cell Death Differ*, 2008, **15**, 678-685.